

Power Loss Minimization with Second Order Cone Programming Relaxation



Miss Akira Chuppawa

A Thesis Submitted in Partial Fulfillment of the Requirements  
for the Degree of Master of Engineering in Electrical Engineering

Department of Electrical Engineering

FACULTY OF ENGINEERING

Chulalongkorn University

Academic Year 2020

Copyright of Chulalongkorn University

การหากำลังสูญเสียต่ำสุดด้วยการผ่อนคลายแบบการโปรแกรมกรวยอันดับสอง



วิทยานิพนธ์นี้เป็นส่วนหนึ่งของการศึกษาตามหลักสูตรปริญญาวิศวกรรมศาสตรมหาบัณฑิต  
สาขาวิชาวิศวกรรมไฟฟ้า ภาควิชาวิศวกรรมไฟฟ้า  
คณะวิศวกรรมศาสตร์ จุฬาลงกรณ์มหาวิทยาลัย  
ปีการศึกษา 2563  
ลิขสิทธิ์ของจุฬาลงกรณ์มหาวิทยาลัย

Thesis Title                      Power Loss Minimization with Second Order Cone  
   Programming Relaxation

By                                      Miss Akira Chuppawa

Field of Study                      Electrical Engineering

Thesis Advisor                      Associate Professor SOTDHIPONG PHICHAISAWAT, Ph.D.

---

Accepted by the FACULTY OF ENGINEERING, Chulalongkorn University in  
Partial Fulfillment of the Requirement for the Master of Engineering

..... Dean of the FACULTY OF  
ENGINEERING  
(Professor SUPOT TEACHAVORASINSKUN, Ph.D.)

THESIS COMMITTEE

..... Chairman  
(Associate Professor SURACHAI CHAITUSANEY, Ph.D.)

..... Thesis Advisor  
(Associate Professor SOTDHIPONG PHICHAISAWAT, Ph.D.)

..... Examiner  
(Assistant Professor Channarong Banmonkol, Ph.D.)

..... External Examiner  
(Att Phayomhom, Ph.D.)

อาศิรา ชูปวา : การหาค่ากำลังสูญเสียต่ำสุดด้วยการผ่อนคลายแบบการโปรแกรมกรวย  
อันดับสอง. ( Power Loss Minimization with Second Order Cone  
Programming Relaxation) อ.ที่ปรึกษาหลัก : รศ. ดร.โสทธิพงศ์ พิชัยสวัสดิ์

ในปัจจุบันปัญหาการลดกำลังสูญเสียในระบบไฟฟ้าเป็นหัวข้อที่น่าสนใจอย่างยิ่ง การลดกำลังสูญเสียในระบบจำหน่ายมีความสำคัญอย่างมากในการเพิ่มความน่าเชื่อถือและประสิทธิภาพของระบบ วิทยานิพนธ์นี้จึงพิจารณาการหาค่ากำลังสูญเสียต่ำสุดในระบบไฟฟ้า กำลังไฟฟ้าจริงสูญเสียต่ำสุดสามารถพิจารณาได้จากการไหลของกระแสไฟฟ้ากระแสสลับที่เหมาะสมที่สุดภายใต้ขีดจำกัดของเครื่องกำเนิดไฟฟ้า แรงดันไฟฟ้าของบัสและสายส่ง ปัญหาการไหลของกระแสไฟฟ้ากระแสสลับที่เหมาะสมโดยทั่วไปสามารถคำนวณได้ยากในทางปฏิบัติ เนื่องจากฟังก์ชันวัตถุประสงค์และข้อจำกัดไม่เป็นเชิงเส้น ดังนั้นปัญหาการไหลของกระแสไฟฟ้ากระแสสลับที่เหมาะสมแบบเดิมจึงเป็นปัญหาการเพิ่มประสิทธิภาพแบบไม่คอนเวกซ์ งานวิจัยนี้จึงได้พัฒนาวิธีการคำนวณของปัญหาการไหลของกระแสไฟฟ้ากระแสสลับที่เหมาะสมโดยประยุกต์ใช้การผ่อนคลายแบบการโปรแกรมกรวยอันดับที่สองเพื่อเปลี่ยนปัญหาแบบไม่คอนเวกซ์ให้เป็นปัญหาแบบคอนเวกซ์ ซึ่งทำให้สามารถหาผลเฉลยที่ดีที่สุดภายในเวลาพหุนามได้ นอกจากนี้อุปกรณ์ระบบไฟฟ้า เช่น การผลิตไฟฟ้าแบบกระจายตัวหรือตัวชดเชยกำลังไฟฟ้าจินตภาพแบบสถิต สามารถทำให้กำลังสูญเสียในระบบเปลี่ยนแปลงได้ ดังนั้นงานวิจัยนี้จะวิเคราะห์การติดตั้งการผลิตไฟฟ้าแบบกระจายตัวและตัวชดเชยกำลังไฟฟ้าจินตภาพแบบสถิตในตำแหน่งที่เหมาะสมด้วยขนาดที่เหมาะสมเพื่อลดกำลังสูญเสียในสายจำหน่ายไฟฟ้า งานวิจัยนี้นำไปใช้ทดสอบกับระบบทดสอบจาก MATPOWER ผลการทดสอบพบว่าตัวแปรของระบบทั้งหมดไม่ละเมิดขีดจำกัดของระบบกำลังไฟฟ้าทั้งหมดที่ผลิตขึ้นสามารถตอบสนองความต้องการใช้ไฟฟ้าทั้งหมดได้อย่างเพียงพอ นอกจากนี้กำลังสูญเสียมีค่าลดลงเมื่อติดตั้งการผลิตไฟฟ้าแบบกระจายตัวและตัวชดเชยกำลังไฟฟ้าจินตภาพแบบสถิตในตำแหน่งที่เหมาะสมด้วยขนาดที่เหมาะสม

สาขาวิชา วิศวกรรมไฟฟ้า

ปีการศึกษา 2563

ลายมือชื่อนิสิต .....

ลายมือชื่อ อ.ที่ปรึกษาหลัก .....

# # 6272104921 : MAJOR ELECTRICAL ENGINEERING

KEYWORD: Power loss minimization, second order cone programming relaxation, AC optimal power flow, distributed generation, static var compensator

Akira Chuppawa : Power Loss Minimization with Second Order Cone Programming Relaxation. Advisor: Assoc. Prof. SOTDHIPONG PHICHAISAWAT, Ph.D.

The minimization of power loss in distribution systems is very important to increase the reliability and performance of the system. Therefore, this thesis determines power loss minimization in a power system. The active power loss can be minimized by the alternating current optimal power flow (ACOPF) under the limits of power generations, bus voltages, and distribution lines. The general ACOPF problem is computationally intractable in practice owing to the nonlinear objective function and nonlinear constraints. Accordingly, the conventional ACOPF is a nonconvex and NP-hard optimization problem. To address this difficulty, this work develops the computation of the ACOPF by applying second order cone program (SOCP) relaxation. Then, the ACOPF problem is a convex optimization problem. In addition, power system devices, such as distributed generation (DG) or static var compensator (SVC) can vary power loss in the system. Consequently, this work analyzes the appropriate site DG and SVC with optimal size to reduce power loss in distribution line. The proposed work was applied to MATPOWER test systems. The results show that all system parameters do not violate the system limits. The total generated power can supply the total load demand sufficiently. A near-global solution can be discovered. Furthermore, power loss is reduced when DG and SVC are installed with the optimal size at the proper site.

Field of Study: Electrical Engineering

Student's Signature .....

Academic Year: 2020

Advisor's Signature .....

## ACKNOWLEDGEMENTS

Firstly, I would like to express my sincere gratefulness to my advisor Assoc. Prof. Sotdhipong Phichaisawat, Ph.D. for giving precious advice. My advisor supports me overcome academic challenges and helps me in the research throughout my master's program. This thesis would not have been complete without his guidance. I also express my thankfulness to my thesis committee: Assoc. Prof. Surachai Chaitusaney, Ph.D., Asst. Prof. Chanarong Banmongkol, Ph.D., and Att Phayomhom, Ph.d. for their helpful comments on this thesis.

I would like to extend my profound thankfulness to all instructors in Department of Electrical Engineering, Faculty of Engineering, Chulalongkorn University for giving me valuable knowledge. In addition, I also express my thankfulness to Pikkanate Angaphiwatchawal who is a senior in the Power System Research Laboratory (PSRL) for giving invaluable advice and wisdom in academic aspects.

Besides, I would like to express my special thanks to Arnon Teawnarong and Jetsada Kantiyawong from PSRL for sharing their assistance and suggestion throughout my thesis, including for their encouragement and helpful comment.

Lastly, and most importantly, I would like to express my acknowledgment to Pongsakorn Sukheeboon who is a co-researcher. He always supports me not only my thesis but also supports master's degree study.

Akira Chuppawa

## TABLE OF CONTENTS

	Page
ABSTRACT (THAI) .....	iii
ABSTRACT (ENGLISH) .....	iv
ACKNOWLEDGEMENTS .....	v
TABLE OF CONTENTS .....	vi
CHAPTER 1 Introduction .....	1
1.1 Background and Motivation .....	1
1.2 Objective .....	2
1.3 Scope of Works .....	3
1.4 Methodology .....	3
1.5 Expected Contribution .....	4
1.6 Literature Review .....	4
CHAPTER 2 Basic Power System .....	7
2.1 Distribution System .....	7
2.1.1 Radial Distribution System .....	8
2.1.2 Loop Distribution System .....	8
2.1.3 Network Distribution System .....	9
2.2 Bus Classification .....	10
2.2.1 Voltage Bus .....	10
2.2.2 Load Bus .....	10
2.2.3 Slack Bus .....	10
2.3 Introduction to Power Loss .....	11

CHAPTER 3 Conventional Alternating Current Optimal Power Flow .....	14
3.1 Power System Modelling .....	14
3.1.1 Generator .....	14
3.1.2 Load .....	15
3.1.3 Shunt Compensation Element .....	16
3.1.4 Conventional Transformer .....	17
3.1.5 Transmission Line .....	20
3.2 Conventional Alternating Current Optimal Power Flow Problem .....	21
3.2.1 Objective Function .....	22
3.2.2 Equality Constraints .....	23
3.2.3 Inequality Constraints .....	24
CHAPTER 4 Power Loss Minimization with SOCP relaxation .....	26
4.1 Convex Optimization .....	26
4.2 Second Order Cone Programming .....	31
4.3 Alternating Current Optimal Power Flow with SOCP Relaxation .....	32
4.3.1 Reformulating the Power Flow Equations .....	33
4.3.2 SOCP Relaxation .....	37
4.3.3 ACOPF Formulation .....	38
4.4 Exactness of the Relaxation .....	39
4.5 ACOPF Computational Algorithm .....	42
CHAPTER 5 Distributed Generation and Static Var Compensator .....	44
5.1 Distributed Generation .....	44
5.2 Static Var Compensator .....	47
CHAPTER 6 Numerical Results .....	51



6.1 Base Case .....	51
6.1.1 9-Bus Test System .....	51
6.1.2 24-Bus Test System .....	55
6.1.3 33-Bus Test System .....	58
6.1.4 118-Bus Test System .....	62
6.2 Installing DG.....	62
6.2.1 One DG.....	63
6.2.2 Two DGs.....	65
6.2.3 Three DGs .....	66
6.3 Installing SVC.....	68
6.3.1 One SVC.....	68
6.3.2 Two SVCs.....	70
6.3.3 Three SVCs .....	72
6.4 Installing DG and SVC .....	73
6.4.1 One DG and One SVC .....	73
6.4.2 Two DGs and Two SVCs.....	75
6.5 Summary.....	76
CHAPTER 7 Conclusion and Future Work .....	78
7.1 Conclusion .....	78
7.2 Future Work.....	79
REFERENCES .....	80
APPENDIX.....	88
A. Data of Test Systems .....	88
A.1 9-Bus Test System .....	88

A.2 24-Bus Test System .....	89
A.3 33-Bus Test System .....	93
A.4 118-Bus Test System .....	96
B. Additional Results .....	109
B.1 24-Bus Test System .....	109
B.2 33-Bus Test System .....	111
B.3 118-Bus Test System .....	112
VITA.....	124



## LIST OF FIGURES

	Page
Figure 2.1 Radial distribution system.....	8
Figure 2.2 Loop distribution system .....	9
Figure 2.3 Network distribution system.....	9
Figure 3.1 Generator model .....	15
Figure 3.2 Load model .....	16
Figure 3.3 Two winding transformer equivalent circuit.....	18
Figure 3.4 Equivalent circuit of the transmission line .....	20
Figure 4.1 The line passing through $x_1$ and $x_2$ .....	27
Figure 4.2 Convex and nonconvex sets .....	27
Figure 4.3 Graph of a convex function .....	28
Figure 4.4 Local optimal solution and global optimal solution .....	29
Figure 4.5 Concept of a convex relaxation and a convex approximation .....	30
Figure 4.6 SOCP relaxation structure .....	33
Figure 4.7 Flow chart of ACOPF algorithm .....	43
Figure 5.1 DG integration diagram .....	45
Figure 5.2 SVC diagram .....	48
Figure 5.3 FC-TCR model.....	49
Figure 6.1 9-bus network system.....	52
Figure 6.2 24-bus network system .....	55
Figure 6.3 Comparison of voltage magnitude and voltage magnitude limit in 24-bus test system .....	58
Figure 6.4 33-bus system structure.....	59

Figure 6.5 Comparison of voltage magnitude and voltage magnitude limit in 33-bus test system .....	61
Figure 6.6 Comparison of total active power loss between base case and one DG installation at each bus .....	64
Figure 6.7 Total active power loss when installing two DGs at each bus .....	65
Figure 6.8 Comparison of total active power loss between base case and one SVC installation at each bus .....	70
Figure 6.9 Total active power loss when installing two SVCs at each bus.....	71
Figure 6.10 Total active power loss when installing DG and SVC at each bus.....	74



## LIST OF TABLES

	<b>Page</b>
Table 2.1 Comparison of bus types.....	11
Table 6.1 Comparison of bus data result in 9-bus test system.....	52
Table 6.2 Comparison of branch data result in 9-bus test system.....	53
Table 6.3 Comparison of power loss in 9-bus test system .....	53
Table 6.4 Comparison of power generation and power generation limit in 9-bus test system .....	54
Table 6.5 Comparison of voltage and voltage limit in 9-bus test system.....	54
Table 6.6 Comparison of bus data result in 24-bus test system.....	56
Table 6.7 Comparison of total power loss in 24-bus test system .....	57
Table 6.8 Comparison of power generation and power generation limit in 24-bus test system .....	57
Table 6.9 Comparison of bus data result in 33-bus test system.....	59
Table 6.10 Comparison of total power loss in 33-bus test system .....	61
Table 6.11 Comparison of total power generation and total power loss .....	62
Table 6.12 Comparison of power loss between base case and one DG installation at each bus .....	63
Table 6.13 Power generation from conventional generator and DG at bus 29 .....	65
Table 6.14 Comparison of power loss between base case and two DGs installation.	66
Table 6.15 Power generation when installing DG at bus 15 and 29 .....	66
Table 6.16 Comparison of power loss between base case and three DGs installation .....	67
Table 6.17 Power generation data when installing DGs at bus 6, 15, and 25 .....	67

Table 6.18 Comparison of power loss between base case and SVC installation at each bus .....	68
Table 6.19 Power generation from conventional generator and SVC at bus30 .....	70
Table 6.20 Comparison of power loss between base case and two SVCs installation	71
Table 6.21 Power generation when installing SVCs at bus 8 and 30 .....	72
Table 6.22 Comparison of power loss between base case and three SVCs installation .....	72
Table 6.23 Power generation data when installing SVCs at bus 8, 24, and 30 .....	73
Table 6.24 Comparison of power loss between base case and DG and SVC installation.....	74
Table 6.25 Power generation data when installing DG at bus 29 and SVC at bus 30..	75
Table 6.26 Comparison of power loss between base case and installing two DGs and two SVCs.....	75
Table 6.27 Power generation when installing two DGs and two SVCs.....	76
Table A.1 Bus data of 9-bus test system.....	88
Table A.2 Generator data of 9-bus test system .....	88
Table A.3 Branch data of 9-bus test system.....	89
Table A.4 Bus data of 24-bus test system.....	89
Table A.5 Generator data of 24-bus test system.....	90
Table A.6 Branch data of 24-bus test system.....	92
Table A.7 Bus data of 33-bus test system.....	93
Table A.8 Generator data of 33-bus test system.....	95
Table A.9 Branch data of 33-bus test system.....	95
Table A.10 Bus data of 118-bus test system .....	96
Table A.11 Generator data of 118-bus test system.....	101

Table A.12 Branch data of 118-bus test system .....	103
Table B.1 Branch data result in 24-bus test system.....	110
Table B.2 Branch data result in 33-bus test system.....	111
Table B.3 Comparison of bus data result in 118-bus test system .....	113
Table B.4 Branch data result in 118-bus test system .....	117



## CHAPTER 1

### Introduction

#### 1.1 Background and Motivation

A power system is a network that consists of a generation system, transmission system, and distribution system. The electric power is delivered to users from the generation system that supplies the electricity through the transmission system and the distribution system [1]. This transmission causes power loss in a power system [2]. In addition, the power demand is increasing every year, and consumers distribute from the power source resulted in increasing the power loss in the system. Therefore, the study of power loss minimization is very important. Power loss minimization can increase the reliability and performance of a power system by generating lower power, but load demand remains unchanged. Moreover, the cost of power loss and energy production can be reduced. Power loss can be minimized by the alternating current optimal power flow (ACOPF) [3].

The ACOPF is a fundamental tool for determining an optimal operating point in an alternating current (AC) power system. The goal of the ACOPF problem is to minimize the total power loss while maintaining the security of the power system operation. This operation is subjected to keep each device in the system within its required operation range at steady state. This includes the limits of power generation, maximum power flow of transmission line, as well as voltage limit at each bus [4]. The general ACOPF problem is a nonconvex and NP-hard optimization problem with nonlinear objective function and constraints [5]. Thus, this problem is computationally expensive and difficult to solve in practice. To reduce the complexity, second order cone program (SOCP) relaxation is applied [6]. SOCP relaxation can convert the conventional ACOPF problem to a convex optimization problem [7]. Thereby, the global optimal solution can be obtained within polynomial time.



Power loss in the system can be varied from power system devices, such as distributed generation (DG) or static var compensator (SVC). DG is playing important role in a power system because DG is a renewable energy generation that can improve the reliability of the system [8]. Moreover, DG can reduce transmission power and power loss of a distributed system since DG is close to the load location, so the transmission distance is reduced [9]. Therefore, the appropriate placement of DG with a suitable size can reduce the power loss and improve the reliability of the power system. While the unreasonable location and capacity of DG lead to greater power loss [10]. As a result, the optimal placement and size of DG are necessary to determine.

SVC is one type of flexible AC transmission system (FACTS) device, which is used to ensure power system reliability and security by appropriate control. SVC can continuously supply or absorb reactive power to the system [11]. Thus, a transmission system and a distribution system use SVC to control voltage and reactive power. The integration of SVC at the appropriate location can reduce the power loss and increase the transmission capability while maintaining the smooth voltage profile [12]. Therefore, the placement of SVC with a suitable size is necessary to consider for minimizing the power loss in the network.

The thesis aims to minimize power loss in the power system by using the ACOPF which is reformulated from SOCP relaxation. The optimal solution can be obtained without violating the power system limit. Additionally, the appropriate location and size of DG and SVC are also considered to reduce power loss.

## 1.2 Objective

The objective of this study is to enhance the power system performance in terms of total power loss minimization by using alternating current optimal power flow (ACOPF) with second order cone program (SOCP) relaxation.

1. To develop the computation of the ACOPF by using SOCP relaxation.

2. To analyze the appropriate site and size of distributed generation (DG) and static var compensator (SVC) to reduce power loss in distribution line.
3. To minimize power loss in distribution line.

### 1.3 Scope of Works

1. The study considers only power system in steady state operation.
2. The study considers only power loss minimization in distribution line and the suitable placement and sizing of DG and SVC.
3. The study considers the ACOPF formulation with SOCP relaxation.
4. The study is applied on the standard MATPOWER test system.
5. The simulations are performed using CVX optimization solver on Matlab.

### 1.4 Methodology

1. Studying literature works related to the thesis as follows:
  - 1.1 Studying the power system analysis and the optimal power flow for power loss minimization.
  - 1.2 Studying the convex optimization and SOCP relaxation.
  - 1.3 Studying CVX optimization solver to solve SOCP relaxation.
  - 1.4 Studying the effects of DG and SVC to the power system.
2. Formulating the ACOPF problem with SOCP relaxation to relax nonconvex problem to convex problem.
3. Defining the scope and methodology of the thesis.
4. Considering data related to the test system.
5. Developing a program for computing the ACOPF of total power loss minimization problem in the system with MATLAB and CVX.

6. Performing the proposed method and program on test systems.
7. Discussing the result and concluding the research.

### 1.5 Expected Contribution

1. The ACOPF formulation with SOCP relaxation for minimizing total power loss in distribution line.
2. The suitable site and sizing of DG and SVC for power loss minimization.
3. The reliable solution of the problem under system constraints.

### 1.6 Literature Review

The minimization of power loss in transmission and distribution system is very important to increase the reliability and efficiency of the system. Nowadays, the problem of loss minimization is an interesting topic. The power loss in transmission lines depends on the admittances, leakage losses, and voltages [13]. Due to this, the power loss can be optimized by the optimal power flow (OPF) under the limits of power generations, bus voltages, and network flows.

The OPF is a fundamental tool in electrical power system analysis. It focuses on finding an optimal operation. Carpentier first defined the OPF problem in the early 1960s [14]. After that, Dommel and Tinney complete the OPF formulation and multiple algorithms in their work [15]. Several optimization methods have been established to efficiently solve the OPF problem. However, this problem is also a challenging optimization problem in the power system.

From [16], there are 2 challenges in the OPF problem. First, the problem is solved every few minutes due to an operational level problem. Consequently, the computational budget is limited. Second, the problem is a nonconvex and NP-hard problem owing to nonlinear constraints. Hence, the algorithms, that are suggested for the OPF problem, are based on approximation or relaxation. Direct current optimal

power flow (DCOPF) approximation is used in the practical electricity industry [17]. In contrast, the original nonconvex OPF is the ACOPF. DCOPF is a linearization of ACOPF by approximating the power flow equations. The important aspects are ignored, such as voltage angle and reactive power so the computation is faster. However, the solution is not precise and cannot guarantee the global optimal solution.

In [18], Newton-method is applied to the OPF problem. Then many methods according to Newton-method and gradient algorithm are arisen [19]–[20]. These methods solved the OPF problem from the iterative method in a specific direction. Hence, the convergence speed near the optimal point is very low. Moreover, the global optimal solution is obtained difficultly. From [21], non-deterministic search techniques like Ant Colony Optimization (ACC), Particle Swarm Optimization (PSO), or Tabu Search (TS) are applied to solve the OPF problem. Moreover, hybrid methods which combine various optimization techniques into one algorithm are also applied to the OPF problem [21]. These methods can handle nonconvex, dynamics, and discrete variables but the calculation speed is very slow.

In recent years, the semidefinite program (SDP) and the second order cone program (SOCP) are applied to the OPF problem. The research [22] converts the power flow model into the SDP model by primal-dual interior point algorithm. For the mesh network, the OPF problem is solved using SDP relaxation from [23]. There are 4 different formations to consider the problem. Only one of the formations provide the exact solution. The research [24] presents the SDP relaxation is exact only if the duality gap is zero. The work shows a necessary and sufficient condition to guarantee the existence of no duality gap for the OPF problem. The SDP relaxation provides the global optimal solution to the OPF problem when the relaxation is exact. However, the exactness can be guaranteed only for some problems within some assumptions, such as radial networks under load over-satisfaction, or lossless networks with cyclic graphs [25]–[27]. When the solution matrices are not rank one, some problems in the terms of recovering an optimal solution are posed [28].

Therefore, the SDP relaxation is difficult to solve in the real large-scale power network.

The work [29] presents SOCP to convexify power flow equations in the radial distribution networks. The research [30] describes an exact SOCP model for reformulating the power flow equation with the branching aspect. In [31], the OPF problem applies SOCP relaxations. The relaxations are proved to be tight with the application of the convex hull. In addition, the research [32] indicates the ACOPF formulation with SOCP relaxation in the radial network. The work shows that the SOCP relaxation is exact under certain conditions. As a result, the SOCP method is less sensitive to the power system scale and less computational time. The SOCP solves the ACOPF problem faster than the SDP.

To reduce power loss in the system, the power system devices, such as distributed generation (DG) or static var compensator (SVC) are considered. The study [33] formulate the optimal photovoltaics sizing problems as SOCP model for loss minimization in a distribution network. The research [10] proposes a distributed generation (DG) siting and sizing for minimizing the total active power loss. The SOCP model is used to solve the problem and provides the optimal solutions. Furthermore, the suitable locations of SVC in the transmission network are determined in [12]. The active power loss can be reduced from several SVCs with appropriate placement.

As a result of all literatures above, this thesis focuses on power loss minimization which can be determined from reformulating the ACOPF with SOCP relaxation. Moreover, DG and SVC with suitable placement and size are considered to reduce power loss in the system.

## CHAPTER 2

### Basic Power System

This chapter describes the basic knowledge in the power system which encloses 3 parts. The first part describes the distribution system which carries electricity through the transmission system to consumers. The distribution system can be classified into 3 types according to feeder connection topologies. The second part describes bus type which is used in power flow analysis. The last part describes an introduction to power loss and the factors that affect power loss minimization.

#### 2.1 Distribution System

From [1], the distribution system is part of the power system that receives electricity from the generation system through the transmission network in order to deliver electric power to the users in different areas. The transmission system and the distribution system are connected through a substation which regulates the voltage to a suitable level for the user application.

The distribution system is divided into 2 system types that are an overhead aerial system and an underground cable system. Several factors are considered to select the system type, such as safety, environment, and investment cost. Generally, the distribution system in Thailand is the overhead aerial system because the price is lower than the underground cable system. However, the underground cable system is used in the high load density area or within industrial estates.

The distribution system consists of 3 typical feeder connection topologies as following.

1. Radial distribution system
2. Loop distribution system
3. Network distribution system

### 2.1.1 Radial Distribution System

The radial distribution system is the most commonly used due to the simplest connection system and the lowest installation cost. The radial system has only one power generation and various feeders radiate from a substation to feed the user at one end as shown in Figure 2.1. Thus, the power flow in radial system has one direction. The reliability of the system is not highly. When a fault occurs at any point in the feeder, power in the entire line is interrupted and there is no alternative feeders to feed load.

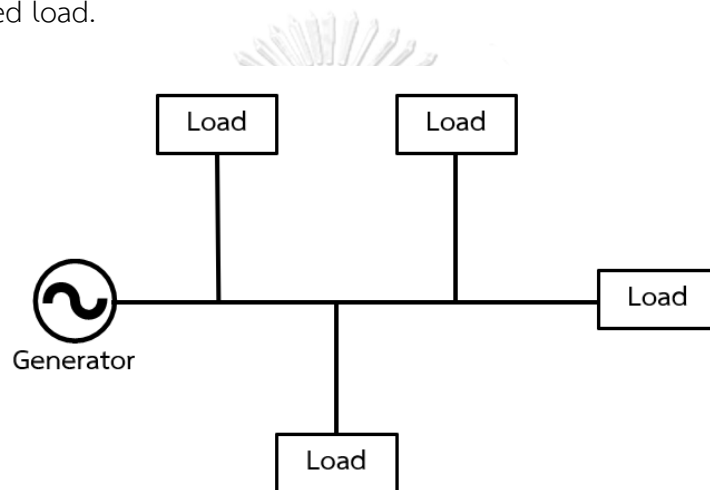


Figure 2.1 Radial distribution system

### 2.1.2 Loop Distribution System

The loop distribution system loops through the load area and returns to the initial point which is the substation bus as shown in Figure 2.2. The strategic placement of switches allows the utility to supply power to customers from either direction. If the fault occurs, the circuit breaker will open the circuit to trip until the fault disappears from all directions. The fault can be eliminated with a minimum of customer interruptions. Hence, the loop system provides better reliability and continuity of service than the radial system. However, this system is more expensive because more switches are required.

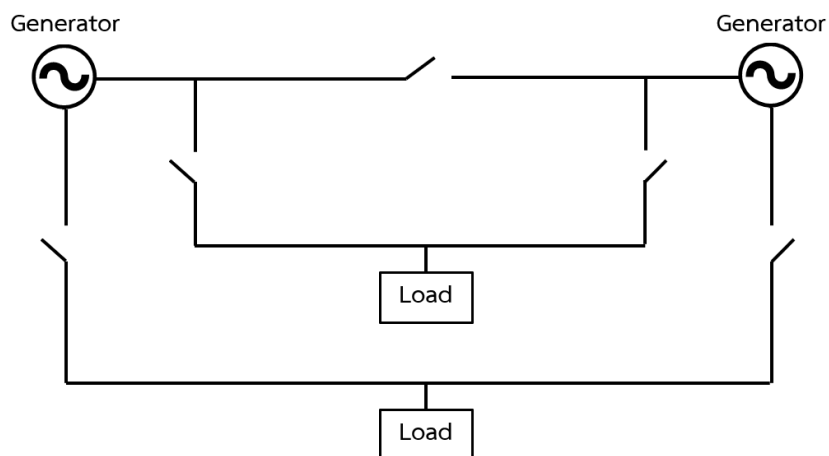


Figure 2.2 Loop distribution system

### 2.1.3 Network Distribution System

The network distribution system is the most complicated system that consists of several interconnecting circuits operating at the same voltage level. The utility can supply loads from two or more power supplies with various direction as shown in Figure 2.3. When one power source fails, the other sources can supply power to the customer without interruption. Therefore, the loss in this system is lower than the radial distribution system. Moreover, the network system is the most reliable in terms of continuity of service. However, it is also the most expensive. For this reason, it is usually used only in high load density area or downtown area.

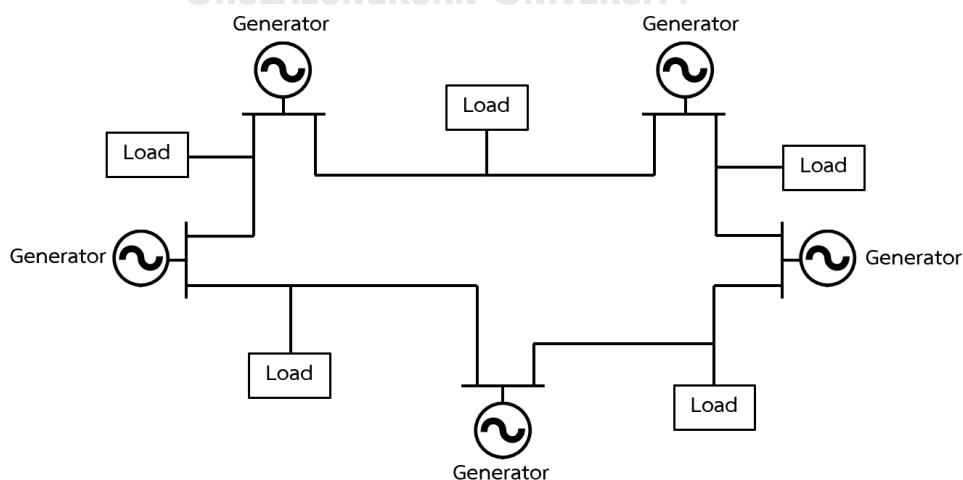


Figure 2.3 Network distribution system



## 2.2 Bus Classification

The buses in a power system are associated with four quantities which are the magnitude of the voltage, the angle of the voltage, the active power, and the reactive power [34]–[35]. Thereby, the buses are placed in three categories: voltage bus, load bus, and slack bus which can be summarized in Table 2.1.

### 2.2.1 Voltage Bus

The voltage bus is also known as the generator bus or PV bus in which the generators are connected. The voltage magnitude corresponding to the generator voltage, and the active power corresponding to the generator rating are specified. The voltage magnitude is set by adjusting the synchronous generator field current. The constant power generation is controlled through a prime mover.

### 2.2.2 Load Bus

The load bus is also called the PQ bus where no generators are connected. Thus, the active and reactive power generation is zero, but the active and reactive power of the load is specified. The bus voltage magnitude may vary within tolerable rates and the voltage angle is not very crucial for the load. The load bus is the most abundant bus in the power system.

### 2.2.3 Slack Bus

The slack bus is also known as the swing bus which is taken as a reference bus. The voltage magnitude and the voltage angle are predefined with the angle set to zero. No load is connected to this bus so the loss can be considered during the transmission of power. The generator bus supplies the active and reactive power, but the load bus is not receiving all the power as a result of power loss in the system. The slack bus supplies the loss and the unfulfilled demand from other buses. Accordingly, the slack bus maintains the balance of the power by absorbing or supplying the active or reactive power.

Table 2.1 Comparison of bus types

Bus type	Active power	Reactive power	Voltage magnitude	Voltage angle
Voltage Bus	constant	unknow	constant	unknow
Load Bus	constant	constant	unknow	unknow
Slack Bus	unknow	unknow	constant	constant

### 2.3 Introduction to Power Loss

From [1], [36] and [37], power loss in the power system is the power that loses in the transmission line by converting from electrical energy to thermal energy. The power loss can be divided into 2 types as follows.

1. Technical loss

Technical loss consists of power loss in the transmission line, transformers, or other components. Moreover, it also includes core loss of transformer and discharge loss.

2. Non-technical loss

Non-technical loss is caused by faulty measurements or defective data collection processes. It is generally calculated from the difference between the total power loss and the technical loss.

In this part, the technical loss is focused. The technical losses can be considered from power flow analysis through power system model such as transmission lines, transformers, or impedance. Therefore, the utility can plan to reduce the power loss for example installing a capacitor or selecting a suitable transformer size. Furthermore, there are two types of causes of the technical loss.

1. Power loss dependent on load loss

This loss comprises power loss in transmission line and transformer. This loss is caused by the electric current flowing through the various components of the power system. The loss is converted into heat, causing high temperatures in components, and energy waste is wasted.

2. Power loss independent of load loss

This loss mostly is transformer core loss. This loss is especially in distribution systems with a large number of distribution transformers.

Generally, the utility computes the power loss occurring in the system to examine the cause and amount of power loss from each component and then determines an effective plan for reducing the loss. The power loss can be calculated from the difference between the power unit generated and the power usage from the customer. This loss is a total loss that includes both the technical loss and the non-technical loss. After that, the technical loss is calculated. For accurate results, power flow analysis is applied to calculate loss. In order to reduce loss, there are 5 factors to consider as follows.

1. Distributed generator size and placement

Installing a distributed generator with a suitable capacity and location can reduce the power loss in the system. The loss will increase when installed too high capacity due to the reverse power flow to the generator at the substation.

2. Load demand capacity

Each electricity user has different power consumption behavior so, there are various load characteristics. Industrial users consume a lot of power during the day while consuming less power at night. Residential users consume a lot of power during the night while consuming less power during the day. The higher the power demand, the higher the power loss. Thus, the power loss depends on the amount of power demand.

### 3. Transmission line type and length

The power loss occurs in transmission lines so, the transmission line type and length have a direct effect on power loss. There are various types of transmission lines that have different conductivity. In addition, the length of the transmission line varies in line impedance. The higher impedance, the higher power loss.

### 4. Capacitor size and placement

The utility requires a high power factor, especially in the load bus with high power demand. The higher the power factor, the lower the power loss in the system. To improve the power factor, the capacitors are installed at the appropriate size and location. Therefore, capacitors can affect the power loss.

### 5. Transformer tap changing

In a radial distribution system, the voltage level decreases along with the distance of the transmission line. The longer the distance, the lower the voltage level and it depends on the amount of power demand in each location. The transformer tap is adjusted to increase or decrease the voltage level. Therefore, adjusting the transformer tap can reduce the power loss in the power system. This method applies the same principle as raising the voltage level to high so that the current in the transmission line is low resulting in lower power loss.

## CHAPTER 3

### Conventional Alternating Current Optimal Power Flow

This chapter describes the conventional alternating current optimal power flow (ACOPF) problem which is a nonlinear optimization program. The ACOPF is power dispatch proposed to satisfy an objective function while system constraints are taken into account, for example power flow equations, generation capacity limits, transmission line flow limits, etc. The explicit ACOPF formulation can be derived from the power system model. Hence, the suitable model and components are very important in the system. This section consists of 2 parts. The first part describes the power system modeling. The last part explains the ACOPF formulation with the objective function and the constraints.

#### 3.1 Power System Modelling

From [38]–[39], a power system model is key factor in the alternating current optimal power flow (ACOPF) analysis. The appropriate model provides accurate results of the ACOPF problem. This section consists of 5 components of the power system which are generators, loads, shunt compensation elements, transformers, and transmission lines.

##### 3.1.1 Generator

A generator is a device that transforms mechanical energy into electrical power in the power system. The complex power which is generated from the generator can be imposed as below.

$$S_{gi} = P_{gi} + jQ_{gi} \quad (3.1)$$

Where  $P_{gi}$  is active power generated at bus  $i$ .

$Q_{gi}$  is reactive power generated at bus  $i$ .

The generator is modeled as a controllable power source as illustrated in Figure 3.1.

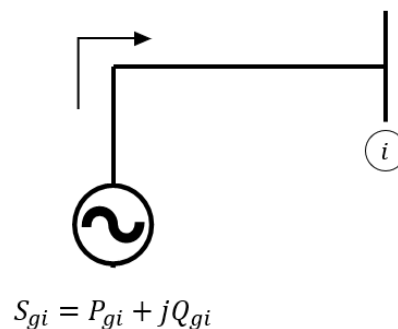


Figure 3.1 Generator model

Most of the based load in the power system is originated from thermal units. Hence, the fuel cost of the generator can be represented as a quadratic function of active power generation,

$$C(P_{gi}) = \alpha_i + \beta_i(P_{gi}) + \gamma_i(P_{gi})^2 \quad (3.2)$$

where  $\alpha_i$  is the thermal plant fixed cost.

$\beta_i$  is first-order coefficient of the cost curve.

$\gamma_i$  is second-order coefficient of the cost curve.

### 3.1.2 Load

A load is one of the portions of the power system which consumes electrical energy in the form of current and converts current into other forms such as heat, light, work, or motion. The load is resistors, inductors, or capacitors. Moreover, the electric load is also called power demand. The power demand is determined as constant complex power consumption which is not dependent on the voltage as express below.

$$S_{di} = P_{di} + jQ_{di} \quad (3.3)$$

Where  $P_{di}$  is active power demand at bus  $i$ .

$Q_{di}$  is reactive power demand at bus  $i$ .

Figure 3.2 shows the load model with constant active and reactive power.

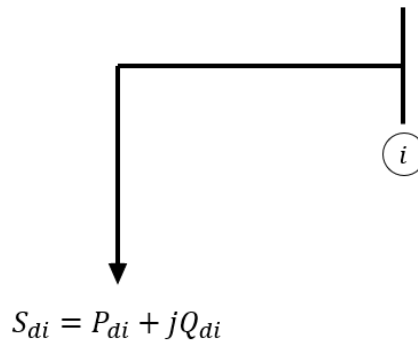


Figure 3.2 Load model

### 3.1.3 Shunt Compensation Element

In shunt compensation, the shunt elements operate as a controllable current source and are connected in parallel with the transmission line in the power system. The current is injected into the transmission line to set the voltage magnitude by changing shunt impedance. There are 2 major types of shunt compensation elements.

#### 1. Shunt inductive compensation

Shunt inductive compensation is used to limit the voltage when the load at receiving end is very low. Due to the light load, a very low current flows through the transmission line then the reactive power demand is less than the reactive power generated. As a result of the shunt capacitance of the line, the voltage tends to rise. To control the voltage, reactive power is necessary to draw out. This is accomplished by connecting the shunt inductors across the transmission line.

#### 2. Shunt capacitive compensation

Shunt capacitive compensation is often used to raise the voltage on the transmission line and reduce power loss in the power system. When the load is high, the large reactive power flows from sending end to the receiving end and resulted in a large voltage drop due to the series inductance of the line.

To improve the voltage, shunt capacitors are connected to feed the reactive power to the load.

Shunt elements are indicated from the voltage magnitude dependent complex power as shown in equation (3.4). Hence, the active and reactive power which are injected via the shunt compensation admittance are presented in equation (3.5)–(3.6).

$$S_i^{sh} = P_i^{inj} + jQ_i^{inj} \quad (3.4)$$

$$P_i^{inj} = U_i^2 G_i \quad (3.5)$$

$$Q_i^{inj} = -U_i^2 B_i \quad (3.6)$$

Where  $P_i^{inj}$  is active power injection at bus  $i$ .

$Q_i^{inj}$  is reactive power injection at bus  $i$ .

$U_i$  is voltage magnitude at bus  $i$ .

$G_i$  is shunt conductance of shunt compensator at bus  $i$ .

$B_i$  is shunt susceptance of shunt compensator at bus  $i$ .

### 3.1.4 Conventional Transformer

A transformer is one of the major components in the power system which transfers power from one voltage level to another level with high efficiency. The power of the primary and the secondary winding are almost equal except for the transformer losses. Accordingly, the secondary voltage is increased by a ratio of  $a$  using a step-up transformer of turn ratio  $a$ . The loss in the line will decrease and the power can be transmitted to the load over long distances.



The two winding transformer is modeled having complex tap ratio on both primary and secondary windings. The model also considers the magnetizing branch under saturated conditions for the core loss. The two winding transformer equivalent circuit is shown in Figure 3.3.

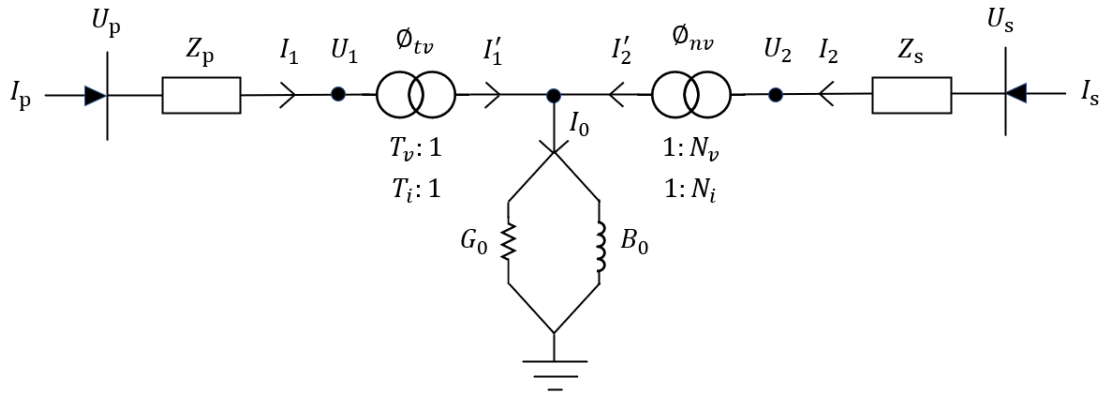


Figure 3.3 Two winding transformer equivalent circuit

The primary winding is represented as an ideal transformer with complex tap ratios  $T_v:1$  and  $T_i:1$  in series with the impedance  $Z_p$ , where  $T_v = T_i^* = T_v \angle \Phi_{tv}$  and the \* denotes the conjugate operation. In the same manner, the secondary winding is represented as an ideal transformer with complex tap ratios  $N_v:1$  and  $N_i:1$  in series with the impedance  $Z_s$ , where  $N_v = N_i^* = N_v \angle \Phi_{nv}$ . The primary voltage  $U_p$  and current  $I_p$  are related to the secondary voltage  $U_s$  and current  $I_s$  through the transfer admittance matrix of the two winding transformer is defined by equation (3.7). In the alternating current (AC) network,  $T$ ,  $N$ ,  $U$ , and  $I$  are all complex variables.

$$\begin{bmatrix} I_p \\ I_s \end{bmatrix} = \begin{bmatrix} G_{pp} & G_{ps} \\ G_{sp} & G_{ss} \end{bmatrix} + j \begin{bmatrix} B_{pp} & B_{ps} \\ B_{sp} & B_{ss} \end{bmatrix} \begin{bmatrix} U_p \\ U_s \end{bmatrix} \quad (3.7)$$

Where

$$G_{pp} = \frac{F_1(N_v^2 + R_1) + F_2R_2}{F_1^2 + F_2^2}$$

$$B_{pp} = \frac{F_1R_2 - F_2(N_v^2 + R_1)}{F_1^2 + F_2^2}$$

$$G_{ss} = \frac{F_1(T_v^2 + R_3) + F_2R_4}{F_1^2 + F_2^2}$$

$$B_{ss} = \frac{F_1R_4 - F_2(T_v^2 + R_3)}{F_1^2 + F_2^2}$$

$$G_{ps} = \frac{-T_vN_v(F_1 \cos(\phi_1) + F_2 \sin(\phi_1))}{F_1^2 + F_2^2}$$

$$B_{ps} = \frac{T_vN_v(F_2 \cos(\phi_1) + F_1 \sin(\phi_1))}{F_1^2 + F_2^2}$$

$$G_{sp} = \frac{-T_vN_v(F_1 \cos(\phi_2) + F_2 \sin(\phi_2))}{F_1^2 + F_2^2}$$

$$B_{sp} = \frac{T_vN_v(F_2 \cos(\phi_2) + F_1 \sin(\phi_2))}{F_1^2 + F_2^2}$$

$$F_1 = T_v^2R_s + N_v^2R_p + R_{eq1}$$

$$F_2 = T_v^2X_s + N_v^2X_p + X_{eq1}$$

$$R_{eq1} = (R_pR_s - X_pX_s)G_0 - (R_pX_s - R_sX_p)B_0$$

$$X_{eq1} = (R_pR_s - X_pX_s)B_0 + (R_pX_s - R_sX_p)G_0$$

$$R_1 = R_sG_0 - X_sB_0$$

$$R_2 = R_sB_0 - X_sG_0$$

$$R_3 = R_pG_0 - X_pB_0$$

$$R_4 = R_pB_0 - X_pG_0$$

$$\phi_1 = \phi_{tv} - \phi_{nv}$$

$$\phi_2 = \phi_{nv} - \phi_{tv}$$

### 3.1.5 Transmission Line

A transmission line is used to transfer electric energy from generating units at various locations to the distribution units which ultimately supply the load. It transmits the wave of voltage and current from sending end to receiving end. The transmission line is characterized by series resistance, series inductance, shunt conductance, and shunt capacitance. Figure 3.4 displays the  $\pi$  equivalent model of the transmission line.

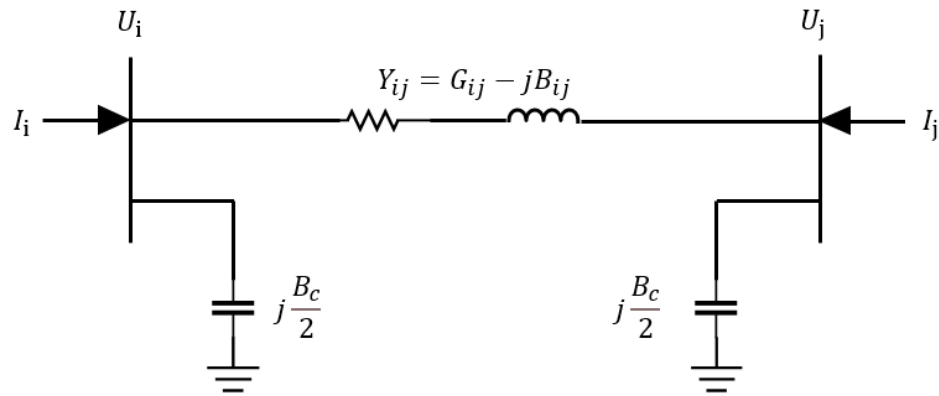


Figure 3.4 Equivalent circuit of the transmission line

Let  $I_i$  and  $U_i$  denote the injection current and the voltage at bus  $i$ . The series resistance, series inductance, and shunt susceptance are indicated as  $R$ ,  $L$ , and  $B_c$ , respectively. The relation of the current and the voltage is presented in equation (3.8) in the form of the bus admittance matrix.

$$\begin{bmatrix} I_i \\ I_j \end{bmatrix} = \begin{bmatrix} Y_{ii} & Y_{ij} \\ Y_{ji} & Y_{jj} \end{bmatrix} \begin{bmatrix} U_i \\ U_j \end{bmatrix} \quad (3.8)$$

Where

$$Y_{ii} = Y_{jj} = \left( y_{ij} + j \frac{B_c}{2} \right) = G_{ii} - jB_{ii}$$

$$Y_{ij} = Y_{ji} = -y_{ij} = G_{ij} - jB_{ij}$$

$$G_{ij} = \frac{R}{R^2 + (\omega L)^2}$$

$$B_{ij} = \frac{\omega L}{R^2 + (\omega L)^2}$$

The power injection at bus  $i$  through the transmission component connected between bus  $i$  and  $j$  is explained as follows.

$$S_i = U_i I_i^* \quad (3.9)$$

$$I_i = Y_{ii} U_i + Y_{ij} U_j \quad (3.10)$$

Therefore, equation (3.9) can be reformulated as

$$S_i = U_i (Y_{ii} U_i + Y_{ij} U_j)^* \quad (3.11)$$

Moreover, the power injection can be presented in the form of the active and reactive power at bus  $i$  as follows.

$$S_i = P_i + jQ_i \quad (3.12)$$

The Euler identity is applied to the voltage at bus  $i$  and bus  $j$  in equation (3.11). Then, the complex power injection is separated into real and imaginary parts as in equation (3.13)–(3.14).

$$P_i = U_i^2 G_{ii} - U_i U_j [G_{ij} \cos(\theta_i - \theta_j) + B_{ij} \sin(\theta_i - \theta_j)] \quad (3.13)$$

$$Q_i = U_i^2 B_{ii} + U_i U_j [G_{ij} \sin(\theta_i - \theta_j) - B_{ij} \cos(\theta_i - \theta_j)] - j \frac{B_c}{2} U_i^2 \quad (3.14)$$

Where  $\theta_i$  is voltage angle at bus  $i$ .

### 3.2 Conventional Alternating Current Optimal Power Flow Problem

The alternating current optimal power flow (ACOPF) problem is concerned with determining a steady state optimal operating point of an alternating current (AC) in the power system. The ACOPF problem minimizes a certain objective function such as generation cost or power loss subject to network and physical constraints. From [6], [32], and [40], the general ACOPF problem can be stated as follows.

$$\text{Minimize } f(x) \quad (3.15)$$

$$\text{Subject to } g(x) = 0 \quad (3.16)$$

$$h(x) \leq 0 \quad (3.17)$$

$$x_{lb} \leq x \leq x_{ub} \quad (3.18)$$

Where  $f(x)$  is the objective function.

$x$  is variable of the power system which encloses voltage magnitude, voltage angle, power generation and power demand.

$g(x)$  are the equality constraints which are power flow equations and control equations.

$h(x)$  are the inequality constraints which are transmission line flow limit.

$x_{lb}$  are lower limit of the variables.

$x_{ub}$  are upper limit of the variables.

Equation (3.14)–(3.17) can be summarized as minimizing the value of the objective function when the equality and inequality constraints are satisfied.

This part is organized by the objective function, the equality constraints, and the inequality constraints.

### 3.2.1 Objective Function

The objective function of the ACOF problem in this study focuses on transmission power loss minimization. The transmission power loss can be determined with the difference in the power generated and the power demand. Furthermore, the total transmission power loss can be also formulated with the sum of power injection at bus  $i$ . However, the total transmission power loss is mostly concerned with the active power only, so the objective function can be represented as below.

$$F = \sum_{i=1}^N \sum_{j=1}^N G_{ij} [U_i^2 + U_j^2 - 2U_i U_j \cos(\theta_i - \theta_j)] \quad i \in N, i, j \in E \quad (3.19)$$

Where  $G_{ij}$  is conductance on branch  $ij$ .

$U_i$  is voltage magnitude at bus  $i$ .

$\theta_i$  is voltage angel at bus  $i$ .

$i$  is from bus.

$j$  is to bus and not equal to from bus.

$N$  is total number of bus.

$E$  is total number of branch.

### 3.2.2 Equality Constraints

The equality constraints are the power balance equation which is formulated from the Kirchhoff law and the power flow equations. The power balance of the power system must be satisfied in order to represent the steady state. Let  $\mathbf{a}^*$  denote the conjugate form of  $\mathbf{a}$ . The power balance equation is as follows.

$$S_i = (\sum P_{gi} - \sum P_{di}) + j(\sum Q_{gi} - \sum Q_{di}) \quad i \in N \quad (3.20)$$

$$S_i = \sum_{j \sim i} S_{ij} \quad i \in N, i, j \in E \quad (3.21)$$

$$S_{ij} = U_i I_{ij}^* \quad i \in N, i, j \in E \quad (3.22)$$

$$I_{ij} = (U_i - U_j)Y_{ij} + j\frac{B_c}{2}U_i \quad i \in N, i, j \in E \quad (3.23)$$

Where  $S_i$  is complex power at bus  $i$ .

$\sum P_{gi}$  is the sum of active power generated at bus  $i$ .

$\sum P_{di}$  is the sum of active power demand at bus  $i$ .

$\sum Q_{gi}$  is the sum of reactive power generated at bus  $i$ .

$\sum Q_{di}$  is the sum of reactive power demand at bus  $i$ .

$S_{ij}$  is complex branch flow from bus  $i$  to bus  $j$ .

$I_{ij}$  is current from bus  $i$  to bus  $j$ .

$Y_{ij}$  is admittance on branch  $ij$ .

Equation (3.22) indicates the relations of the bus voltage, the current, and the complex power flow according to equation (3.9). Equation (3.23) shows the Kirchhoff law which explains the relations between the current and the voltage difference of the branch according to the model in Figure 3.4.

The complex power in equation (3.22) can be separated into the active and reactive power according to equation (3.13)–(3.14). The power flow equations can be represented as follows.

$$S_{ij} = P_{ij} + jQ_{ij} \quad i, j \in E \quad (3.24)$$

$$P_{ij} = G_{ij}U_i^2 - G_{ij}U_iU_j \cos(\theta_{ij}) + B_{ij}U_iU_j \sin(\theta_{ij}) \quad i \in N, i, j \in E \quad (3.25)$$

$$Q_{ij} = B_{ij}U_i^2 - B_{ij}U_iU_j \cos(\theta_{ij}) - G_{ij}U_iU_j \sin(\theta_{ij}) - \frac{B_c}{2}U_i^2 \quad i \in N, i, j \in E \quad (3.26)$$

Where  $P_{ij}$  is active power flow on branch  $ij$ .

$Q_{ij}$  is reactive power flow on branch  $ij$ .

$B_{ij}$  is susceptance on branch  $ij$ .

$\theta_{ij}$  is  $\theta_i - \theta_j$ .

### 3.2.3 Inequality Constraints

The inequality constraints are considered to assure the safe and stable operation of the power system. The inequality constraints include the bus voltage limit and the capacity of active and reactive power generation limit. In the stable operation, the bus voltage should not fluctuate much, so the bus voltage limit is typically  $\pm 5\%$  within the base voltage. The inequality constraints are shown as follows.

$$P_{gi,min} \leq P_{gi} \leq P_{gi,max} \quad i \in N \quad (3.27)$$

$$Q_{gi,min} \leq Q_{gi} \leq Q_{gi,max} \quad i \in N \quad (3.28)$$

$$U_{i,min} \leq U_i \leq U_{i,max} \quad i \in N \quad (3.29)$$

Where  $P_{gi,min}$  is the lower bound of the active power generation at bus  $i$ .

$P_{gi,max}$  is the upper bound of the active power generation at bus  $i$ .

$Q_{gi,min}$  is the lower bound of the reactive power generation at bus  $i$ .

$Q_{gi,max}$  is the upper bound of the reactive power generation at bus  $i$ .

$U_{i,min}$  is the lower bound of the voltage at bus  $i$ .

$U_{i,max}$  is the upper bound of the voltage at bus  $i$ .

All the above inequality constraints are for the PQ bus and the PV bus. For the slack bus, the active and reactive power generation are not limited. Moreover, the voltage is fixed so the lower and upper bounds are equivalent to the voltage at the slack bus.

The inequality constraints also include the limit on power transmission line between bus  $i$  to bus  $j$  which can be manifested as follows.

$$|S_{ij}| \leq S_{ij,max} \quad i, j \in E \quad (3.30)$$

$$|S_{ji}| \leq S_{ij,max} \quad i, j \in E \quad (3.31)$$

Where  $S_{ij,max}$  is the upper bound of the complex power in the branch  $ij$ .



## CHAPTER 4

### Power Loss Minimization with SOCP relaxation

The conventional alternating current optimal power flow (ACOPF) problem is a nonconvex problem from a nonlinear objective function and nonlinear constraints that is difficult to find the global optimal solution. Therefore, the ACOPF problem is computationally intractable in practice. To reduce the complexity of the computation, the ACOPF problem is transformed into a convex optimization format. In this chapter, second order cone program (SOCP) relaxation is applied to minimize total power loss in the ACOPF problem. The proposed method can obtain the global optimal solution within polynomial time. This chapter consists of 4 parts. The first part describes the convex optimization problem and the convex relaxation. The second part explains the SOCP format. The third part illustrates SOCP relaxation which is applied to the ACOPF problem for power loss minimization. The last part presents the flowchart of the ACOPF computational algorithm.

#### 4.1 Convex Optimization

Convex optimization is a special class of mathematical optimization problem which has applications in a wide range of disciplines. There are many advantages to formulate a problem as a convex optimization problem, for instance the problem can be solved efficiently and reliably. Moreover, convex optimization can interpret the original problem to obtain an efficient method for solving the problem. Affine set, convex set, and convex function must be also considered to determine a convex optimization problem [41]–[42].

Suppose  $x_1 \neq x_2$  are 2 points in  $\mathbb{R}^n$ . The line passing through  $x_1$  and  $x_2$  can be indicated as

$$y = \theta x_1 + (1 - \theta)x_2, \quad (4.1)$$

where  $\theta \in \mathbb{R}$ . The line can be displayed as Figure 4.1.

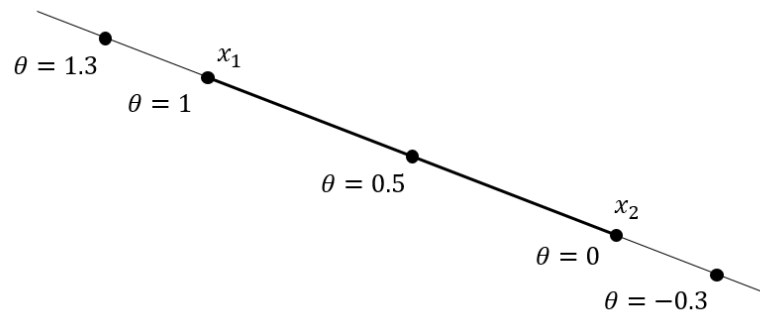


Figure 4.1 The line passing through  $x_1$  and  $x_2$

A set  $C$  is affine if it contains the line through any 2 distinct points in the set, i.e., for any  $x_1, x_2 \in C$  and  $\theta \in \mathbb{R}$  then  $\theta x_1 + (1 - \theta)x_2 \in C$ . However, a set  $C$  is convex if it contains line segment between any 2 points in the set, i.e., for any  $x_1, x_2 \in C$  and any  $\theta$  with  $0 \leq \theta \leq 1$  then  $\theta x_1 + (1 - \theta)x_2 \in C$ . Accordingly, every affine set is also convex because it contains the whole line between any two distinct points, and also the line segment between the points. Figure 4.2 shows the example of simple convex and nonconvex set.

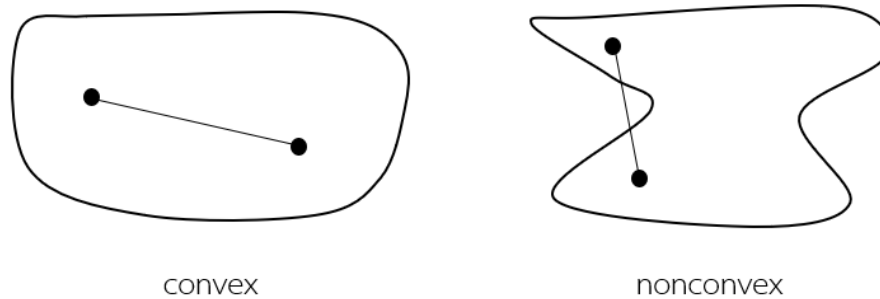


Figure 4.2 Convex and nonconvex sets

A function  $f : \mathbb{R}^n \rightarrow \mathbb{R}$  is convex if the domain of the function  $f$  ( $\text{dom } f$ ) is a convex set and if for all  $x, y \in \text{dom } f$ , and  $\theta$  where  $0 \leq \theta \leq 1$  then

$$f(\theta x + (1 - \theta)y) \leq \theta f(x) + (1 - \theta)f(y). \quad (4.2)$$

From equation (4.2), the inequality means that the line segment between  $(x, f(x))$  and  $(y, f(y))$  lies above the graph of  $f$ . Moreover, the line segment is also the chord from  $x$  to  $y$ . Graph of convex function is demonstrated in Figure 4.3.

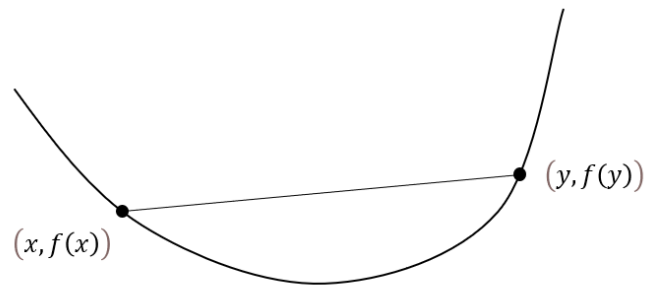


Figure 4.3 Graph of a convex function

From all above, the convex optimization can be written in standard form as

$$\text{minimize } f_0(x) \quad (4.3)$$

$$\text{subject to } f_i(x) \leq 0, \quad i = 1, \dots, m, \quad (4.4)$$

$$a_i^T x = b_i, \quad i = 1, \dots, p, \quad (4.5)$$

where  $f_0, \dots, f_m$  are convex function. There are 3 requirements of the convex problem. The first, the objective function must be convex. The second, the inequality constraint functions must be convex. The last, the equality constraint functions must be affine. Besides, there has an important property which is the feasible set of a convex optimization problem is convex. Consequently, a convex objective function is minimized over a convex set in a convex optimization problem which means they satisfy the equation (4.2). The problem may have zero, one, or many solutions but there is only one optimal solution, which is globally optimal.

Global optimal solution is the solution of an optimization problem that is the most optimal among all feasible solutions whereas a local optimal solution is a solution that is optimal within a neighboring set of feasible solutions. The concept of local optimal solution and the global optimal solution is illustrated in Figure 4.4.

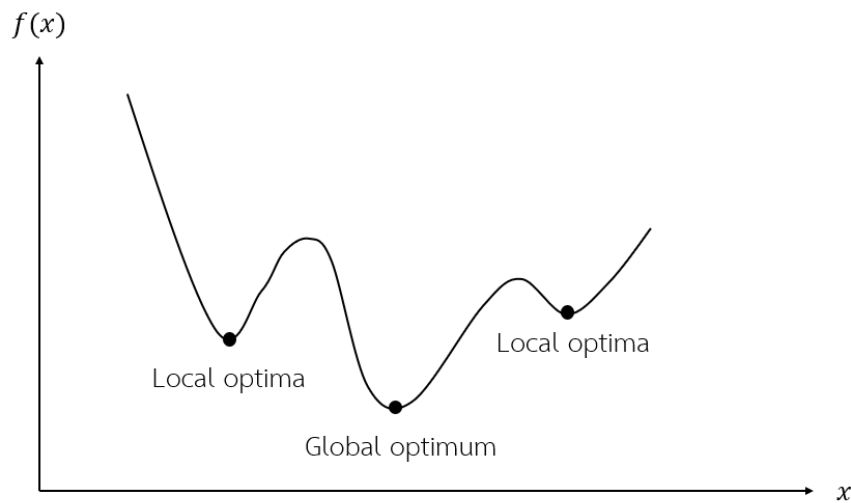


Figure 4.4 Local optimal solution and global optimal solution

In a convex optimization problem, there is only one optimal solution, so any locally optimal point is also globally optimal. On the other hand, a nonconvex problem has many optimal solutions which are local optima and global optimum. Therefore, a convex optimization problem is more efficient to find the true global solution than a nonconvex problem.

Many problems are nonconvex problems, such as matrix completion, deep neural networks, or principal component analysis. The power flow equation is also one of the nonconvex optimization problems. In order to convexify the nonconvex problem, relaxation, and approximation are applied [7].

Approximation is an approximate representation of the feasible space. The feasible space is the space where all variable assignments satisfying all problem constraints. Approximations simplify the nonconvex problem by using assumptions regarding certain quantities. A convex approximation can closely display the behavior of the problem when the relevant ascriptions are exact. Moreover, many convex approximation problems are reasonably accurate for problem constraints. However, the approximation may not contain all feasible points and may also contain points that are not feasible.

A relaxation is an extension of the feasible space which contains all feasible points. Relaxation encircles the nonconvex feasible spaces in a larger space. Therefore, relaxation can be nonconvex, nonlinear, or linear. However, the larger space is typically considered as convex to determine the problem as convex optimization problems.

The conceptual examples of the relaxation and the approximation of a nonconvex feasible space are shown in Figure 4.5.

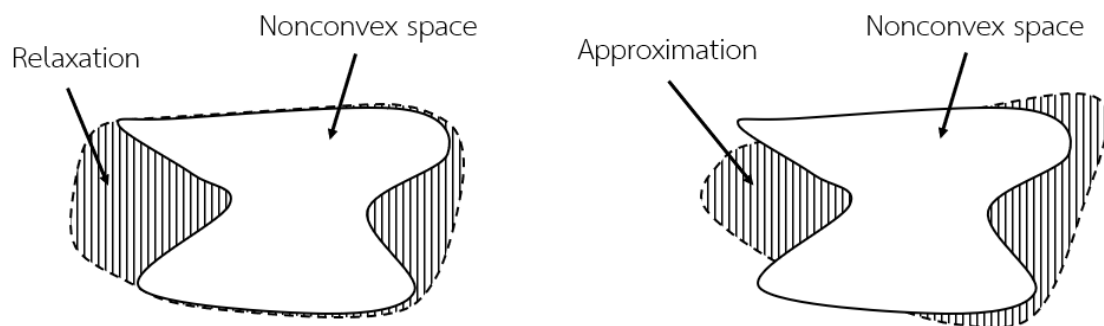


Figure 4.5 Concept of a convex relaxation and a convex approximation

Optimization problems that use convex relaxations provide bounds on the optimal objective value for the original nonconvex problem. Moreover, sufficient conditions for certifying problem infeasibility are also obtained. Some convex relaxations provide global optima for limited classes of power system optimization problems which can be guaranteed by related sufficient conditions. In contrast, any of the above theoretical guarantees which is obtained by relaxation are not obtained from approximations.

In this study, the relaxation of the ACOPF problem is only considered due to the mathematical guarantees. Moreover, relaxations are superior to approximations because relaxations can provide bounds on true optima.

## 4.2 Second Order Cone Programming

A second order cone program (SOCP) is the class of convex optimization problem which is closely related to quadratic programming [41]–[42]. The SOCP problem includes linear and quadratic programming. The objective function which is a linear function is minimized subject to linear constraints and the intersection of an affine set and the product of second order (quadratic) cones. The standard form of the SOCP problem is shown as

$$\text{minimize} \quad f^T x \quad (4.6)$$

$$\text{subject to} \quad \|A_i x + b_i\|_2 \leq c_i^T x + d_i, \quad i = 1, \dots, m \quad (4.7)$$

$$F x = g, \quad (4.8)$$

where  $x \in \mathbb{R}^n$  is the optimization variable. The problem parameters are  $f \in \mathbb{R}^n$ ,  $A_i \in \mathbb{R}^{n_i \times n}$ ,  $b_i \in \mathbb{R}^{n_i}$ ,  $c_i \in \mathbb{R}^n$ ,  $d_i \in \mathbb{R}$ ,  $F \in \mathbb{R}^{p \times n}$ , and  $g \in \mathbb{R}^p$ . The norm  $\|x\|_2$  in the constraints is the Euclidean norm and  $c_i^T$  denotes the transpose of  $c_i$ .

A constraint in equation (4.8) is called a second order cone constraint which is represented as

$$\|Ax + b\|_2 \leq c^T x + d, \quad (4.9)$$

where  $A \in \mathbb{R}^{k \times n}$ . The second order cone constraint in SOCP arises from the constraints which are the same as requiring the affine function  $(Ax + b, c^T x + d)$  to lie in the second-order cone in  $\mathbb{R}^{k+1}$ .

To demonstrate the convexity of SOCP, the standard second order (convex) cone of dimension is determined as follows.

$$\mathcal{C}_k = \left\{ \begin{bmatrix} u \\ t \end{bmatrix} \mid u \in \mathbb{R}^{k-1}, t \in \mathbb{R}, \|u\| \leq t \right\}$$

For  $k = 1$ , the unit second order cone as

$$\mathcal{C}_1 = \{t \mid t \in \mathbb{R}, 0 \leq t\}.$$

The set of points satisfying a second order cone constraint is the inverse image of the unit second order cone under an affine mapping as below.

$$\|A_i x + b_i\|_2 \leq c_i^T x + d_i \Leftrightarrow \begin{bmatrix} A_i \\ c_i^T \end{bmatrix} x + \begin{bmatrix} b_i \\ d_i \end{bmatrix} \in \mathcal{C}_n$$

Therefore, the SOCP in equation (4.5)–(4.7) is a convex programming problem with the convexity of the objective function and constraints.

Second order cone constraints can be employed to represent many general convex constraints. For instance, when  $A_i = \mathbf{0}$ ,  $i = 1, \dots, m$ , then the SOCP reduces to a general linear program (LP). Similarly, when  $c_i = \mathbf{0}$ ,  $i = 1, \dots, m$ , the SOCP equivalent to a quadratically constrained quadratic program (QCQP). The SOCP is more general than LP, QCQP, and other nonlinear convex optimization problems. Accordingly, many nonlinear convex optimization problems can be reformulated from SOCP. Additionally, a variety of engineering problems can be formulated as second order cone problems to solve more complicated problems. In this research, the SOCP is only focused to apply in the ACOPF problem.

### 4.3 Alternating Current Optimal Power Flow with SOCP Relaxation

In this part, the power system model is exploited to reformulate the power flow equations. Moreover, SOCP relaxation is applied to the traditional ACOPF problem. The proposed ACOPF for power loss minimization is solved through 2 steps. In the first step, the conventional power flow constraints are reformulated by reformulating the power flow equations with new variables. In the second step, SOCP relaxation relaxes the nonconvex equations into convex format. The structure of this method is predicated in Figure 4.6.

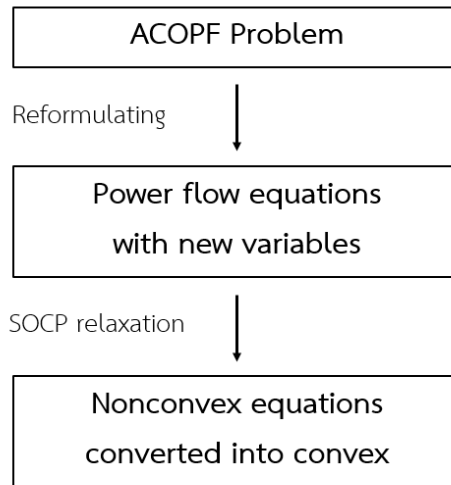


Figure 4.6 SOCP relaxation structure

#### 4.3.1 Reformulating the Power Flow Equations

In order to reformulate the conventional power flow equation, the new variables are introduced by exploiting the network structure. Let  $\mathbf{a}^*$  denote the conjugate form of  $\mathbf{a}$ . The power flow equation is presented as follows.

$$S_{ij} = U_i I_{ij}^* \quad i \in N, i, j \in E \quad (4.10)$$

$$S_{ji} = U_j I_{ji}^* \quad i \in N, i, j \in E \quad (4.11)$$

$$I_{ij} = -I_{ji} \quad i, j \in E \quad (4.12)$$

$$I_{ij} = (U_i - U_j)Y_{ij} + j\frac{B_c}{2}U_i \quad i \in N, i, j \in E \quad (4.13)$$

$$I_{ji} = (U_j - U_i)Y_{ij} + j\frac{B_c}{2}U_j \quad i \in N, i, j \in E \quad (4.14)$$

Where  $S_{ij}$  is complex power flow from bus  $i$  to bus  $j$ .

$U_i$  is voltage at bus  $i$ .

$I_{ij}$  is current from bus  $i$  to bus  $j$ .

$Y_{ij}$  is admittance on branch  $ij$ .

$B_c$  is shunt susceptance.



From the transmission line model in Figure 3.4, the variables  $S_{ij}$  and  $S_{ji}$  are introduced at the same time for a branch  $ij$ . The power loss of the branch  $ij$  can be imposed by the sum of  $S_{ij}$  and  $S_{ji}$ . Although  $I_{ij}$  equals to  $-I_{ji}$  from equation (4.12), the complex power  $S_{ij}$  is not equal to  $-S_{ji}$  thanks to the voltage difference. The power flow formulation can be reformulated by eliminating the current  $I_{ij}$  and  $I_{ji}$  as below.

$$S_{ij} = Y_{ij}^* U_i U_i^* - Y_{ij}^* U_i U_j^* - j \frac{B_c}{2} U_i U_i^* \quad (4.15)$$

$$S_{ji} = Y_{ij}^* U_j U_j^* - Y_{ij}^* U_j U_i^* - j \frac{B_c}{2} U_j U_j^* \quad (4.16)$$

From the complex number property, the product of a complex conjugate pair is a positive real number. Therefore, the new variables are defined in terms of the bus voltage as follows.

$$V_i = U_i U_i^* \quad i \in N \quad (4.17)$$

$$V_{ij} = U_i U_j^* \quad i \in N, i, j \in E \quad (4.18)$$

$$V_{ij} = V_{ji}^* \quad i, j \in E \quad (4.19)$$

Where  $V_i \in \mathbb{R}$  and  $V_i \geq 0$ ,  $V_{ij} \in \mathbb{C}$ .

The power flow equations can be rewritten by the new variables as follows.

$$S_{ij} = Y_{ij}^* V_i - Y_{ij}^* V_{ij} - j \frac{B_c}{2} V_i \quad (4.20)$$

$$S_{ji} = Y_{ij}^* V_j - Y_{ij}^* V_{ij}^* - j \frac{B_c}{2} V_j \quad (4.21)$$

From all above, the relation between the bus voltage and the branch voltage can be displayed as below.

$$|V_{ij}|^2 = V_i V_j \quad (4.22)$$

Since  $V_{ij}$  is the complex number, the real and imaginary part of  $V_{ij}$  is defined as new variables  $a_{ij}$  and  $b_{ij}$ , respectively.  $V_{ij}$  can be represented as

$$V_{ij} = a_{ij} + jb_{ij}. \quad (4.23)$$

Then, equation (4.22) can be illustrated as follows.

$$a_{ij}^2 + b_{ij}^2 = V_i V_j \quad (4.24)$$

Equation (4.20)–(4.21) are the new power flow equation that eliminates the current term and indicates the new voltage variables in each branch of the power system topology. Therefore, equation (3.22)–(3.23) are replaced with new variables and a new format.

From the convex optimization problem, the objective function and the inequality constraints must be convex. Moreover, the equality constraints must be affine. Both  $S_{ij}$  and  $S_{ji}$  in equation (4.20)–(4.21) are the general affine function depending on the variables  $V_i$ ,  $V_j$  and  $V_{ij}$  where  $V_{ij}^*$  is the constant. When combining the 2 equations together, the affine functions disappear owing to the nonaffine relation between  $V_{ij}$  and  $V_{ij}^*$ .

In order to modify the equality constraints to be affine,  $V_{ij}$  and  $V_{ij}^*$  are replaced by  $a_{ij}$  and  $b_{ij}$ . Then, the complex power  $S_{ij}$  and  $S_{ji}$  are decoupled into the active and reactive power. Hence, the complex problem is a real convex problem. From equation (3.25)–(3.26), the power flow equations are represented as follows.

$$P_{ij} = G_{ij}(V_i - a_{ij}) + B_{ij}b_{ij} \quad (4.25)$$

$$P_{ji} = G_{ij}(V_j - a_{ij}) - B_{ij}b_{ij} \quad (4.26)$$

$$Q_{ij} = -G_{ij}b_{ij} + B_{ij}(V_i - a_{ij}) - \frac{B_c}{2}V_i \quad (4.27)$$

$$Q_{ji} = G_{ij}b_{ij} + B_{ij}(V_j - a_{ij}) - \frac{B_c}{2}V_j \quad (4.28)$$

Where  $P_{ij}$  is active power flow on branch  $ij$ .

$Q_{ij}$  is reactive power flow on branch  $ij$ .

$G_{ij}$  is conductance on branch  $ij$ .

$B_{ij}$  is susceptance on branch  $ij$ .

Equation (4.25)–(4.28) are totally linear and convex in simple form. Furthermore, all the variables are in real format. Accordingly, the active and reactive power flow on branch  $ij$  are only considered with  $V_i, V_j, a_{ij}$ , and  $b_{ij}$ .

From all the above mentioned, the power balance equations which are the equality constraints can be represented as follows.

$$\sum_{j \sim i} S_{ij} = (\sum P_{gi} - \sum P_{di}) + j(\sum Q_{gi} - \sum Q_{di}) \quad (4.29)$$

$$\sum_{j \sim i} P_{ij} = \sum P_{gi} - \sum P_{di} \quad (4.30)$$

$$\sum_{j \sim i} Q_{ij} = \sum Q_{gi} - \sum Q_{di} \quad (4.31)$$

Where  $P_{gi}$  is active power generated at bus  $i$ .

$P_{di}$  is active power demand at bus  $i$ .

$Q_{gi}$  is reactive power generated at bus  $i$ .

$Q_{di}$  is reactive power demand at bus  $i$ .

Since the power flow equations are modified, the objective function for power loss minimization must be reformulated. The total power loss is mostly considered the active power only, so the objective function can be represented as follows.

$$F = \sum P_{loss} \quad (4.32)$$

$$\sum P_{loss} = \sum P_{ij} + \sum P_{ji} \quad (4.33)$$

$$\sum P_{loss} = \sum G_{ij}(V_i + V_j - 2a_{ij}) \quad (4.34)$$

For the inequality constraints, the voltage constraint in equation (3.29) must be reformulated as below.

$$U_{i,min}^2 \leq V_i \leq U_{i,max}^2 \quad (4.35)$$

$$V_i = U_{ref}^2 \quad (4.36)$$

Where  $U_{ref}$  is reference voltage at the slack bus.

Moreover, the limit of  $a_{ij}$  must be considered. Since the value of  $a_{ij}$  is greater than the value of  $b_{ij}$ , the limit of  $a_{ij}$  is only considered. The  $a_{ij}$  constraints are determined as below.

$$U_{i,min}U_{j,min} \leq a_{ij} \leq U_{i,max}U_{j,max} \quad (4.37)$$

### 4.3.2 SOCP Relaxation

To consider the ACOPF problem as a convex optimization problem, SOCP relaxation is applied to the quadratic equation which is not affine. Equation (4.24) is the nonconvex quadratic equality constraint. The relaxation of the sign of equality into the sign of inequality in equation (4.24) can transform the quadratic equation into a rotating cone. The SOCP relaxation is as below.

$$a_{ij}^2 + b_{ij}^2 \leq V_i V_j \quad (4.38)$$

Equation (4.38) can be written as

$$(2a_{ij})^2 + (2b_{ij})^2 + (V_i - V_j)^2 \leq (V_i + V_j)^2. \quad (4.39)$$

Equation (4.38) can be presented as a cone in a 2-norm form as follows.

$$\left\| \begin{array}{c} 2a_{ij} \\ 2b_{ij} \\ V_i - V_j \end{array} \right\|_2 \leq V_i + V_j \quad (4.40)$$

Equation (4.38) is the inequality constraint in conic format. Therefore, the ACOPF problem is a convex optimization problem that can be computed more tractable.

### 4.3.3 ACOPF Formulation

After 2 steps of relaxation, the conventional ACOPF problem which is a nonlinear and nonconvex problem is converted to the proposed ACOPF problem with convex objective function and constraints. The proposed ACOPF problem can be summarized as follows.

$$\begin{aligned}
 &\text{Minimize} && \sum G_{ij}(V_i + V_j - 2a_{ij}) \\
 &\text{Subject to} && \sum_{j \sim i} P_{ij} = \sum P_{gi} - \sum P_{di} \\
 &&& \sum_{j \sim i} Q_{ij} = \sum Q_{gi} - \sum Q_{di} \\
 &&& P_{ij} = G_{ij}(V_i - a_{ij}) + B_{ij}b_{ij} \\
 &&& P_{ji} = G_{ij}(V_j - a_{ij}) - B_{ij}b_{ij} \\
 &&& Q_{ij} = -G_{ij}b_{ij} + B_{ij}(V_i - a_{ij}) - \frac{B_c}{2}V_i \\
 &&& Q_{ji} = G_{ij}b_{ij} + B_{ij}(V_j - a_{ij}) - \frac{B_c}{2}V_j \\
 &&& \left\| \begin{array}{l} 2a_{ij} \\ 2b_{ij} \\ V_i - V_j \end{array} \right\|_2 \leq V_i + V_j \\
 &&& P_{ij}^2 + Q_{ij}^2 \leq S_{ij,max}^2 \\
 &&& P_{ji}^2 + Q_{ji}^2 \leq S_{ij,max}^2 \\
 &&& P_{gi,min} \leq P_{gi} \leq P_{gi,max} \\
 &&& Q_{gi,min} \leq Q_{gi} \leq Q_{gi,max} \\
 &&& U_{i,min}^2 \leq V_i \leq U_{i,max}^2 \\
 &&& U_{i,min}U_{j,min} \leq a_{ij} \leq U_{i,max}U_{j,max}
 \end{aligned}$$

From the ACOPF formulation,  $P_{gi}$ ,  $Q_{gi}$ ,  $V_i$ ,  $a_{ij}$ , and  $b_{ij}$  are variables while  $P_{ij}$ ,  $P_{ji}$ ,  $Q_{ij}$ , and  $Q_{ji}$  are just the intermediate variables. All the variables are real numbers. In addition, the objective function and the inequality constraints are convex. The equality constraints are affine.

#### 4.4 Exactness of the Relaxation

To guarantee the correctness of the solution, the final result of the relaxation must exist within the boundary of the cone. The relaxation is exact if the optimal solution is obtained from the problem when changing the inequal sign to the equal sign in equation (4.40). Moreover, the relaxation is exact if there is no upper bound on  $P_{d,max}$  and  $Q_{d,max}$ .

To describe the exactness, branch  $kl$  is introduced where  $k$  is from bus and  $l$  is to bus.  $V_i, V_j, a_{ij}$ , and  $b_{ij}$  which are a group of optimal solutions are obtained from the relaxation problem. The exact solutions on branch  $ij$  are obtained where  $i, j \neq 0$  except the branch  $kl$ . That is,  $\{i, j\} \cap \{k, l\} \neq \emptyset$  and

$$a_{ij}^2 + b_{ij}^2 = V_i V_j \quad \{i, j\} \neq \{k, l\}, \quad (4.41)$$

$$a_{ij}^2 + b_{ij}^2 < V_i V_j \quad \{i, j\} = \{k, l\}. \quad (4.42)$$

On branch  $kl$ , new variables are indicated as follows.

$$a_{kl}^H = \sqrt{V_k V_l - b_{kl}} \quad (4.43)$$

$$b_{kl}^H = b_{kl} \quad (4.44)$$

$$V_k^H = V_k \quad (4.45)$$

$$V_l^H = V_l \quad (4.46)$$

The power flow equations in equation (4.25)–(4.28) are rewritten with the following variables as

$$P_{kl}^H = G_{kl}(V_k^H - a_{kl}^H) + B_{kl}b_{kl}^H, \quad (4.47)$$

$$P_{lk}^H = G_{kl}(V_l^H - a_{kl}^H) - B_{kl}b_{kl}^H, \quad (4.48)$$

$$Q_{kl}^H = -G_{kl}b_{kl}^H + B_{kl}(V_k^H - a_{kl}^H) - \frac{B_c}{2}V_k^H, \quad (4.49)$$

$$Q_{lk}^H = G_{kl}b_{kl}^H + B_{kl}(V_l^H - a_{kl}^H) - \frac{B_c}{2}V_l^H. \quad (4.50)$$

Since  $a_{kl}^2 + b_{kl}^2 < V_k V_l$ ,  $a_{kl}^H$  is greater than  $a_{kl}$ . Then

$$P_{kl}^H - P_{kl} = G_{kl}(a_{kl}^H - a_{kl}), \quad (4.51)$$

$$G_{kl}(a_{kl}^H - a_{kl}) < 0, \quad (4.52)$$

$$Q_{kl}^H - Q_{kl} = B_{kl}(a_{kl}^H - a_{kl}), \quad (4.53)$$

$$B_{kl}(a_{kl}^H - a_{kl}) < 0, \quad (4.54)$$

The difference of the active and reactive power flow on branch  $kl$  are shown in equation (4.51) and (4.53). From the power balance equation, the active power at bus  $k$  can be determined as

$$\begin{aligned} \sum P_{gk}^H - \sum P_{dk}^H &= P_{kl}^H + \sum_{kH \sim i} P_{ki}^H \\ \sum P_{gk}^H - \sum P_{dk}^H &= P_{kl}^H + \sum_{kH \sim i} P_{ki} \end{aligned} \quad (4.55)$$

$$P_{kl}^H + \sum_{kH \sim i} P_{ki} < \sum P_{gk} - \sum P_{dk}$$

Similarly, the active power at bus  $l$  can be represented as

$$\begin{aligned} \sum P_{gl}^H - \sum P_{dl}^H &= P_{lk}^H + \sum_{lH \sim i} P_{li}^H \\ \sum P_{gl}^H - \sum P_{dl}^H &= P_{lk}^H + \sum_{lH \sim i} P_{li} \end{aligned} \quad (4.56)$$

$$P_{lk}^H + \sum_{lH \sim i} P_{li} < \sum P_{gl} - \sum P_{dl}$$

For the reactive power, the reactive power at bus  $k$  can be indicated as

$$\begin{aligned} \sum Q_{gk}^H - \sum Q_{dk}^H &= Q_{kl}^H + \sum_{kH \sim i} Q_{ki}^H \\ \sum Q_{gk}^H - \sum Q_{dk}^H &= Q_{kl}^H + \sum_{kH \sim i} Q_{ki} \end{aligned} \quad (4.57)$$

$$Q_{kl}^H + \sum_{kH \sim i} Q_{ki} < \sum Q_{gk} - \sum Q_{dk}$$

Similarly, the reactive power at bus  $l$  can be represented as

$$\begin{aligned}\Sigma Q_{gl}^H - \Sigma Q_{dl}^H &= Q_{lk}^H + \Sigma_{lH \sim i} Q_{li}^H \\ \Sigma Q_{gl}^H - \Sigma Q_{dl}^H &= Q_{lk}^H + \Sigma_{lH \sim i} Q_{li} \\ Q_{lk}^H + \Sigma_{lH \sim i} Q_{ki} &< \Sigma Q_{gl} - \Sigma Q_{dl}\end{aligned}\tag{4.58}$$

From all above mentioned,  $P_{gk}^H < P_{dk}$  and  $P_{gl}^H < P_{dl}$  when the active power demand at bus  $k$  and bus  $l$  still unchanged. Likewise,  $Q_{gk}^H < Q_{dk}$  and  $Q_{gl}^H < Q_{dl}$  when the reactive power demand at bus  $k$  and bus  $l$  still unchanged.

The value of  $P_{di}$  and  $Q_{di}$  can be changed when the value of  $P_g$  and  $Q_g$  has already reached the minimum limit which is  $P_{g,min}$  and  $Q_{g,min}$  thanks to theorem1 which is there is no upper bound for  $P_{d,max}$  and  $Q_{d,max}$ . The value of  $P_{gi}$  and  $Q_{gi}$  cannot be changed because it must satisfy the upper and lower limit of the power generation. In addition, the objective function which is the transmission power loss can be represented as follows.

$$P_{kl}^H + P_{lk}^H - (P_{kl} + P_{lk}) = G_{kl}(V_k^H - V_l^H + V_l^H - V_k - 2a_{kl}^H + 2a_{kl}) < 0.\tag{4.59}$$

Thereby, the objective function which is  $P_{ij} + P_{ji}$  has a lower value.

The set of solution which is  $V_k^H$ ,  $V_l^H$ ,  $a_{kl}^H$ , and  $b_{kl}^H$  satisfies equation (4.25)–(4.28), (4.35)–(4.36) and (4.38). The optimal solution is obtained when inequality sign in equation (4.40) converts to equality sign.



#### 4.5 ACOPF Computational Algorithm

In this thesis, the ACOPF problem with SOCP relaxation is solved by using CVX optimization solver. CVX is a Matlab-based modeling system for convex optimization. CVX turns Matlab into a modeling language which objective function and constraints can be determined Matlab expression syntax. Hence, The ACOPF algorithm can be summarized as the following step.

1. Download system data case.
2. Convert the power system data to per unit in order to normalize the system quantities.
3. Set optimization variables which is  $x = [V^T \ a^T \ b^T \ P_g^T \ Q_g^T]^T$ .
4. Formulate the ACOPF problem.
  - 4.1 Formulate the objective function which is total power loss.
  - 4.2 Formulate constraints which include equality and inequality constraints.
  - 4.3 Set boundary of the variables, especially the voltage magnitude and voltage angle of slack bus.
5. Run CVX optimization solver to obtain the solution of the ACOPF problem.
6. Compute the power flow of the network from the optimal solution  $x$ .
7. Report all results.

The ACOPF computational procedure can be illustrated as the flowchart in Figure 4.7.

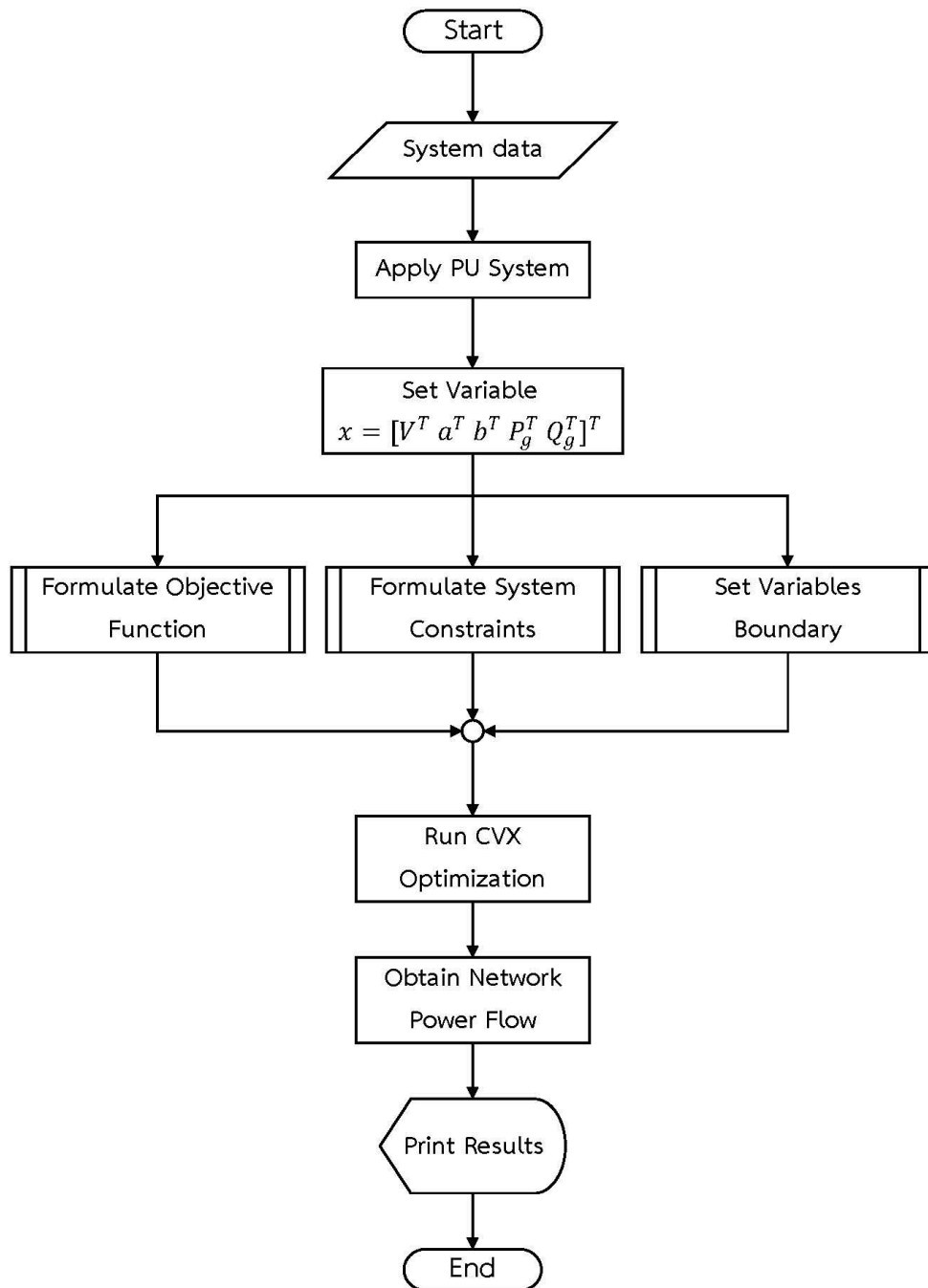


Figure 4.7 Flow chart of ACOPF algorithm

## CHAPTER 5

### Distributed Generation and Static Var Compensator

Power loss in a power system can be varied from power system devices, especially distributed generation (DG) or static var compensator (SVC). The appropriate site of DG and SVC with suitable size can reduce the power loss and improve the efficiency of a power system. However, the inappropriate location and size of DG and SVC can result in negative impacts such as power loss increment. As a result, the optimal site of DG and SVC with optimal size are necessary to determine. Therefore, this chapter describes basic knowledge of DG and SVC.

#### 5.1 Distributed Generation

The traditional power generation system is the centralized power generation system. Large power plants are built near energy sources to generate electricity with an emphasis on economic cost. In addition, power plants are built in remote areas to prevent negative effects on the environment and the livelihoods of residents. Therefore, the popularity of centralized power generation system is declining. This system should be properly addressed to meet economic and environmental challenges. Moreover, fossil fuels are steadily decreasing and conventional power plants are difficult to construct at present. Thus, the distributed generation system is formed to alleviate the problem governs by a centralized system. The objective is to deliver electricity to end-users within the network continuously at a lower price without polluting the environment. Thereby, DG is important in the power system.

DG is defined as a small-scale generator with a capacity less than 100 MW. DG should be installed within a distribution network or the customer side of the network near end-users. Moreover, DG can be based on non-renewable energy such as natural gas, coal, or diesel fuel and renewable energy such as solar energy, wind power, or hydroelectric power. In addition, DG can be categorized based on output characteristic into 4 types as follow.

1. DG generating only active power, e.g., fuel cells, photovoltaic.
2. DG generating only reactive power, e.g., capacitors, synchronous compensator.
3. DG generating both active and reactive power, e.g., synchronous machines.
4. DG generating active power but absorbing reactive power, e.g., induction generators used in the wind turbines.

The integration of DG in the distribution system can significantly impact the power flow and voltage at customer side and utility equipment. The optimal placement of DG with suitable size can bring about various benefits to a power system such as transmission loss reduction, voltage profile improvement, increased reliability, grid reinforcement, and reduced greenhouse gas emission. Additionally, DG is economically beneficial in terms of investment cost reduction. DG can upgrade the system when the load is increased. DG can be operated stand-alone, however, DG is normally connected to the main grid as shown in Figure 5.1.

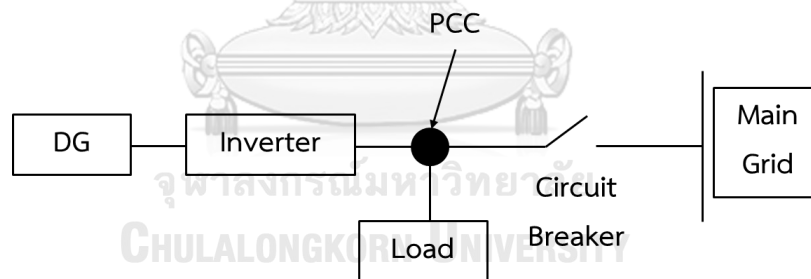


Figure 5.1 DG integration diagram

DG is usually installed close to the load but the determination of the location from Point of Common Coupling (PCC) is also very important. Inappropriate location and size of DG can result in a negative effect on the power system. Hence, many optimization techniques are reported to find the optimal site for DG. There are 2 major types of techniques as follows.

### 1. Conventional optimization techniques

Conventional techniques are widely used due to simple in implementation and less convergence issues. For example, a 2/3 rule which said DG capacity should be 2/3 of the load demand and installed at 2/3 of the feeder length. This rule cannot apply to non-uniform load because this rule is a simple approximation. Additionally, an analytical method is one of the conventional techniques. In this method, the model is developed for identifying problems in the same manner as optimization analysis. This approach includes optimal power flow (OPF), linear programming, and mixed-integer linear programming. The analytical method is simple, fast, and accurate.

### 2. Non-conventional optimization techniques

Non-conventional optimization techniques include artificial intelligence (AI) method, Metaheuristic method, and Hybrid method. These methods are widely used due to their ability to solve complex problems. AI is a soft computing technique inspired by nature which can provide local optimal solutions. This method can apply with both continuous and discrete parameters. However, this method sometimes does not converge and less accurate in a large-scale system. Metaheuristic method is a high-level procedure with optimal controlling parameters. This method can bring near-optimal solutions, but reliability is not considered during modeling. Examples of this method are Tabu search (TS), Particle swarm optimization (PSO), and Ant colony optimization (ACO). Hybrid method is the method that combine various optimization techniques into one algorithm. This approach can provide fast convergence with a smaller number of iterations. In addition, this method brings more accurate results and works as a better decision-making tool.

The integration of DG leads to consideration of distribution system planning and operations. Inappropriate capacity of DG can cause voltage fluctuation and harmonic. Therefore, the appropriate DG size should be determined. Each DG is treated as a generator which injects power to the system. Voltage and line limits are major determining factors for the installation size of DG. A commonly used rule in the U.S. allows peak powers of DG installation up to 15% of the peak load on a feeder without a detailed system effect study. In this work, the maximum allowable integration of DG is determined by Metropolitan Electricity Authority (MEA) Grid Code [46]. The total installed capacity of DG installed in the same feeder must not exceed 8 MW/feeder for 24 kV system and 4 MW/feeder for 12 kV system. In addition, the total installed capacity from all feeders must be no reverse current to the transmission side of the Electricity Generating Authority of Thailand (EGAT). Thus, the total DG installation capacity constraint can be considered as follow.

$$P_{dg,min} \leq P_{dg} \leq P_{dg,max} \quad (5.1)$$

Where  $P_{dg}$  is the total power generated from DG.

$P_{dg,min}$  is the lower bound of the total DG installation capacity.

$P_{dg,max}$  is the upper bound of the total DG installation capacity.

Additionally, the constraint of DG capacity should be added to the ACOPF formulation in Chapter 4 part 3.3.

## 5.2 Static Var Compensator

Mostly, the optimal operating point in a power system is determined based on economic criteria. However, other criteria like power loss, voltage profile, and so on should also be considered. Flexible AC Transmission System (FACTS) devices are considered to maximize the use of existing transmission facilities. FACTS devices can increase power system reliability and security as well as minimize transmission power loss of the system. Moreover, FACTS devices can improve power factor by absorbing

or delivering reactive power. There are various types of FACTS devices such as SVC, Static Synchronous Compensator (STATCOM), Thyristor-Controlled Series Capacitor (TCSC), and Unified Power Flow Controller (UPFC). In this work, SVC is only considered since SVC is the best option for voltage control.

SVC is a shunt compensation component that is used in transmission and distribution systems to control voltage and reactive power. SVC responds very fast and has high reliability compared with mechanically switched capacitor banks. In addition, SVC can be used in steady-state and transient voltage control with high efficiency. There are many advantages of SVC such as transient stability improvement, transmission capacity increment, and power system damping improvement. SVC can improve voltage profile by supplying or absorbing reactive power to the system. The appropriate placement of SVC in the network can reduce real power loss and enhance the system transfer capability while maintaining smooth voltage profile.

SVC is modeled as a shunt variable admittance. SVC can be installed at the terminal bus or the middle of a long transmission line. SVC is usually treated as a shunt connected static VAR generator which can transfer inductive or capacitive current to control bus voltage. SVC comprises one thyristor-controlled reactor (TCR), several thyristor-switched capacitors (TSC) and filters as shown in Figure 5.2.

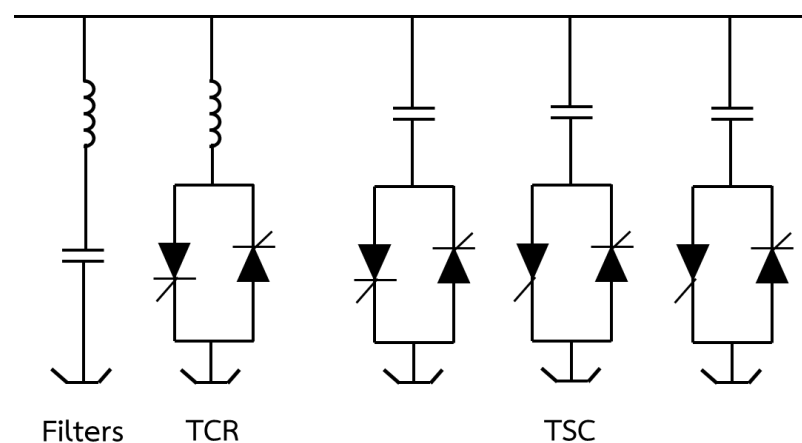


Figure 5.2 SVC diagram

The most popular simple configuration of SVC is a fixed capacitor with a thyristor-controlled reactor (FC-TCR) as presented in Figure 5.3. In this model, an inductance is connected as shunt impedance in order to produce the required compensating current. When an overvoltage occurs, inductance operates as an inductor. On the other hand, when an undervoltage occurs, inductance operates as a capacitor.

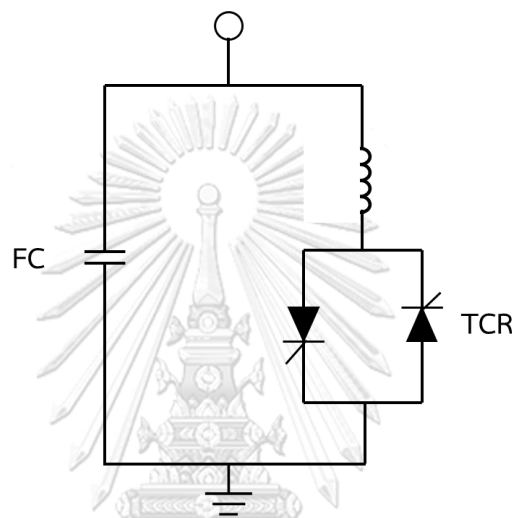


Figure 5.3 FC-TCR model

Reactive power is absorbed or supplied by SVC and current through SVC are expressed as follows.

$$Q_{SVCi} = B_{SVCi} V_i^2 \quad (5.2)$$

$$I_{SVC} = B_{SVCi} V_i \quad (5.3)$$

Where  $Q_{SVCi}$  is reactive power of SVC at bus  $i$ .

$B_{SVCi}$  is susceptance of SVC at bus  $i$ .

$V_i$  is voltage at bus  $i$ .

$I_{SVC}$  is current through SVC at bus  $i$ .



If  $B$  is positive, SVC delivers reactive power. However, if  $B$  is negative, SVC absorbs reactive power. The limit of reactive power is dependent on susceptance as follows.

$$B_{SVC,min} \leq B_{SVC} \leq B_{SVC,max} \quad (5.4)$$

$$B_{SVC,min} = \frac{1}{\left| \frac{S_b}{Q_{ind}} \right| - |X_{tlpu}|} \quad (5.5)$$

$$B_{SVC,max} = \frac{1}{\left| \frac{S_b}{Q_{cap}} \right| + |X_{tlpu}|} \quad (5.6)$$

Where  $S_b$  is base apparent power of the system.

$Q_{ind}$  is reactive power of inductance in SVC.

$Q_{cap}$  is reactive power of capacitance in SVC.

$X_{tlpu}$  is SVC transformer reactance in per unit.

## CHAPTER 6

### Numerical Results

In this chapter, the proposed alternating current optimal power flow (ACOPF) problem with second order cone program (SOCP) relaxation has been applied to MATPOWER test systems and carried out into 4 cases as follows.

1. Base case
2. Installing distributed generation (DG)
3. Installing static var compensator (SVC)
4. Installing DG and SVC

The simulations were performed using MATLAB software with CVX optimization solver. The total power loss of the power system was determined by using the proposed ACOPF. Moreover, the results from the proposed method were compared with the conventional ACOPF problem.

#### 6.1 Base Case

This part illustrates the simulations on base test systems which are the system without installing any device. Base test systems are 9-bus, 24-bus, 33-bus, and 118-bus MATPOWER test systems.

##### 6.1.1 9-Bus Test System

This part presents the results for the 9-bus test system obtained by the proposed ACOPF for power loss minimization. The test system is the network topology which consists of 3 generators, 6 load buses, and 9 branches. The total load demand is 315 MW and 115 MVar. The additional data of the system is in appendix A.1 from [49]. The network is shown in Figure 6.1.

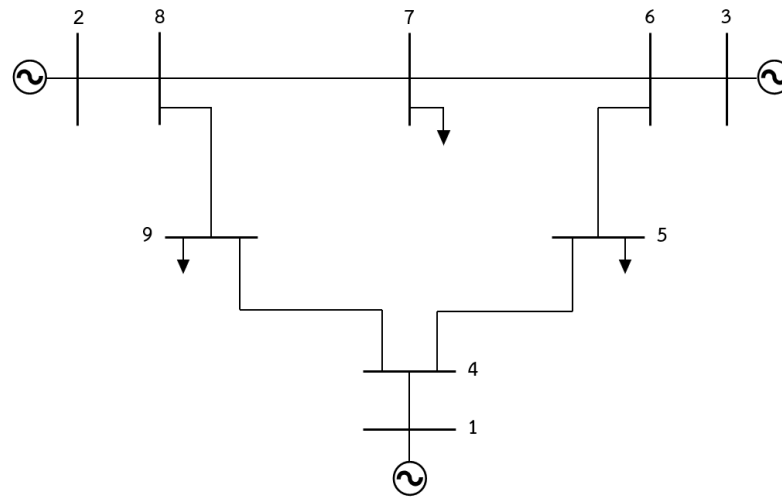


Figure 6.1 9-bus network system

The results of the proposed method compared with the conventional ACOPF method are shown in Table 6.1-6.3. Table 6.1 shows all voltage magnitudes, active power, and reactive power at each bus. Table 6.2 shows active and reactive power flow between each transmission line where FB is from bus and TB is to bus. The active power loss and reactive power loss on each branch are shown in Table 6.3.

Table 6.1 Comparison of bus data result in 9-bus test system

Bus	Conventional ACOPF			ACOPF with SOCP Relaxation		
	$V$ (p.u.)	$P_g$ (MW)	$Q_g$ (MVar)	$V$ (p.u.)	$P_g$ (MW)	$Q_g$ (MVar)
1	1.100	157.65	12.12	1.100	158.19	12.37
2	1.097	88.10	-2.37	1.097	89.48	-2.52
3	1.088	71.57	-21.80	1.088	69.63	-20.44
4	1.097	-	-	1.097	-	-
5	1.087	-	-	1.087	-	-
6	1.100	-	-	1.100	-	-
7	1.089	-	-	1.089	-	-
8	1.100	-	-	1.100	-	-
9	1.076	-	-	1.076	-	-
Total		317.32	-12.06		317.13	-10.59

Table 6.2 Comparison of branch data result in 9-bus test system

FB	TB	Conventional ACOPF				ACOPF with SOCP Relaxation			
		$P_{ij}$ (MW)	$Q_{ij}$ (MVar)	$P_{ji}$ (MW)	$Q_{ji}$ (MVar)	$P_{ij}$ (MW)	$Q_{ij}$ (MVar)	$P_{ji}$ (MW)	$Q_{ji}$ (MVar)
1	4	157.65	12.12	-157.65	-0.21	158.19	12.37	-158.19	-0.39
4	5	65.45	-8.64	-64.85	-6.92	63.03	-8.32	-62.47	-7.48
5	6	-25.15	-23.08	25.36	-18.83	-27.53	-22.52	27.78	-19.20
3	6	71.57	-21.8	-71.57	24.57	69.63	-20.44	-69.63	24.37
6	7	46.20	-5.75	-45.99	-17.48	41.85	-5.17	-41.67	-18.37
7	8	-54.01	-17.52	54.23	1.48	-58.33	-16.63	58.57	0.88
8	2	-88.10	6.40	88.10	-2.37	-89.48	6.69	89.48	-2.52
8	9	33.87	-7.88	-33.54	-26.65	30.91	-7.57	-30.62	-27.20
9	4	-91.46	-23.35	92.20	8.86	-94.38	-22.80	95.16	8.70

Table 6.3 Comparison of power loss in 9-bus test system

From Bus	To Bus	Conventional ACOPF		ACOPF with SOCP Relaxation	
		$P_{loss}$ (MW)	$Q_{loss}$ (MVar)	$P_{loss}$ (MW)	$Q_{loss}$ (MVar)
1	4	0.00	11.90	0.00	11.99
4	5	0.61	3.28	0.56	3.04
5	6	0.21	0.92	0.25	1.09
3	6	0.00	2.77	0.00	3.93
6	7	0.21	1.82	0.18	1.51
7	8	0.21	1.82	0.25	2.10
8	2	0.00	4.03	0.00	4.16
8	9	0.33	1.68	0.28	1.43
9	4	0.74	6.27	0.78	6.66
Total		2.32	34.48	2.31	35.91

Furthermore, power generation and voltage magnitude from the proposed method is compared with the power generation limit to verify the results as shown in Table 6.4 and Table 6.5, respectively.

Table 6.4 Comparison of power generation and power generation limit in 9-bus test system

Bus	Power Generation		Power Generation Limit			
	$P_g$ (MW)	$Q_g$ (MVar)	$P_{max}$ (MW)	$P_{min}$ (MVar)	$Q_{max}$ (MVar)	$Q_{min}$ (MVar)
1	157.65	12.12	250.00	10.00	300.00	-300.00
2	88.10	-2.37	300.00	10.00	300.00	-300.00
3	71.57	-21.80	270.00	10.00	300.00	-300.00

Table 6.5 Comparison of voltage and voltage limit in 9-bus test system

Bus	$V$ (p.u.)	Voltage Limit	
		$V_{max}$ (p.u.)	$V_{min}$ (p.u.)
1	1.100	1.100	0.900
2	1.097	1.100	0.900
3	1.088	1.100	0.900
4	1.097	1.100	0.900
5	1.087	1.100	0.900
6	1.100	1.100	0.900
7	1.089	1.100	0.900
8	1.100	1.100	0.900
9	1.076	1.100	0.900

The result shows that voltage at each bus of the 2 methods are equal. The summation of power generated can supply the total load demand sufficiently. Furthermore, the summation of the active power generated of the proposed ACOPF is lower than the conventional ACOPF while the reactive power generated is greater. The total active power loss which is the objective function of the proposed method

is slightly lower than the other method whereas the total reactive power is higher. In addition, voltage magnitudes, active and reactive power generation of the proposed method are inside the limits. However, voltage magnitude at bus 1, 6, and 8 are equal to the maximum voltage limit.

### 6.1.2 24-Bus Test System

The results of the proposed method compared with the conventional method on the 24-bus test system are presented in this part. Moreover, Figure 6.2 displays the network structure.

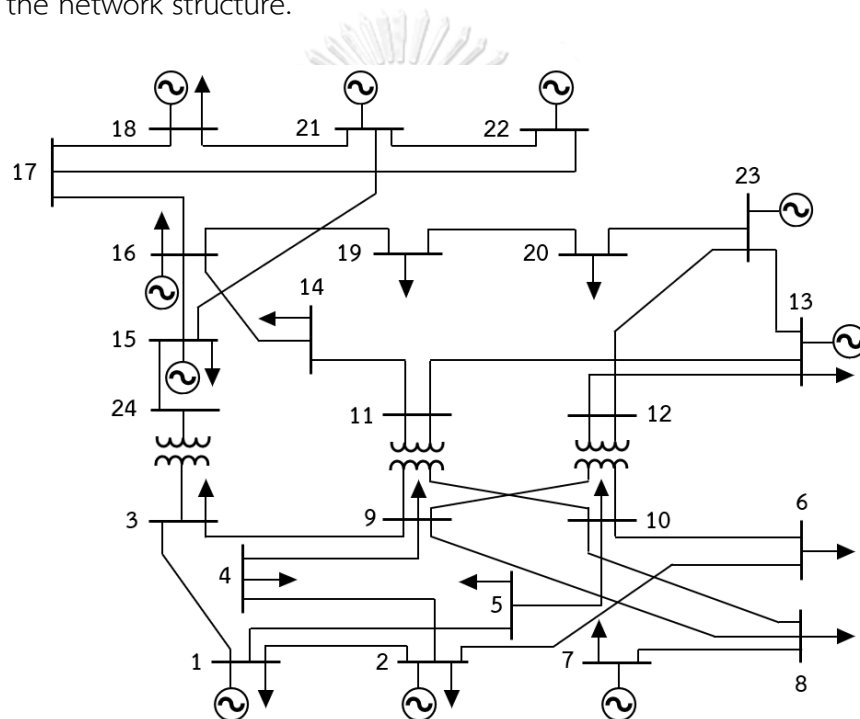


Figure 6.2 24-bus network system

The test system is the network topology. There are 33 generators, 17 load buses, and 38 branches. The total load demand is 2,850 MW and 580 MVar. Furthermore, the system is divided into 4 area. The additional information of the system is in appendix A.2 from [50].

The bus data result which is voltage magnitude, active and reactive power generation from 2 methods is shown in Table 6.6. The total power loss obtained by the proposed implementation are compared to the conventional ACOPF and present in Table 6.7. The supplementary result is in appendix B.1.

Table 6.6 Comparison of bus data result in 24-bus test system

Bus	Conventional ACOPF			ACOPF with SOCP Relaxation		
	$V$ (p.u.)	$P_g$ (MW)	$Q_g$ (MVar)	$V$ (p.u.)	$P_g$ (MW)	$Q_g$ (MVar)
1	1.013	163.94	14.15	0.967	192.00	-42.17
2	1.013	165.04	14.15	0.968	192.00	-50.00
3	0.973	-	-	0.968	-	-
4	0.981	-	-	0.957	-	-
5	1.00	-	-	0.984	-	-
6	0.995	-	-	1.042	-	-
7	1.022	234.63	61.13	1.031	281.15	56.44
8	0.985	-	-	0.992	-	-
9	0.988	-	-	0.984	-	-
10	1.013	-	-	1.029	-	-
11	0.984	-	-	1.014	-	-
12	0.983	-	-	1.012	-	-
13	1.006	532.16	106.7	1.028	591.00	55.15
14	0.992	0.00	75.82	1.022	0.00	34.63
15	0.995	168.86	47.56	1.041	215.00	110.00
16	0.998	134.52	17.9	1.040	155.00	57.27
17	1.009	-	-	1.047	-	-
18	1.012	356.23	44.41	1.049	400.00	58.19
19	0.996	-	-	1.034	-	-
20	1.005	-	-	1.038	-	-
21	1.016	348.02	45.34	1.050	298.44	-8.61
22	1.031	194.33	6.7	1.050	60.00	-24.13
23	1.014	587.45	50.58	1.044	495.78	35.68
24	0.965	-	-	1.005	-	-
Total		2885.18	484.43		2880.40	282.46

Table 6.7 Comparison of total power loss in 24-bus test system

	Conventional ACOPF		ACOPF with SOCP Relaxation	
	$P_{loss}$ (MW)	$Q_{loss}$ (MVar)	$P_{loss}$ (MW)	$Q_{loss}$ (MVar)
Total Power Loss	35.26	337.61	30.37	255.67

Additionally, power generation and voltage magnitude from the proposed method is compared with the power generation limit to verify the results as shown in Table 6.8 and Figure 6.3, respectively.

Table 6.8 Comparison of power generation and power generation limit in 24-bus test system

Bus	Power Generation		Power Generation Limit			
	$P_g$ (MW)	$Q_g$ (MVar)	$P_{max}$ (MW)	$P_{min}$ (MVar)	$Q_{max}$ (MVar)	$Q_{min}$ (MVar)
1	192.00	-42.47	192.00	62.40	80.00	-50.00
2	192.00	-50.00	192.00	62.40	80.00	-50.00
7	281.15	56.44	300.00	75.00	180.00	0.00
13	591.00	55.15	591.00	207.00	240.00	0.00
14	0.00	34.63	0.00	0.00	200.00	-50.00
15	215.00	110.00	227.00	66.30	110.00	-50.00
16	155.00	57.27	155.00	54.30	80.00	-50.00
18	400.00	58.19	400.00	100.00	200.00	-50.00
21	298.44	-8.61	400.00	100.00	200.00	-50.00
22	60.00	-24.13	300.00	50.00	80.00	-50.00
23	495.78	35.68	660.00	248.60	310.00	-125.00



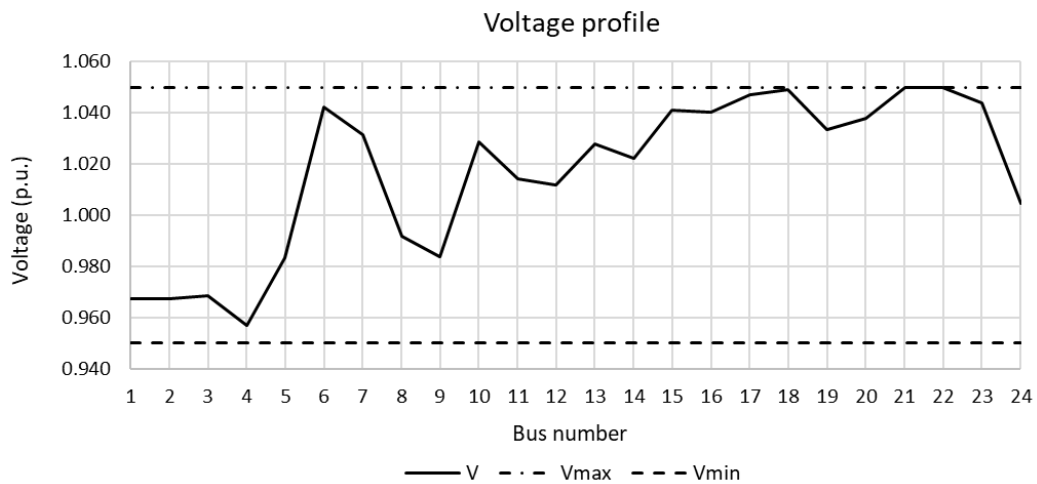


Figure 6.3 Comparison of voltage magnitude and voltage magnitude limit in 24-bus test system

From Table 6.6, the total power generation can supply the total load demand sufficiently. The total active power generation between 2 methods is slightly different. However, the total reactive power generation of the traditional methods is lower than the proposed method. Additionally, the total active and reactive power loss of the proposed ACOPF are lower than the traditional ACOPF 4.89 MW and 81.94 MVAR, respectively. In addition, voltage magnitudes, active and reactive power generation of the proposed method are inside the limits. However, active power generation from bus 1, 2, 13, 16, and 18 are equal to the upper limit. Reactive power generation from bus 15 is equal to the upper limit while reactive power generation from bus 2 is equal to the lower limit. Moreover, voltage magnitude at bus 21 and 22 are equal to the maximum voltage limit.

### 6.1.3 33-Bus Test System

This part illustrates the comparison results between the proposed ACOPF and the conventional ACOPF which the objective function is power loss minimization. The 33-bus system structure is shown in Figure 6.4.

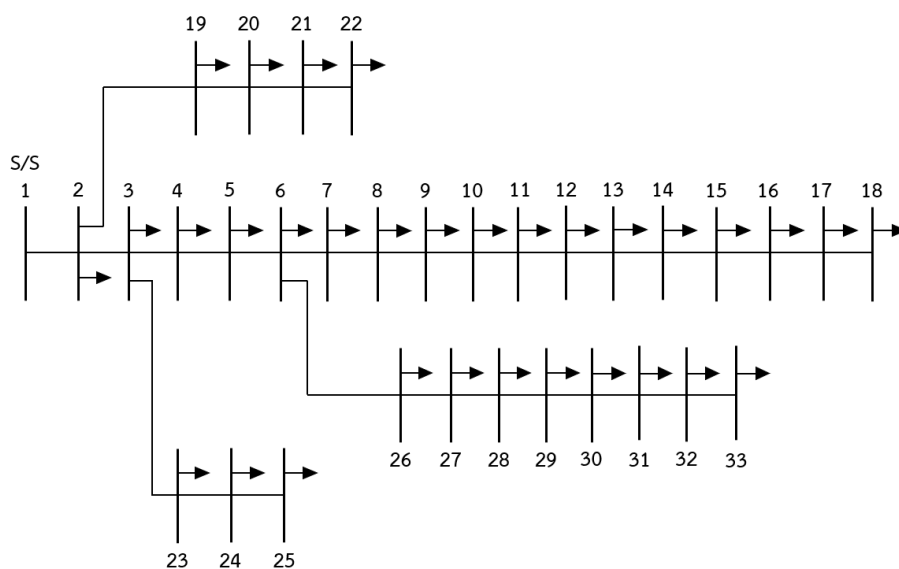


Figure 6.4 33-bus system structure

The test system is a radial topology. The system includes 1 generator at bus 1 which is a slack bus and 32 load buses. There are 32 transmission lines. Besides, the total load demand is 3.715 MW and 2.3 MVar. The additional data of the system is in appendix A.3 from [51].

The comparison results between the proposed method and the conventional method are presented in Table 6.9-6.10. The bus voltage magnitudes, active and reactive power generation is in Table 6.9. Table 6.10 shows the total active and reactive power loss. Moreover, the additional result is also in appendix B.2.

Table 6.9 Comparison of bus data result in 33-bus test system

Bus	Conventional ACOPF			ACOPF with SOCP Relaxation		
	$V$ (p.u.)	$P_g$ (MW)	$Q_g$ (MVar)	$V$ (p.u.)	$P_g$ (MW)	$Q_g$ (MVar)
1	1.000	3.86	2.39	1.000	3.86	2.39
2	0.997	-	-	0.997	-	-
3	0.986	-	-	0.986	-	-
4	0.983	-	-	0.983	-	-
5	0.979	-	-	0.979	-	-
6	0.971	-	-	0.971	-	-

Bus	Conventional ACOFP			ACOPF with SOCP Relaxation		
	$V$ (p.u.)	$P_g$ (MW)	$Q_g$ (MVA <sub>r</sub> )	$V$ (p.u.)	$P_g$ (MW)	$Q_g$ (MVA <sub>r</sub> )
7	0.970	-	-	0.970	-	-
8	0.969	-	-	0.969	-	-
9	0.966	-	-	0.966	-	-
10	0.965	-	-	0.965	-	-
11	0.966	-	-	0.966	-	-
12	0.966	-	-	0.966	-	-
13	0.962	-	-	0.962	-	-
14	0.961	-	-	0.961	-	-
15	0.961	-	-	0.961	-	-
16	0.959	-	-	0.959	-	-
17	0.955	-	-	0.955	-	-
18	0.954	-	-	0.954	-	-
19	0.995	-	-	0.995	-	-
20	0.981	-	-	0.981	-	-
21	0.977	-	-	0.977	-	-
22	0.973	-	-	0.973	-	-
23	0.981	-	-	0.981	-	-
24	0.970	-	-	0.970	-	-
25	0.963	-	-	0.963	-	-
26	0.970	-	-	0.970	-	-
27	0.969	-	-	0.969	-	-
28	0.964	-	-	0.964	-	-
29	0.960	-	-	0.960	-	-
30	0.957	-	-	0.957	-	-
31	0.954	-	-	0.954	-	-
32	0.954	-	-	0.954	-	-
33	0.954	-	-	0.954	-	-
Total		3.86	2.39		3.86	2.39

Table 6.10 Comparison of total power loss in 33-bus test system

	Conventional ACOPF		ACOPF with SOCP Relaxation	
	$P_{loss}$ (MW)	$Q_{loss}$ (MVar)	$P_{loss}$ (MW)	$Q_{loss}$ (MVar)
Total Power Loss	0.12	0.09	0.12	0.09

Additionally, power generation and voltage magnitude from the proposed method is compared with the power generation limit to verify the results as shown in Table 6.11 and Figure 6.5, respectively.

Table 6.11 Comparison of power generation and power generation limit in 33-bus test system

Bus	Power Generation		Power Generation Limit			
	$P_g$ (MW)	$Q_g$ (MVar)	$P_{max}$ (MW)	$P_{min}$ (MVar)	$Q_{max}$ (MVar)	$Q_{min}$ (MVar)
1	3.86	2.39	10.00	0	10.00	-10.00

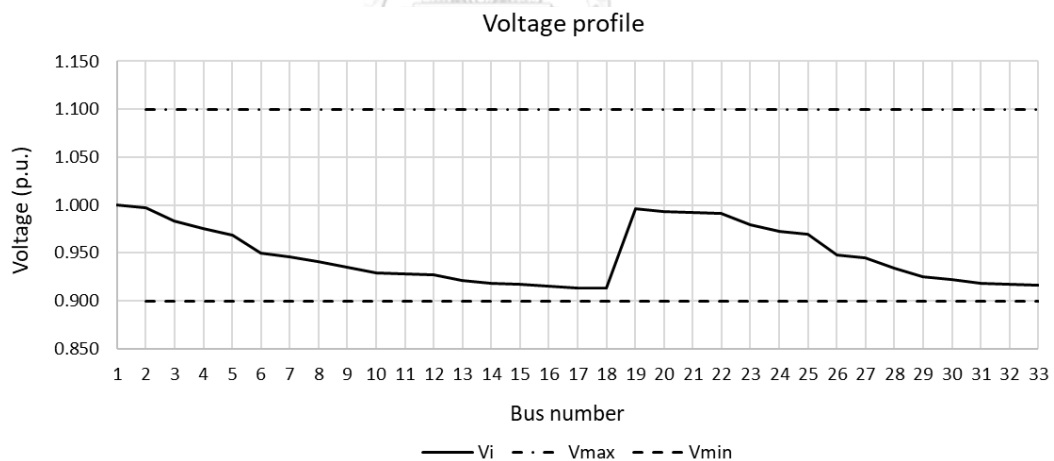


Figure 6.5 Comparison of voltage magnitude and voltage magnitude limit in 33-bus test system

The result shows that all bus variables which are voltage magnitude, active and reactive power generation are within the power system constraints. All power generators can supply all loads sufficiently. Moreover, the total active and reactive power generation using the proposed ACOPF are equal to the conventional ACOPF.

Similarly, the total active and reactive power loss from the proposed method are also equal to the other method.

#### 6.1.4 118-Bus Test System

In this part, the results from the proposed ACOPF are compared with the results from the conventional ACOPF. The 118-test system is a network topology that comprises 54 generators, 64 load buses, and 186 branches. The total load demand is 4,242 MW and 1,438 MVar. The additional data is in appendix A.4 from [52].

The total active and reactive power generated between the 2 methods are displayed in Table 6.11. The total active and reactive power loss are also compared in Table 6.11. In addition, more results are in appendix B.3.

Table 6.11 Comparison of total power generation and total power loss

	Conventional ACOPF		ACOPF with SOCP Relaxation	
	$P$ (MW)	$Q$ (MVar)	$P$ (MW)	$Q$ (MVar)
Total Power generation	4319.40	388.26	4314.50	1378.10
Total Power Loss	77.40	483.52	72.54	1423.40

From Table 6.11, the results show that the total active power generation and the total active power loss from the traditional ACOPF is greater than the ACOPF with SOCP relaxation. Whereas the total reactive power generation and the total reactive power loss are greatly lower. Besides, the total power generation can supply the total load demand sufficiently.

#### 6.2 Installing DG

This part presents the results obtained by the proposed ACOPF when installing DG in the 33-bus MATPOWER test system. In this system, the total load demand is 3.715 MW and 2.3 MVar. DG which generates only active power is used as a new generator in the system. The maximum allowable integration of DG which is 4 MW/feeder is set by Metropolitan Electricity Authority (MEA) Grid Code. Moreover, this part is divided into 3 cases which are one DG, two DGs, and three DGs.

### 6.2.1 One DG

In this case, the optimal size of one DG is determined by the proposed method for power loss minimization. DG is installed at each bus to analyze the appropriate site. Table 6.12 shows total power loss when installing DG at each bus and compares with total power loss from the base case. Besides, the optimal size of DG is also presented. Figure 6.6 displays total active power loss when installing DG at each bus compared with total active power loss from the base case.

Table 6.12 Comparison of power loss between base case and one DG installation at each bus

Base Case		DG Installation			
$P_{loss}$ (MW)	$Q_{loss}$ (MVar)	Bus Number	Size (MW)	$P_{loss}$ (MW)	$Q_{loss}$ (MVar)
0.1225	0.0875	1	1.4677	0.1225	0.0875
0.1225	0.0875	2	3.8285	0.1135	0.0828
0.1225	0.0875	3	3.0122	0.0910	0.0691
0.1225	0.0875	4	2.4694	0.0899	0.0683
0.1225	0.0875	5	2.2953	0.0863	0.0667
0.1225	0.0875	6	2.4306	0.0714	0.0547
0.1225	0.0875	7	2.3420	0.0722	0.0558
0.1225	0.0875	8	2.1909	0.0738	0.0540
0.1225	0.0875	9	1.8652	0.0765	0.0552
0.1225	0.0875	10	1.6325	0.0819	0.0579
0.1225	0.0875	11	1.6316	0.0820	0.0580
0.1225	0.0875	12	1.6599	0.0816	0.0585
0.1225	0.0875	13	1.5066	0.0815	0.0602
0.1225	0.0875	14	1.5625	0.0788	0.0580
0.1225	0.0875	15	1.6789	0.0751	0.0558
0.1225	0.0875	16	1.5828	0.0756	0.0568
0.1225	0.0875	17	1.5646	0.0731	0.0553
0.1225	0.0875	18	1.6245	0.0700	0.0537

Base Case		DG Installation			
$P_{loss}$ (MW)	$Q_{loss}$ (MVar)	$P_{loss}$ (MW)	$Q_{loss}$ (MVar)	$P_{loss}$ (MW)	$Q_{loss}$ (MVar)
0.1225	0.0875	19	2.2309	0.1146	0.0841
0.1225	0.0875	20	1.7217	0.0981	0.0742
0.1225	0.0875	21	1.8294	0.0917	0.0689
0.1225	0.0875	22	1.5685	0.0924	0.0691
0.1225	0.0875	23	2.3795	0.0884	0.0674
0.1225	0.0875	24	2.1919	0.0751	0.0572
0.1225	0.0875	25	2.2279	0.0638	0.0491
0.1225	0.0875	26	2.2923	0.0727	0.0551
0.1225	0.0875	27	2.1593	0.0736	0.0557
0.1225	0.0875	28	2.0541	0.0699	0.0532
0.1225	0.0875	29	2.2849	0.0596	0.0452
0.1225	0.0875	30	2.0586	0.0617	0.0462
0.1225	0.0875	31	1.8038	0.0647	0.0490
0.1225	0.0875	32	1.7523	0.0655	0.0497
0.1225	0.0875	33	1.6905	0.0675	0.0521

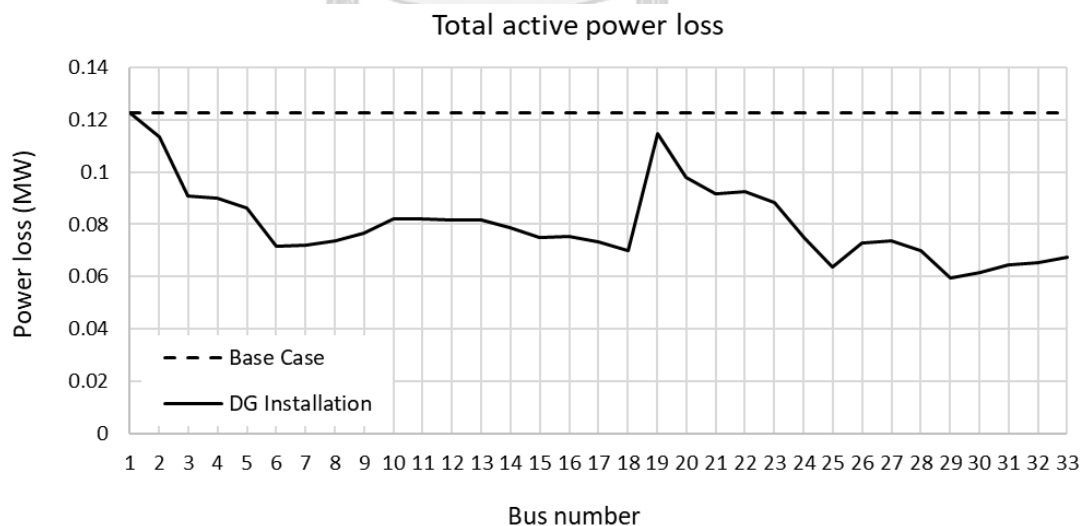


Figure 6.6 Comparison of total active power loss between base case and one DG installation at each bus

From Table 6.12 and Figure 6.6, the best location of DG for total power loss minimization is bus 29. Installing DG at bus 29 with a size of 2.2849 MW can reduce the total active power loss from 0.1225 to 0.0596 MW or equal to 51.38%. Moreover, power generation from conventional generator and DG do not violate the power generation limit as shown in Table 6.13.

Table 6.13 Power generation from conventional generator and DG at bus 29

Bus	Power Generation		Power Generation Limit			
	$P_g$ (MW)	$Q_g$ (MVar)	$P_{max}$ (MW)	$P_{min}$ (MVar)	$Q_{max}$ (MVar)	$Q_{min}$ (MVar)
1	1.4897	2.3452	10	0	10	-10
29	2.2849	0	4	0	0	0

### 6.2.2 Two DGs

The optimal size of two DGs at different bus is determined by the proposed ACOPF and presented in this part. Figure 6.7 shows total active power loss when installing two DGs at each bus. The color scale shows the total active power loss from maximum to minimum by red to green scale.

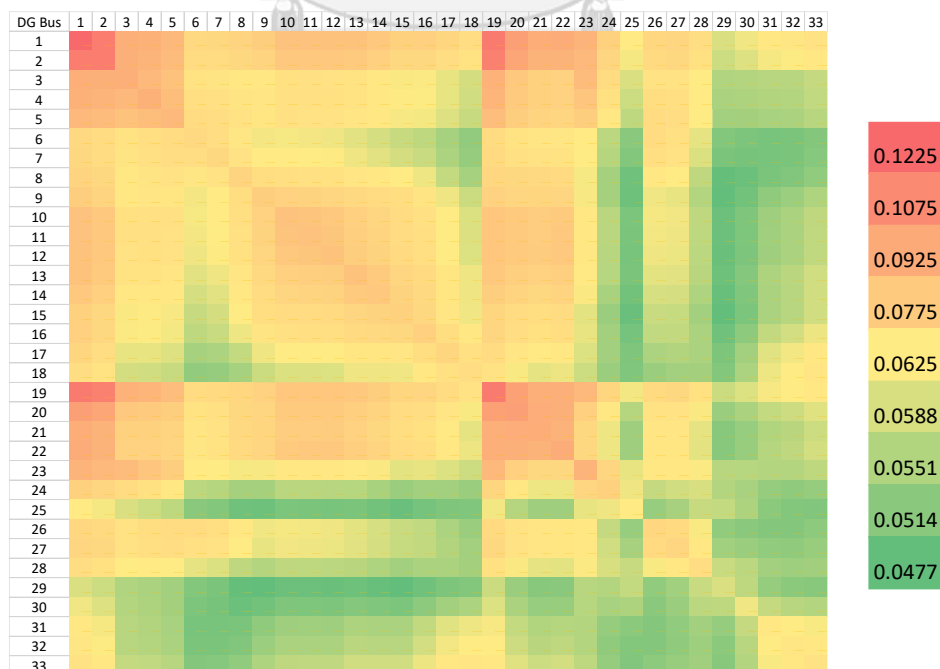


Figure 6.7 Total active power loss when installing two DGs at each bus



From Figure 6.7, installing DG at bus 15 and 29 provides the minimum total active power loss. Furthermore, the optimal size of DGs at bus 15 and 29 are shown in Table 6.14.

Table 6.14 Comparison of power loss between base case and two DGs installation

	DG Location (bus number)	DG Size (MW)	Power Loss	
			$P_{loss}$ (MW)	$Q_{loss}$ (MVar)
Base Case	-	-	0.1225	0.0875
Two DGs	15	0.9641	0.0477	0.0351
	29	1.7285		

Installing DG at bus 15 with the size of 0.9641 MW and bus 29 with the size of 1.7285 MW can minimize power loss. This installation can reduce power loss from 0.1225 to 0.0477 MW or equal to 61.06%. Moreover, active and reactive power generation and total load demand are shown in Table 6.15.

Table 6.15 Power generation when installing DG at bus 15 and 29

Bus	Power Generation		Total Load Demand	
	$P_g$ (MW)	$Q_g$ (MVar)	$P_l$ (MW)	$Q_l$ (MVar)
1	1.0700	2.3351	-	-
15	0.9641	-	-	-
29	1.7285	-	-	-
Total	3.7626	2.3351	3.7150	2.300

### 6.2.3 Three DGs

This part presents the optimal DG sizes and their corresponding sites by employing the proposed method. The optimal site and size of three DGs for power loss minimization are shown in Table 6.16. Moreover, the table shows the comparison results between this case and the base case by sorting the best 3 performance groups which these groups are a set of DG installing sites.

Table 6.16 Comparison of power loss between base case and three DGs installation

	DG Location (bus number)	DG Size (MW)	Power Loss	
			$P_{loss}$ (MW)	$Q_{loss}$ (MVAr)
Base Case	-	-	0.1225	0.0875
Group 1	6	0.9646	0.0435	0.0324
	15	0.8288		
	25	1.3413		
Group 2	6	0.8791	0.0439	0.0326
	15	0.7779		
	29	1.3873		
Group 3	15	0.9549	0.0457	0.0333
	25	0.8485		
	29	0.9998		

From Table 6.16, Installing DG at bus 6 with the size of 0.9646 MW, bus 15 with the size of 0.8288 MW and bus 25 with the size of 1.3413 MW can minimize power loss. This installation can reduce power loss from 0.1225 to 0.0435 MW or equal to 64.49%. Moreover, Table 6.17 shows active and reactive power generation and total load demand.

Table 6.17 Power generation data when installing DGs at bus 6, 15, and 25

Bus	Power Generation		Total Load Demand	
	$P_g$ (MW)	$Q_g$ (MVAr)	$P_l$ (MW)	$Q_l$ (MVAr)
1	0.6238	2.3324	-	-
6	0.9646	-	-	-
15	0.8288	-	-	-
25	1.3413	-	-	-
Total	3.7585	2.3324	3.7150	2.300

### 6.3 Installing SVC

This part presents the results obtained by the proposed ACOPF when installing SVC in the 33-bus MATPOWER test system. In this system, the total load demand is 3.715 MW and 2.3 MVar. SVC is considered as a new generator which supplying reactive power. SVC sizing is varied from 0–4 MVar. In addition, this part is divided into 3 cases which are one SVC, two SVCs, and three SVCs.

#### 6.3.1 One SVC

In this case, the optimal size of one SVC is determined by the proposed method for power loss minimization. SVC is installed at each bus to analyze the appropriate site. Table 6.18 shows total power loss when installing SVC at each bus and compares with total power loss from the base case. Besides, the optimal size of SVC is also presented. Figure 6.8 displays total active power loss when installing SVC at each bus compared with total active power loss from the base case.

Table 6.18 Comparison of power loss between base case and SVC installation at each bus

Base Case		SVC Installation			
$P_{loss}$ (MW)	$Q_{loss}$ (MVar)	Bus number	$Q_{loss}$ (MVar)	$P_{loss}$ (MW)	$Q_{loss}$ (MVar)
0.1225	0.0875	1	0.3209	0.1225	0.0875
0.1225	0.0875	2	2.4465	0.1191	0.0857
0.1225	0.0875	3	1.9234	0.1095	0.0805
0.1225	0.0875	4	1.5634	0.1092	0.0803
0.1225	0.0875	5	1.4412	0.1078	0.0798
0.1225	0.0875	6	1.5328	0.1018	0.0749
0.1225	0.0875	7	1.4643	0.1026	0.0756
0.1225	0.0875	8	1.3508	0.1037	0.0756
0.1225	0.0875	9	1.1386	0.1050	0.0763
0.1225	0.0875	10	0.9906	0.1072	0.0773
0.1225	0.0875	11	0.9900	0.1072	0.0774

Base Case		SVC Installation			
$P_{loss}$ (MW)	$Q_{loss}$ (MVar)	Bus Number	Size (MVar)	$P_{loss}$ (MW)	$Q_{loss}$ (MVar)
0.1225	0.0875	12	1.0046	0.1070	0.0776
0.1225	0.0875	13	0.9206	0.1067	0.0780
0.1225	0.0875	14	0.9636	0.1055	0.0771
0.1225	0.0875	15	1.0402	0.1039	0.0763
0.1225	0.0875	16	0.9909	0.1037	0.0764
0.1225	0.0875	17	1.0148	0.1012	0.0749
0.1225	0.0875	18	1.0760	0.0990	0.0737
0.1225	0.0875	19	1.3648	0.1196	0.0863
0.1225	0.0875	20	1.0383	0.1136	0.0830
0.1225	0.0875	21	1.1095	0.1110	0.0813
0.1225	0.0875	22	0.9489	0.1113	0.0816
0.1225	0.0875	23	1.5357	0.1081	0.0795
0.1225	0.0875	24	1.4379	0.1017	0.0746
0.1225	0.0875	25	1.5113	0.0949	0.0697
0.1225	0.0875	26	1.4559	0.1019	0.0749
0.1225	0.0875	27	1.3859	0.1018	0.0748
0.1225	0.0875	28	1.3831	0.0980	0.0718
0.1225	0.0875	29	1.5955	0.0911	0.0662
0.1225	0.0875	30	1.4958	0.0893	0.0653
0.1225	0.0875	31	1.2426	0.0943	0.0697
0.1225	0.0875	32	1.1919	0.0955	0.0708
0.1225	0.0875	33	1.1389	0.0970	0.0725

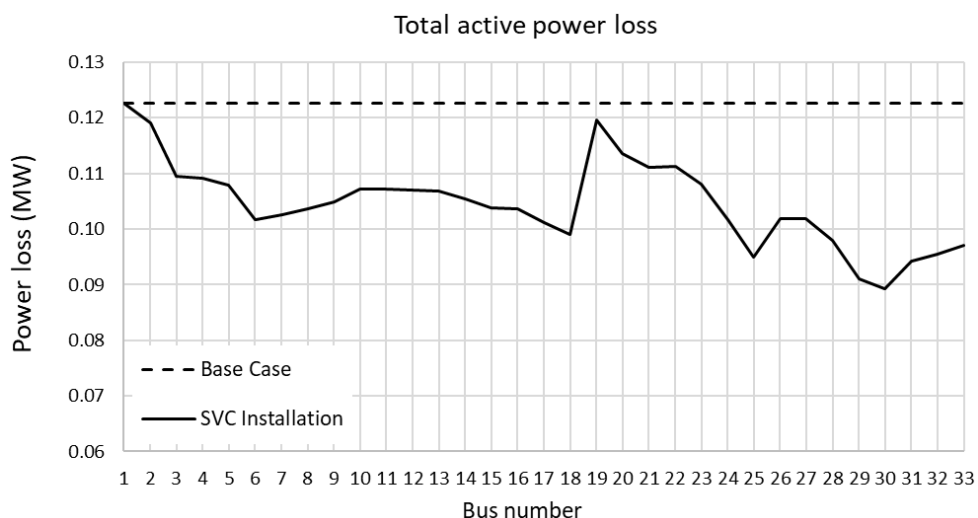


Figure 6.8 Comparison of total active power loss between base case and one SVC installation at each bus

From Table 6.18 and Figure 6.4, the best location of SVC for total active power loss minimization is bus 30. Installing SVC with a size of 0.1496 MVar can reduce the total active power loss from 0.1225 to 0.0893 MW or equal to 27.12%. Moreover, power generation from conventional generator and SVC do not violate the power generation limit as shown in Table 6.19.

Table 6.19 Power generation from conventional generator and SVC at bus30

Bus	Power Generation		Power Generation Limit			
	$P_g$ (MW)	$Q_g$ (MVar)	$P_{max}$ (MW)	$P_{min}$ (MVar)	$Q_{max}$ (MVar)	$Q_{min}$ (MVar)
1	3.8043	0.8695	10	0	10	-10
30	0	1.4958	0	0	4	0

### 6.3.2 Two SVCs

The optimal size of two SVCs at different bus is determined by the proposed ACOPF and presented in this part. Figure 6.9 shows total active power loss when installing two SVC at each bus. The color scale shows the total active power loss from maximum to minimum by red to green scale.

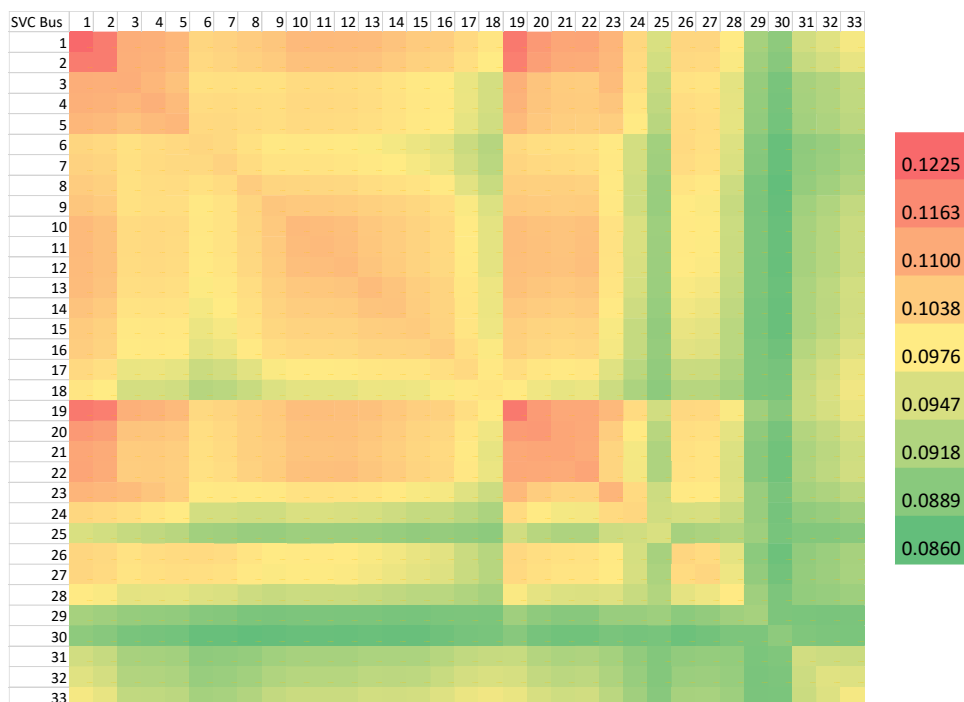


Figure 6.9 Total active power loss when installing two SVCs at each bus

From Figure 6.9, installing SVC at bus 8 and 30 provide the minimum total active power loss. Additionally, the optimal size of SVCs at bus 8 and 30 are shown in Table 6.20.

Table 6.20 Comparison of power loss between base case and two SVCs installation

	SVC Location (bus number)	SVC Size (MVar)	Power Loss	
			$P_{loss}$ (MW)	$Q_{loss}$ (MVar)
Base Case	-	-	0.1225	0.0875
Two SVCs	8	0.6399	0.0860	0.0627
	30	1.2404		

From Table 6.20, Installing SVC at bus 8 with the size of 0.6399 MVar and bus 30 with the size of 1.2404 MVar can minimize power loss. This installation can reduce power loss from 0.1225 to 0.0860 MW or equal to 29.80%. Moreover, active and reactive power generation and total load demand are shown in Table 6.21.

Table 6.21 Power generation when installing SVCs at bus 8 and 30

Bus	Power Generation		Total Load Demand	
	$P_g$ (MW)	$Q_g$ (MVar)	$P_l$ (MW)	$Q_l$ (MVar)
1	3.8010	0.4824	-	-
8	-	0.6399	-	-
30	-	1.2404	-	-
Total	3.8010	2.3627	3.7150	2.300

### 6.3.3 Three SVCs

This part presents the optimal SVC sizes and their corresponding location by employing the proposed method. The optimal site and size of three SVC for power loss minimization are shown in Table 6.22. Moreover, the table shows the comparison results between this case and the base case by sorting the best 3 performance groups which these groups are a set of SVC installing sites.

Table 6.22 Comparison of power loss between base case and three SVCs installation

	SVC Location (bus number)	SVC Size (MVar)	Power Loss	
			$P_{loss}$ (MW)	$Q_{loss}$ (MVar)
Base Case	-	-	0.1225	0.0875
Group 1	8	0.5792	0.0848	0.0619
	24	0.4347		
	30	1.0488		
Group 2	6	0.5207	0.0851	0.0623
	13	0.3143		
	30	1.1241		
Group 3	6	0.5841	0.0855	0.0629
	24	0.4045		
	30	1.0493		

From Table 6.22, Installing SVC at bus 8 with the size of 0.5792 MVar, bus 24 with the size of 0.4347 MVar and bus 30 with the size of 1.0488 MVar can minimize power loss. This installation can reduce power loss from 0.1225 to 0.0848 MW or equal to 30.78%. Moreover, Table 6.23 shows active and reactive power generation and total load demand.

Table 6.23 Power generation data when installing SVCs at bus 8, 24, and 30

Bus	Power Generation		Total Load Demand	
	$P_g$ (MW)	$Q_g$ (MVar)	$P_l$ (MW)	$Q_l$ (MVar)
1	3.7998	0.2992	-	-
8	-	0.5792	-	-
24	-	0.4347	-	-
30	-	1.0488	-	-
Total	3.7998	2.3619	3.7150	2.300

#### 6.4 Installing DG and SVC

This part presents the results obtained by the proposed ACOPF when installing DG and SVC in the 33-bus MATPOWER test system. In this system, the total load demand is 3.715 MW and 2.3 MVar. DG type 1 which generates only active power is used as a new generator. DG sizing is varied from 0–4 MW while SVC sizing is varied from 0–4 MVar. Moreover, this part is divided into 2 cases. The first case is one DG and one SVC. The second case is two DGs and two SVCs.

##### 6.4.1 One DG and One SVC

In this case, the optimal size of one DG and one SVC are determined by the proposed method for power loss minimization. DG and SVC are installed at each bus to analyze the appropriate sites. Figure 6.10 shows total active power loss when installing DG and SVC at each bus. X-axis is defined as DG installed bus, Y-axis is imposed as SVC installed bus, and Z-axis is defined as the total active power loss. In addition, the total active power loss is varied from 0 to 1 MW with blue to yellow.



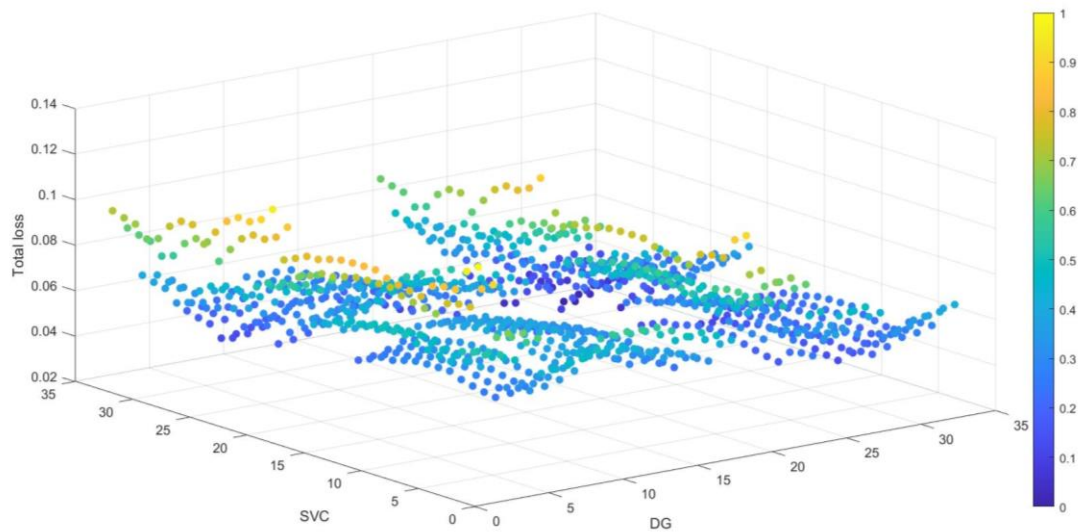


Figure 6.10 Total active power loss when installing DG and SVC at each bus

Installing DG at bus 29 with the size of 2.2844 MW and SVC at bus 30 with the size of 1.5022 MVar is the best site with the optimal sizes for total active power loss minimization. This installation can reduce the power loss from 0.1225 to 0.0281 MW or equal to 77.06%. The result can be summarized as in Table 6.24.

Table 6.24 Comparison of power loss between base case and DG and SVC installation

	DG Bus Number	DG Size (MW)	SVC Bus Number	SVC Size (MVar)	Power Loss	
					$P_{loss}$ (MW)	$Q_{loss}$ (MVar)
Base Case	-	-	-	-	0.1225	0.0875
DG and SVC Installation	29	2.2844	30	1.5022	0.0281	0.0235

In addition, active and reactive power generation data and total load demand are shown in Table 6.25.

Table 6.25 Power generation data when installing DG at bus 29 and SVC at bus 30

Bus	Power Generation		Total Load Demand	
	$P_g$ (MW)	$Q_g$ (MVAr)	$P_l$ (MW)	$Q_l$ (MVAr)
1	1.4587	0.8213	-	-
29	2.2844	-	-	-
30	-	1.5022	-	-
Total	3.7431	2.3235	3.7150	2.300

#### 6.4.2 Two DGs and Two SVCs

The optimal size of two DGs and two SVCs at different bus is determined by the proposed ACOPTF and presented in this part. The optimal site and size of DGs and SVCs for power loss minimization are shown in Table 6.26.

Table 6.26 Comparison of power loss between base case and installing two DGs and two SVCs.

	DG Bus Number	DG Size (MW)	SVC Bus Number	SVC Size (MVAr)	Power Loss	
					$P_{loss}$ (MW)	$Q_{loss}$ (MVAr)
Base Case	-	-	-	-	0.1225	0.0875
DG and SVC Installation	15	0.9613	13	0.4127	0.0144	0.0117
	29	1.7196	30	1.2863		

The best sites of DGs for total active power loss minimization are bus 15 with the size of 0.9613 MW and bus 29 with the size of 1.7196 MW. Additionally, the best sites of SVCs are bus 13 with the size of 0.4127 MVAr and bus 30 with the size of 1.2863 MVAr. This installation can reduce power loss from 0.1225 to 0.0144 MW or equal to 88.24%. Moreover, active and reactive power generation data and total load demand are shown in Table 6.27.

Table 6.27 Power generation when installing two DGs and two SVCs

Bus	Power Generation		Total Load Demand	
	$P_g$ (MW)	$Q_g$ (MVar)	$P_l$ (MW)	$Q_l$ (MVar)
1	1.0485	0.6127	-	-
13	-	0.4127	-	-
15	0.9613	-	-	-
29	1.7196	-	-	-
30	-	1.2863	-	-
Total	3.7294	2.3117	3.7150	2.300

### 6.5 Summary

This section summarizes the numerical results of this work. From the first part, the simulations on base cases which are 9-bus, 24-bus, 33-bus, and 118-bus MATPOWER test systems without installing any device are illustrated. The implementations show that all power system variables do not violate the power system constraints. Some variables reach the limit to verify global optimal solution from optimization theory as shown in the result. Moreover, power generation can supply total loads sufficiently. The total active and reactive power loss using the proposed ACOPF are close to the conventional ACOPF. Thus, the proposed method can solve ACOPF efficiently and reliable. Additionally, the proposed method is not sensitive to the system scale. This method still solves large-scale power systems within polynomial time.

From the remaining case, the simulation results are obtained by the proposed ACOPF in the 33-bus test system are carried out into 3 cases. The first case is installing only DG. The second case is installing only SVC. The last case is installing DG and SVC. The implementations show that the proposed method is applicable to optimize the site and size of DG and SVC. The total active power loss is less than the base case for all cases when DG and SVC are installed in an appropriate site with optimal size. However, the total loss reduction for each case is different. The best case of power loss minimization is the last case. Installing both DG and SVC which

generates active and reactive power to the system provides the lowest power loss. Hence, DG should be deployed close to the load center or high load demand bus. While SVC should be deployed at high reactive power demand bus. When DG cannot be installed at the appropriate site and power system has a small size generation capacity, DG should be installed at the end of the distribution line to reduce the distance between generator and load. Moreover, the more DG and SVC installed, the total power loss is greatly reduced. However, installing DG and SVC too much may provide increased power loss.



## CHAPTER 7

### Conclusion and Future Work

This thesis proposes the conventional alternating current optimal power flow (ACOPF) with second order cone program (SOCP) relaxation for power loss minimization in the power system. In this chapter, the proposed method and the simulation results are summarized. Additionally, the future work of the power loss minimization problem is also presented.

#### 7.1 Conclusion

The conventional ACOPF problem for the power loss objective is formulated as a nonlinear and nonconvex problem. To convexify the ACOPF problem, the SOCP relaxation is applied to minimize the total power loss. The global optimal solution can be obtained from the proposed ACOPF within polynomial time.

To formulate the ACOPF with SOCP relaxation, the thesis has already done on the following methodologies. First, the basic knowledge of the power system is reviewed to consider the power flow analysis. Second, the power system model is reviewed in order to formulate the power flow equations. The conventional ACOPF formulation can be derived in this step. Lastly, convex optimization and SOCP relaxation are considered to convexify the general ACOPF by reformulating the power flow constraints with new variables. Then, the ACOPF becomes the convex optimization. Moreover, one sufficient condition is proposed in this step to guarantee the exactness of the relaxation.

The proposed ACOPF with SOCP relaxation was tested in 4 cases. The first case is a base case which is the test system without installing any device. The second case is a 33-bus test system with installing distributed generation (DG). The third case is a 33-bus test system with installing static var compensator (SVC). The last case is a 33-bus test system with installing DG and SVC. For benchmarking between the proposed ACOPF and the conventional ACOPF in the first case, the

MATPOWER 9-bus, 24-bus, 33-bus, and 118-bus systems are employed as test cases. The numerical results show that all the bus voltage magnitudes, active power generation, and reactive power generation do not violate the system limits. The total power generated can supply the total load demand sufficiently. The optimal value of the objective function from the 2 methods is close. Thereby, the optimal value shows that the proposed method is exact and reliable. Moreover, this method can solve the power loss minimization problem in both radial topology and network topology within polynomial time. For large-scale power systems, the proposed method still solves the ACOPF problem efficiently. From the remaining cases, the results show that installing DG and SVC with optimal size at the appropriate site can reduce the total active power loss from the base case. DG and SVC should be deployed close to the load center or bus with high load demand to have minimum power loss. Additionally, the larger the number of DG and SVC stands, the greater the reduction in power loss. Finally, power loss minimization presents the performance of the power system transmission.

## 7.2 Future Work

This thesis develops the computation of ACOPF problem for power loss minimization with SOCP relaxation and illustrates the example of implementation. However, the work is only applied to the MATPOWER test system which is not the real power system. Therefore, future work can apply the proposed ACOPF to the real power system such as central region power system or Thailand power system to obtain a better objective function value. Moreover, power loss minimization can be adopted in a real power system for planning, scheduling, or improving the power system performance. Furthermore, the proposed ACOPF can solve the power loss minimization problem in large-scale systems but result in higher computational time. Hence, future research can find other convex optimization solvers to improve the computation time. Lastly, the other energy related problems should be explored to use the proposed ACOPF.

## REFERENCES



จุฬาลงกรณ์มหาวิทยาลัย  
**CHULALONGKORN UNIVERSITY**

- [1] บัณฑิต เอื้ออาภรณ์, การวิเคราะห์ระบบไฟฟ้ากำลังเบื้องต้น, กรุงเทพฯ, สำนักพิมพ์ จุฬาลงกรณ์มหาวิทยาลัย, 2547.
- [2] J. D. Glover, M. S. Sarama, and T. Overbye, "Power System Analysis and Design", 5<sup>th</sup> edition, Australia 2011.
- [3] J. A. Momoh, "Optimal power flow with multiple objective functions," The Proceedings of the Twenty-First Annual North American Power Symposium, Rolla, MO, USA, pp. 105-108, 1989.
- [4] J. A. Momoh, R. Adapa and M. E. El-Hawary, "A review of selected optimal power flow literature to 1993. I. Nonlinear and quadratic programming approaches," in IEEE Transactions on Power Systems, vol. 14, no. 1, pp. 96-104, Feb. 1999.
- [5] S. Frank, I. Steponavice, and S. Rebennack, "Optimal power flow: a bibliographic survey I," Energy Syst 3, 221–258, 2012.
- [6] Y. Chen, Y. Li, J. Xiang and X. Shen, "An Optimal Power Flow Formulation with SOCP Relaxation in Radial Network\*," 2018 IEEE 14th International Conference on Control and Automation (ICCA), Anchorage, AK, pp. 921-926, 2018.
- [7] D. K. Molzahn, and I. A. Hiskens, A Survey of Relaxations and Approximations of the Power Flow Equations, now, 2019
- [8] N. Acharya, P. Mahat, and N. Mithulananthan, "An analytical approach for dg allocation in primary distribution network," International Journal of Electrical Power & Energy Systems, vol. 28, no. 10, pp. 669–678, 2006.
- [9] T. Khatib, A. Mohamed, and K. Sopian, "A review of photovoltaic systems size optimization techniques," Renewable and Sustainable Energy Reviews, vol. 22, no. Supplement C, pp. 454 – 465, 2013.



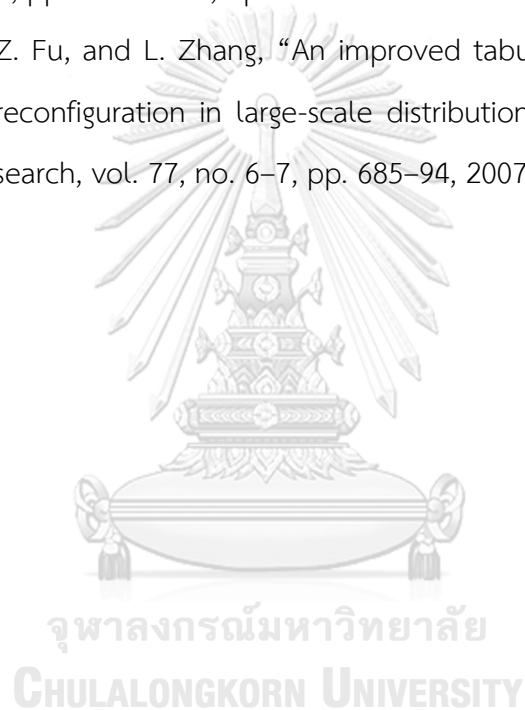
- [10] S. Hong, G. Huang, H. Ren, Y. Hu and H. Xing, "Multi-objective siting and sizing of distributed generation based on the mixed integer second-order cone programming," 8th Renewable Power Generation Conference (RPG 2019), Shanghai, China, pp. 1-6, 2019.
- [11] N. G. Hingorani and L. Gyugyi, Understanding FACTS: Concepts and Technology of Flexible AC Transmission System. New York, NY, USA: Wiley-IEEE Press, 1999.
- [12] X. Zhang et al., "Optimal allocation of static var compensator via mixed integer conic programming," 2017 IEEE Power & Energy Society General Meeting, Chicago, IL, pp. 1-5, 2017.
- [13] F. R. Cabezas Soldevilla and F. A. Cabezas Huerta, "Minimization of Losses in Power Systems by Reactive Power Dispatch using Particle Swarm Optimization," 2019 54th International Universities Power Engineering Conference (UPEC), Bucharest, Romania, pp. 1-5, 2019.
- [14] J. Carpentier, "Contribution to the economic dispatch problem," Bull.sac.france Elect, vol. 3, no. 4, pp. 836–845, 1962.
- [15] H. W. Dommel and W. F. Tinney, "Optimal power flow solutions," IEEE Transactions on Power Apparatus & Systems, vol. PAS-87, no. 10, pp. 1866–1876, 1968.
- [16] B. Kocuk, S. S. Dey, and X. A. Sun, "Strong SOCP Relaxations for the Optimal Power Flow Problem," Operations Research, INFORMS, vol. 64(6), pp. 1177-1196, 2016.
- [17] FERC, "Recent ISO Software Enhancements and Future Software and Modeling Plans," <http://www.ferc.gov/industries/electric/indus-act/rto/rto-iso-soft-2011.pdf>, 2011.
- [18] A. M. Sasson, F. Vilorio, and F. Aboytes, "Optimal load flow solution using the hessian matrix," Power Apparatus & Systems IEEE Transactions on, vol. PAS-92, no. 1, pp. 31–41, 1973.

- [19] W. F. Tinney and C. E. Hart, "Power flow solution by newton's method," *Power Apparatus & Systems IEEE Transactions on*, vol. PAS-86, no. 11, pp. 1449–1460, 2007.
- [20] A. M. H. Rashed and D. H. Kelly, "Optimal load flow solution using lagrangian multipliers and the hessian matrix," *IEEE Transactions on Power Apparatus & Systems*, vol. 94, no. 5, pp. 1292–1297, 1974.
- [21] S. Frank, I. Steponavice, and S. Rebennack, "Optimal power flow: a bibliographic survey II," *Energy Syst* 3, 221–258, 2012.
- [22] X. Bai, H. Wei, K. Fujisawa, and Y. Wang, "Semidefinite programming for optimal power flow problems," *International Journal of Electrical Power & Energy Systems*, vol. 30, no. 67, pp. 383–392, 2008.
- [23] R. Madani, S. Sojoudi, and J. Lavaei, "Convex relaxation for optimal power flow problem: Mesh networks," *IEEE Transactions on Power Systems*, vol. 30, no. 1, pp. 199–211, 2014.
- [24] LavaeiJ and LowSH, "Zero duality gap in optimal power flow problem," *Power Systems IEEE Transactions on*, vol. 27, no. 1, pp. 92–107, 2012.
- [25] B. Zhang, and D. Tse, "Geometry of feasible injection region of power networks," 49th Annual Allerton Conference on Communication, Control, and Computing (Allerton), Dec. 2011.
- [26] S. Sojoudi, and J. Lavaei, "Physics of power networks makes hard optimization problems easy to solve," *IEEE Power and Energy Society General Meeting*, pp. 1–8, 2012.
- [27] B. Zhang, and D. Tse, "Geometry of feasible injection region of power networks," *IEEE Transactions on Power Systems*, vol. 28, no. 2, pp. 788–797, 2013.
- [28] J. Lavaei, D. Tse and B. Zhang, "Geometry of Power Flows and Optimization in Distribution Networks," in *IEEE Transactions on Power Systems*, vol. 29, no. 2, pp. 572–583, March 2014.

- [29] R. A. Jabr, "Radial distribution load flow using conic programming," in *IEEE Transactions on Power Systems*, vol. 21, no. 3, pp. 1458-1459, Aug. 2006.
- [30] M. Farivar and S. H. Low, "Branch flow model: Relaxations and convexification," in *Decision and Control*, pp. 3672–3679, 2012.
- [31] B. Kocuk, S. S. Dey, and X. A. Sun, "Strong socp relaxations for the optimal power flow problem," *Operations Research*, vol. 64, pp. 1177–1196, 2015.
- [32] Y. Chen, J. Xiang, and Y. Li, "SOCP Relaxations of Optimal Power Flow Problem Considering Current Margins in Radial Networks," *Energies*, vol. 11, pp. 1-17, Nov. 2018.
- [33] S. Ikeda, A. Takeda, and H. Ohmori, "Optimal sizing of photovoltaic systems for loss minimization in distribution network," 2018 SICE International Symposium on Control Systems (SICE ISCS), Tokyo, Japan, pp. 185-192, 2018.
- [34] M. S. Srinivas, "Distribution load flows: a brief review," 2000 IEEE Power Engineering Society Winter Meeting. Conference Proceedings (Cat. No.00CH37077), Singapore, pp. 942-945, 2000.
- [35] J. Arrillaga, and N. Watson, "Computer Modelling of Electrical Power Systems, Second Edition," A Wiley-Interscience publication, 2013.
- [36] R. Nadira, S. Benchluch and C. A. Dortolina, "A novel approach to computing distribution losses," 2003 IEEE PES Transmission and Distribution Conference and Exposition (IEEE Cat. No.03CH37495), Dallas, TX, USA, pp. 659-663, 2003.
- [37] C. C. B. Oliveira, N. Kagan, A. Meffe, S. Jonathan, S. Caparroz and J. L. Cavaretti, "A new method for the computation of technical losses in electrical power distribution systems," 16th International Conference and Exhibition on Electricity Distribution, 2001.
- [38] E. Acha, C. R. Fuerte Esquivel, H. Ambriz Pérez, C. Angeles Camacho: *FACTS: Modelling and Simulation in Power Networks*. John Wiley and Sons, 2004.
- [39] W. D. Jr. Stevenson, *Elements of Power System Analysis*, 4th ed. New York, McGraw-Hill, 1982.

- [40] J. Rahul, Y. Sharma and D. Birla, "A New Attempt to Optimize Optimal Power Flow Based Transmission Losses Using Genetic Algorithm," 2012 Fourth International Conference on Computational Intelligence and Communication Networks, Mathura, 2012, pp. 566-570.
- [41] S. P. Boyd and L. Vandenberghe, *Convex Optimization*, Cambridge, U.K. Cambridge Univ. Press, 2004.
- [42] M. Lobo, L. Vandenberghe, S. Boyd, and H. Lebert, "Applications of second-order cone programming," *Linear Algebra and Its Applications*, pp.193-284, 1998.
- [43] สุรชัย ชัยทัศนีย์, พลังงานหมุนเวียนและการผลิตไฟฟ้าแบบกระจายตัว, กรุงเทพฯ, สำนักพิมพ์จุฬาลงกรณ์มหาวิทยาลัย, 2557.
- [44] B. Hussain, A. Amin, A. Mahmood and M. Usman, "An Optimal Site Selection for Distributed Generation in the Distribution Network by QPSO Algorithm," 2020 International Conference on Engineering and Emerging Technologies (ICEET), pp. 1-6, 2020.
- [45] P. Gupta, M. Pandit and D. P. Kothari, "A review on optimal sizing and siting of distributed generation system: Integrating distributed generation into the grid," 2014 6th IEEE Power India International Conference (PIICON), pp. 1-6, 2014.
- [46] การไฟฟ้านครหลวง, ระเบียบการไฟฟ้านครหลวงว่าด้วยข้อกำหนดการเชื่อมต่อระบบโครงข่ายไฟฟ้า พ.ศ. 2558. 2558: กรุงเทพมหานคร.
- [47] A. A. Abdulrazzaq, M. Eremia, L. Toma and C. A. Mandis, "Optimal location and size of SVC for power losses minimization and voltage security improvement," 2015 9th International Symposium on Advanced Topics in Electrical Engineering (ATEE), pp. 858-863, 2015.
- [48] B. Vardani, "Optimum Location of SVC in an IEEE 33 Bus Radial Distribution System Using Power Sensitivity Index," 2019 International Conference on Electrical, Electronics and Computer Engineering (UPCON), pp. 1-5, 2019.

- [49] R.P. Schulz, A.E. Turner and D.N. Ewart, “Long Term Power System Dynamics,” EPRI Report 90-7-0, Palo Alto, California, 1974.
- [50] IEEE Reliability Test System Task Force of Applications of Probability Methods Subcommittee, “IEEE reliability test system-96,” IEEE Transactions on Power Systems, Vol. 14, No. 3, pp. 1010-1020, Aug. 1999.
- [51] M. E. Baran and F. F. Wu, “Network reconfiguration in distribution systems for loss reduction and load balancing,” in IEEE Transactions on Power Delivery, vol. 4, no. 2, pp. 1401-1407, Apr 1989.
- [52] D. Zhang, Z. Fu, and L. Zhang, “An improved tabu search algorithm for loss minimum reconfiguration in large-scale distribution systems,” Electric Power System Research, vol. 77, no. 6–7, pp. 685–94, 2007.





## APPENDIX

## A. Data of Test Systems

## A.1 9-Bus Test System

The test system consists of 3 generators, 6 load buses, and 9 branches. Let bus type 1 denotes load bus, 2 denotes voltage bus, and 3 denotes slack bus. The data of the system is shown in Table A.1-A.3 where the system complex power base is 100 MVA.

Table A.1 Bus data of 9-bus test system

Bus	Bus type	$P_d$ (MW)	$Q_d$ (MVar)	Area	$ V $ (p.u.)	$\theta$ (deg.)	Voltage base (kV)	$V_{max}$ (p.u.)	$V_{min}$ (p.u.)
1	3	0	0	1	1	0	345	1.1	0.9
2	2	0	0	1	1	0	345	1.1	0.9
3	2	0	0	1	1	0	345	1.1	0.9
4	1	0	0	1	1	0	345	1.1	0.9
5	1	90	30	1	1	0	345	1.1	0.9
6	1	0	0	1	1	0	345	1.1	0.9
7	1	100	35	1	1	0	345	1.1	0.9
8	1	0	0	1	1	0	345	1.1	0.9
9	1	125	50	1	1	0	345	1.1	0.9

Table A.2 Generator data of 9-bus test system

Bus	$P_g$ (MW)	$Q_g$ (MVar)	$Q_{max}$ (MVar)	$Q_{min}$ (MVar)	$V_g$ (p.u.)	$P_{max}$ (MW)	$P_{min}$ (MW)
1	72.30	27.03	300	-300	1.040	250	10
2	163.00	6.54	300	-300	1.025	300	10
3	85.00	-10.95	300	-300	1.025	270	10

Table A.3 Branch data of 9-bus test system

Branch	From bus	To bus	$R$ (p.u.)	$X$ (p.u.)	$B_c$ (p.u.)	Line limit (MVA)
1	1	4	0.000	0.058	0.000	250
2	4	5	0.017	0.092	0.158	250
3	5	6	0.039	0.170	0.358	150
4	3	6	0.000	0.059	0.000	300
5	6	7	0.0119	0.101	0.209	150
6	7	8	0.009	0.072	0.149	250
7	8	2	0.000	0.062	0.000	250
8	8	9	0.032	0.161	0.306	250
9	9	4	0.010	0.085	0.176	250

## A.2 24-Bus Test System

The test system consists of 33 generators, 17 load buses, and 38 branches. The system is divided into 4 area. The information of the system is shown in Table A.4-A.6 where the system complex power base is 100 MVA.

Table A.4 Bus data of 24-bus test system

Bus	Bus type	$P_d$ (MW)	$Q_d$ (MVar)	Area	$ V $ (p.u.)	$\theta$ (deg.)	$V_{base}$ (kV)	$V_{max}$ (p.u.)	$V_{min}$ (p.u.)
1	2	108	22	1	1	0	138	1.05	0.95
2	2	97	20	1	1	0	138	1.05	0.95
3	1	180	37	1	1	0	138	1.05	0.95
4	1	74	15	1	1	0	138	1.05	0.95
5	1	71	14	1	1	0	138	1.05	0.95
6	1	136	28	2	1	0	138	1.05	0.95
7	2	125	25	2	1	0	138	1.05	0.95
8	1	171	35	2	1	0	138	1.05	0.95
9	1	175	36	1	1	0	138	1.05	0.95



Bus	Bus type	$P_d$ (MW)	$Q_d$ (MVar)	Area	$ V $ (p.u.)	$\theta$ (deg.)	$V_{base}$ (kV)	$V_{max}$ (p.u.)	$V_{min}$ (p.u.)
10	1	195	40	2	1	0	138	1.05	0.95
11	1	0	0	3	1	0	230	1.05	0.95
12	1	0	0	3	1	0	230	1.05	0.95
13	3	265	54	3	1	0	230	1.05	0.95
14	2	194	39	3	1	0	230	1.05	0.95
15	2	317	64	4	1	0	230	1.05	0.95
16	2	100	20	4	1	0	230	1.05	0.95
17	1	0	0	4	1	0	230	1.05	0.95
18	2	333	68	4	1	0	230	1.05	0.95
19	1	181	37	3	1	0	230	1.05	0.95
20	1	128	26	3	1	0	230	1.05	0.95
21	2	0	0	4	1	0	230	1.05	0.95
22	2	0	0	4	1	0	230	1.05	0.95
23	2	0	0	3	1	0	230	1.05	0.95
24	1	0	0	4	1	0	230	1.05	0.95

Table A.5 Generator data of 24-bus test system

Bus	$P_g$ (MW)	$Q_g$ (MVar)	$Q_{max}$ (MVar)	$Q_{min}$ (MVar)	$V_g$ (p.u.)	$P_{max}$ (MW)	$P_{min}$ (MW)
1	10.0	0	10	0	1.035	20.0	16.0
1	10.0	0	10	0	1.035	20.0	16.0
1	76.0	0	30	-25	1.035	76.0	15.2
1	76.0	0	30	-25	1.035	76.0	15.2
2	10.0	0	10	0	1.035	20.0	16.0
2	10.0	0	10	0	1.035	20.0	16.0
2	76.0	0	30	-25	1.035	76.0	15.2
2	76.0	0	30	-25	1.035	76.0	15.2

Bus	$P_g$ (MW)	$Q_g$ (MVar)	$Q_{max}$ (MVar)	$Q_{min}$ (MVar)	$V_g$ (p.u.)	$P_{max}$ (MW)	$P_{min}$ (MW)
7	80.0	0	60	0	1.025	100.0	25.0
7	80.0	0	60	0	1.025	100.0	25.0
7	80.0	0	60	0	1.025	100.0	25.0
13	95.1	0	80	0	1.020	197.0	69.0
13	95.1	0	80	0	1.020	197.0	69.0
13	95.1	0	80	0	1.020	197.0	69.0
14	0.0	35.3	200	-50	0.980	0.0	0.0
15	12.0	0	6	0	1.014	12.0	2.4
15	12.0	0	6	0	1.014	12.0	2.4
15	12.0	0	6	0	1.014	12.0	2.4
15	12.0	0	6	0	1.014	12.0	2.4
15	12.0	0	6	0	1.014	12.0	2.4
15	155.0	0	80	-50	1.014	155.0	54.3
16	155.0	0	80	-50	1.017	155.0	54.3
18	400.0	0	200	-50	1.050	400.0	100.0
21	400.0	0	200	-50	1.050	400.0	100.0
22	50.0	0	16	-10	1.050	50.0	10.0
22	50.0	0	16	-10	1.050	50.0	10.0
22	50.0	0	16	-10	1.050	50.0	10.0
22	50.0	0	16	-10	1.050	50.0	10.0
22	50.0	0	16	-10	1.050	50.0	10.0
22	50.0	0	16	-10	1.050	50.0	10.0
22	50.0	0	16	-10	1.050	50.0	10.0
23	155.0	0	80	-50	1.050	155.0	54.3
23	155.0	0	80	-50	1.050	155.0	54.3
23	350.0	0	150	-25	1.050	350.0	140.0

Table A.6 Branch data of 24-bus test system

Branch	From bus	To bus	$R$ (p.u.)	$X$ (p.u.)	$B_c$ (p.u.)	Line limit (MVA)
1	1	2	0.0026	0.0139	0.4611	175
2	1	3	0.0546	0.2112	0.0572	175
3	1	5	0.0218	0.0845	0.0229	175
4	2	4	0.0328	0.1267	0.0343	175
5	2	6	0.0497	0.1920	0.0520	175
6	3	9	0.0308	0.1190	0.0322	175
7	3	24	0.0023	0.0839	0.0000	400
8	4	9	0.0268	0.1037	0.0281	175
9	5	10	0.0228	0.0883	0.0239	175
10	6	10	0.0139	0.0605	2.4590	175
11	7	8	0.0159	0.0614	0.0166	175
12	8	9	0.0427	0.1651	0.0447	175
13	8	10	0.0427	0.1651	0.0447	175
14	9	11	0.0023	0.0839	0.0000	400
15	9	12	0.0023	0.0839	0.0000	400
16	10	11	0.0023	0.0839	0.0000	400
17	10	12	0.0023	0.0839	0.0000	400
18	11	13	0.0061	0.0476	0.0999	500
19	11	14	0.0054	0.0418	0.0879	500
20	12	13	0.0061	0.0476	0.0999	500
21	12	23	0.0124	0.0966	0.2030	500
22	13	23	0.0111	0.0865	0.1818	500
23	14	16	0.005	0.0389	0.0818	500
24	15	16	0.0022	0.0173	0.0364	500
25	15	21	0.0063	0.0490	0.1030	500
26	15	21	0.0063	0.0490	0.1030	500

Branch	From bus	To bus	$R$ (p.u.)	$X$ (p.u.)	$B_c$ (p.u.)	Line limit (MVA)
27	15	24	0.0067	0.0519	0.1091	500
28	16	17	0.0033	0.0259	0.0545	500
29	16	19	0.003	0.0231	0.0485	500
30	17	18	0.0018	0.0144	0.0303	500
31	17	22	0.0135	0.1053	0.2212	500
32	18	21	0.0033	0.0259	0.0545	500
33	18	21	0.0033	0.0259	0.0545	500
34	19	20	0.0051	0.0396	0.0833	500
35	19	20	0.0051	0.0396	0.0833	500
36	20	23	0.0028	0.0216	0.0455	500
37	20	23	0.0028	0.0216	0.0455	500
38	21	22	0.0087	0.0678	0.1424	500

### A.3 33-Bus Test System

The test system consists of 1 generator, 32 load buses, and 37 branches. The information of the system is shown in Table A.7-A.9 where the system complex power base is 100 MVA.

Table A.7 Bus data of 33-bus test system

Bus	Bus type	$P_d$ (kW)	$Q_d$ (kVAr)	Area	$ V $ (p.u.)	$\theta$ (deg.)	$V_{base}$ (kV)	$V_{max}$ (p.u.)	$V_{min}$ (p.u.)
1	3	0	0	1	1	0	12.66	1.0	1.0
2	1	100	60	1	1	0	12.66	1.1	0.9
3	1	90	40	1	1	0	12.66	1.1	0.9
4	1	120	80	1	1	0	12.66	1.1	0.9
5	1	60	30	1	1	0	12.66	1.1	0.9
6	1	60	20	1	1	0	12.66	1.1	0.9
7	1	200	100	1	1	0	12.66	1.1	0.9

Bus	Bus type	$P_d$ (kW)	$Q_d$ (kVAr)	Area	$ V $ (p.u.)	$\theta$ (deg.)	$V_{base}$ (kV)	$V_{max}$ (p.u.)	$V_{min}$ (p.u.)
8	1	200	100	1	1	0	12.66	1.1	0.9
9	1	60	20	1	1	0	12.66	1.1	0.9
10	1	60	20	1	1	0	12.66	1.1	0.9
11	1	45	30	1	1	0	12.66	1.1	0.9
12	1	60	35	1	1	0	12.66	1.1	0.9
13	1	60	35	1	1	0	12.66	1.1	0.9
14	1	120	80	1	1	0	12.66	1.1	0.9
15	1	60	10	1	1	0	12.66	1.1	0.9
16	1	60	20	1	1	0	12.66	1.1	0.9
17	1	60	20	1	1	0	12.66	1.1	0.9
18	1	90	40	1	1	0	12.66	1.1	0.9
19	1	90	40	1	1	0	12.66	1.1	0.9
20	1	90	40	1	1	0	12.66	1.1	0.9
21	1	90	40	1	1	0	12.66	1.1	0.9
22	1	90	40	1	1	0	12.66	1.1	0.9
23	1	90	50	1	1	0	12.66	1.1	0.9
24	1	420	200	1	1	0	12.66	1.1	0.9
25	1	420	200	1	1	0	12.66	1.1	0.9
26	1	60	25	1	1	0	12.66	1.1	0.9
27	1	60	25	1	1	0	12.66	1.1	0.9
28	1	60	20	1	1	0	12.66	1.1	0.9
29	1	120	70	1	1	0	12.66	1.1	0.9
30	1	200	600	1	1	0	12.66	1.1	0.9
31	1	150	70	1	1	0	12.66	1.1	0.9
32	1	210	100	1	1	0	12.66	1.1	0.9
33	1	60	40	1	1	0	12.66	1.1	0.9

Table A.8 Generator data of 33-bus test system

Bus	$P_g$ (MW)	$Q_g$ (MVar)	$Q_{max}$ (MVar)	$Q_{min}$ (MVar)	$V_g$ (p.u.)	$P_{max}$ (MW)	$P_{min}$ (MW)
1	0	0	10	-10	1	10	0

Table A.9 Branch data of 33-bus test system

Branch	From bus	To bus	$R$ (p.u.)	$X$ (p.u.)	$B_c$ (p.u.)	Line limit (MVA)
1	1	2	0.0922	0.0470	0	0
2	2	3	0.4930	0.2511	0	0
3	3	4	0.3660	0.1864	0	0
4	4	5	0.3811	0.1941	0	0
5	5	6	0.8190	0.7070	0	0
6	6	7	0.1872	0.6188	0	0
7	7	8	0.7114	0.2351	0	0
8	8	9	1.0300	0.7400	0	0
9	9	10	1.0440	0.7400	0	0
10	10	11	0.1966	0.0650	0	0
11	11	12	0.3744	0.1238	0	0
12	12	13	1.4680	1.1550	0	0
13	13	14	0.5416	0.7129	0	0
14	14	15	0.5910	0.5260	0	0
15	15	16	0.7463	0.5450	0	0
16	16	17	1.2890	1.7210	0	0
17	17	18	0.7320	0.5740	0	0
18	2	19	0.1640	0.1565	0	0
19	19	20	1.5042	1.3554	0	0
20	20	21	0.4095	0.4784	0	0
21	21	22	0.7089	0.9373	0	0
22	3	23	0.4512	0.3083	0	0

Branch	From bus	To bus	$R$ (p.u.)	$X$ (p.u.)	$B_c$ (p.u.)	Line limit (MVA)
23	23	24	0.8980	0.7091	0	0
24	24	25	0.8960	0.7011	0	0
25	6	26	0.2030	0.1034	0	0
26	26	27	0.2842	0.1447	0	0
27	27	28	1.0590	0.9337	0	0
28	28	29	0.8042	0.7006	0	0
29	29	30	0.5075	0.2585	0	0
30	30	31	0.9744	0.9630	0	0
31	31	32	0.3105	0.3619	0	0
32	32	33	0.3410	0.5302	0	0

#### A.4 118-Bus Test System

The test system comprises 54 generators, 64 load buses, and 186 branches. The information of the system is shown in Table A.10-A.12 where the system complex power base is 100 MVA.

Table A.10 Bus data of 118-bus test system

Bus	Bus type	$P_d$ (MW)	$Q_d$ (MVar)	Area	$ V $ (p.u.)	$\theta$ (deg.)	$V_{base}$ (kV)	$V_{max}$ (p.u.)	$V_{min}$ (p.u.)
1	2	51	27	1	0.955	10.67	138	1.06	0.94
2	1	20	9	1	0.971	11.22	138	1.06	0.94
3	1	39	10	1	0.968	11.56	138	1.06	0.94
4	2	39	12	1	0.998	15.28	138	1.06	0.94
5	1	0	0	1	1.002	15.73	138	1.06	0.94
6	2	52	22	1	0.990	13.00	138	1.06	0.94
7	1	19	2	1	0.989	12.56	138	1.06	0.94
8	2	28	0	1	1.015	20.77	345	1.06	0.94
9	1	0	0	1	1.043	28.02	345	1.06	0.94

Bus	Bus type	$P_d$ (MW)	$Q_d$ (MVar)	Area	$ V $ (p.u.)	$\theta$ (deg.)	$V_{base}$ (kV)	$V_{max}$ (p.u.)	$V_{min}$ (p.u.)
10	2	0	0	1	1.050	35.61	345	1.06	0.94
11	1	70	23	1	0.985	12.72	138	1.06	0.94
12	2	47	10	1	0.990	12.20	138	1.06	0.94
13	1	34	16	1	0.968	11.35	138	1.06	0.94
14	1	14	1	1	0.984	11.50	138	1.06	0.94
15	2	90	30	1	0.970	11.23	138	1.06	0.94
16	1	25	10	1	0.984	11.91	138	1.06	0.94
17	1	11	3	1	0.995	13.74	138	1.06	0.94
18	2	60	34	1	0.973	11.53	138	1.06	0.94
19	2	45	25	1	0.963	11.05	138	1.06	0.94
20	1	18	3	1	0.958	11.93	138	1.06	0.94
21	1	14	8	1	0.959	13.52	138	1.06	0.94
22	1	10	5	1	0.970	16.08	138	1.06	0.94
23	1	7	3	1	1.000	21.00	138	1.06	0.94
24	2	13	0	1	0.992	20.89	138	1.06	0.94
25	2	0	0	1	1.050	27.93	138	1.06	0.94
26	2	0	0	1	1.015	29.71	345	1.06	0.94
27	2	71	13	1	0.968	15.35	138	1.06	0.94
28	1	17	7	1	0.962	13.62	138	1.06	0.94
29	1	24	4	1	0.963	12.63	138	1.06	0.94
30	1	0	0	1	0.968	18.79	345	1.06	0.94
31	2	43	27	1	0.967	12.75	138	1.06	0.94
32	2	59	23	1	0.964	14.80	138	1.06	0.94
33	1	23	9	1	0.972	10.63	138	1.06	0.94
34	2	59	26	1	0.986	11.30	138	1.06	0.94
35	1	33	9	1	0.981	10.87	138	1.06	0.94
36	2	31	17	1	0.980	10.87	138	1.06	0.94
37	1	0	0	1	0.992	11.77	138	1.06	0.94



Bus	Bus type	$P_d$ (MW)	$Q_d$ (MVar)	Area	$ V $ (p.u.)	$\theta$ (deg.)	$V_{base}$ (kV)	$V_{max}$ (p.u.)	$V_{min}$ (p.u.)
38	1	0	0	1	0.962	16.91	345	1.06	0.94
39	1	27	11	1	0.970	8.41	138	1.06	0.94
40	2	66	23	1	0.970	7.35	138	1.06	0.94
41	1	37	10	1	0.967	6.92	138	1.06	0.94
42	2	96	23	1	0.985	8.53	138	1.06	0.94
43	1	18	7	1	0.978	11.28	138	1.06	0.94
44	1	16	8	1	0.985	13.82	138	1.06	0.94
45	1	53	22	1	0.987	15.67	138	1.06	0.94
46	2	28	10	1	1.005	18.49	138	1.06	0.94
47	1	34	0	1	1.017	20.73	138	1.06	0.94
48	1	20	11	1	1.021	19.93	138	1.06	0.94
49	2	87	30	1	1.025	20.94	138	1.06	0.94
50	1	17	4	1	1.001	18.90	138	1.06	0.94
51	1	17	8	1	0.967	16.28	138	1.06	0.94
52	1	18	5	1	0.957	15.32	138	1.06	0.94
53	1	23	11	1	0.946	14.35	138	1.06	0.94
54	2	113	32	1	0.955	15.26	138	1.06	0.94
55	2	63	22	1	0.952	14.97	138	1.06	0.94
56	2	84	18	1	0.954	15.16	138	1.06	0.94
57	1	12	3	1	0.971	16.36	138	1.06	0.94
58	1	12	3	1	0.959	15.51	138	1.06	0.94
59	2	277	113	1	0.985	19.37	138	1.06	0.94
60	1	78	3	1	0.993	23.15	138	1.06	0.94
61	2	0	0	1	0.995	24.04	138	1.06	0.94
62	2	77	14	1	0.998	23.43	138	1.06	0.94
63	1	0	0	1	0.969	22.75	345	1.06	0.94
64	1	0	0	1	0.984	24.52	345	1.06	0.94
65	2	0	0	1	1.005	27.65	345	1.06	0.94

Bus	Bus type	$P_d$ (MW)	$Q_d$ (MVar)	Area	$ V $ (p.u.)	$\theta$ (deg.)	$V_{base}$ (kV)	$V_{max}$ (p.u.)	$V_{min}$ (p.u.)
66	2	39	18	1	1.050	27.48	138	1.06	0.94
67	1	28	7	1	1.020	24.84	138	1.06	0.94
68	1	0	0	1	1.003	27.55	345	1.06	0.94
69	3	0	0	1	1.035	30.00	138	1.06	0.94
70	2	66	20	1	0.984	22.58	138	1.06	0.94
71	1	0	0	1	0.987	22.15	138	1.06	0.94
72	2	12	0	1	0.980	20.98	138	1.06	0.94
73	2	6	0	1	0.991	21.94	138	1.06	0.94
74	2	68	27	1	0.958	21.64	138	1.06	0.94
75	1	47	11	1	0.967	22.91	138	1.06	0.94
76	2	68	36	1	0.943	21.77	138	1.06	0.94
77	2	61	28	1	1.006	26.72	138	1.06	0.94
78	1	71	26	1	1.003	26.42	138	1.06	0.94
79	1	39	32	1	1.009	26.72	138	1.06	0.94
80	2	130	26	1	1.040	28.96	138	1.06	0.94
81	1	0	0	1	0.997	28.10	345	1.06	0.94
82	1	54	27	1	0.989	27.24	138	1.06	0.94
83	1	20	10	1	0.985	28.42	138	1.06	0.94
84	1	11	7	1	0.980	30.95	138	1.06	0.94
85	2	24	15	1	0.985	32.51	138	1.06	0.94
86	1	21	10	1	0.987	31.14	138	1.06	0.94
87	2	0	0	1	1.015	31.40	161	1.06	0.94
88	1	48	10	1	0.987	35.64	138	1.06	0.94
89	2	0	0	1	1.005	39.69	138	1.06	0.94
90	2	163	42	1	0.985	33.29	138	1.06	0.94
91	2	10	0	1	0.980	33.31	138	1.06	0.94
92	2	65	10	1	0.993	33.80	138	1.06	0.94
93	1	12	7	1	0.987	30.79	138	1.06	0.94

Bus	Bus type	$P_d$ (MW)	$Q_d$ (MVar)	Area	$ V $ (p.u.)	$\theta$ (deg.)	$V_{base}$ (kV)	$V_{max}$ (p.u.)	$V_{min}$ (p.u.)
94	1	30	16	1	0.991	28.64	138	1.06	0.94
95	1	42	31	1	0.981	27.67	138	1.06	0.94
96	1	38	15	1	0.993	27.51	138	1.06	0.94
97	1	15	9	1	1.011	27.88	138	1.06	0.94
98	1	34	8	1	1.024	27.40	138	1.06	0.94
99	2	42	0	1	1.010	27.04	138	1.06	0.94
100	2	37	18	1	1.017	28.03	138	1.06	0.94
101	1	22	15	1	0.993	29.61	138	1.06	0.94
102	1	5	3	1	0.991	32.30	138	1.06	0.94
103	2	23	16	1	1.001	24.44	138	1.06	0.94
104	2	38	25	1	0.971	21.69	138	1.06	0.94
105	2	31	26	1	0.965	20.57	138	1.06	0.94
106	1	43	16	1	0.962	20.32	138	1.06	0.94
107	2	50	12	1	0.952	17.53	138	1.06	0.94
108	1	2	1	1	0.967	19.38	138	1.06	0.94
109	1	8	3	1	0.967	18.93	138	1.06	0.94
110	2	39	30	1	0.973	18.09	138	1.06	0.94
111	2	0	0	1	0.980	19.74	138	1.06	0.94
112	2	68	13	1	0.975	14.99	138	1.06	0.94
113	2	6	0	1	0.993	13.74	138	1.06	0.94
114	1	8	3	1	0.960	14.46	138	1.06	0.94
115	1	22	7	1	0.960	14.46	138	1.06	0.94
116	2	184	0	1	1.005	27.12	138	1.06	0.94
117	1	20	8	1	0.974	10.67	138	1.06	0.94
118	1	33	15	1	0.949	21.92	138	1.06	0.94

Table A.11 Generator data of 118-bus test system

Bus	$P_g$ (MW)	$Q_g$ (MVar)	$Q_{max}$ (MVar)	$Q_{min}$ (MVar)	$V_g$ (p.u.)	$P_{max}$ (MW)	$P_{min}$ (MW)
1	0	0	15	-5	0.955	100	0
4	0	0	300	-300	0.998	100	0
6	0	0	50	-13	0.990	100	0
8	0	0	300	-300	1.015	100	0
10	450	0	200	-147	1.050	550	0
12	85	0	120	-35	0.990	185	0
15	0	0	30	-10	0.970	100	0
18	0	0	50	-16	0.973	100	0
19	0	0	24	-8	0.962	100	0
24	0	0	300	-300	0.992	100	0
25	220	0	140	-47	1.050	320	0
26	314	0	1000	-1000	1.015	414	0
27	0	0	300	-300	0.968	100	0
31	7	0	300	-300	0.967	107	0
32	0	0	42	-14	0.963	100	0
34	0	0	24	-8	0.984	100	0
36	0	0	24	-8	0.980	100	0
40	0	0	300	-300	0.970	100	0
42	0	0	300	-300	0.985	100	0
46	19	0	100	-100	1.005	119	0
49	204	0	210	-85	1.025	304	0
54	48	0	300	-300	0.955	148	0
55	0	0	23	-8	0.952	100	0
56	0	0	15	-8	0.954	100	0
59	155	0	180	-60	0.985	255	0
61	160	0	300	-100	0.995	260	0
62	0	0	20	-20	0.998	100	0

Bus	$P_g$ (MW)	$Q_g$ (MVar)	$Q_{max}$ (MVar)	$Q_{min}$ (MVar)	$V_g$ (p.u.)	$P_{max}$ (MW)	$P_{min}$ (MW)
65	391	0	200	-67	1.005	491	0
66	392	0	200	-67	1.050	492	0
69	516.4	0	300	-300	1.035	805.2	0
70	0	0	32	-10	0.984	100	0
72	0	0	100	-100	0.980	100	0
73	0	0	100	-100	0.991	100	0
74	0	0	9	-6	0.958	100	0
76	0	0	23	-8	0.943	100	0
77	0	0	70	-20	1.006	100	0
80	477	0	280	-165	1.040	577	0
85	0	0	23	-8	0.985	100	0
87	4	0	1000	-100	1.015	104	0
89	607	0	300	-210	1.005	707	0
90	0	0	300	-300	0.985	100	0
91	0	0	100	-100	0.980	100	0
92	0	0	9	-3	0.990	100	0
99	0	0	100	-100	1.010	100	0
100	252	0	155	-50	1.017	352	0
103	40	0	40	-15	1.010	140	0
104	0	0	23	-8	0.971	100	0
105	0	0	23	-8	0.965	100	0
107	0	0	200	-200	0.952	100	0
110	0	0	23	-8	0.973	100	0
111	36	0	1000	-100	0.980	136	0
112	0	0	1000	-100	0.975	100	0
113	0	0	200	-100	0.993	100	0
116	0	0	1000	-1000	1.005	100	0

Table A.12 Branch data of 118-bus test system

Branch	From bus	To bus	$R$ (p.u.)	$X$ (p.u.)	$B_c$ (p.u.)	Line limit (MVA)
1	1	2	0.0303	0.0999	0.0254	0
2	1	3	0.0129	0.0424	0.0108	0
3	4	5	0.0018	0.0080	0.0021	0
4	3	5	0.0241	0.1080	0.0284	0
5	5	6	0.0119	0.0540	0.0143	0
6	6	7	0.0046	0.0208	0.0055	0
7	8	9	0.0024	0.0305	1.1620	0
8	8	5	0.0000	0.0267	0.0000	0
9	9	10	0.0026	0.0322	1.2300	0
10	4	11	0.0209	0.0688	0.0175	0
11	5	11	0.0203	0.0682	0.0174	0
12	11	12	0.0060	0.0196	0.0050	0
13	2	12	0.0187	0.0616	0.0157	0
14	3	12	0.0484	0.1600	0.0406	0
15	7	12	0.0086	0.0340	0.0087	0
16	11	13	0.0223	0.0731	0.0188	0
17	12	14	0.0215	0.0707	0.0182	0
18	13	15	0.0744	0.2444	0.0627	0
19	14	15	0.0595	0.1950	0.0502	0
20	12	16	0.0212	0.0834	0.0214	0
21	15	17	0.0132	0.0437	0.0444	0
22	16	17	0.0454	0.1801	0.0466	0
23	17	18	0.0123	0.0505	0.0130	0
24	18	19	0.0112	0.0493	0.0114	0
25	19	20	0.0252	0.1170	0.0298	0
26	15	19	0.0120	0.0394	0.0101	0

Branch	From bus	To bus	$R$ (p.u.)	$X$ (p.u.)	$B_c$ (p.u.)	Line limit (MVA)
27	20	21	0.0183	0.0849	0.0216	0
28	21	22	0.0209	0.0970	0.0246	0
29	22	23	0.0342	0.1590	0.0404	0
30	23	24	0.0135	0.0492	0.0498	0
31	23	25	0.0156	0.0800	0.0864	0
32	26	25	0.0000	0.0382	0.0000	0
33	25	27	0.0318	0.1630	0.1764	0
34	27	28	0.0191	0.0855	0.0216	0
35	28	29	0.0237	0.0943	0.0238	0
36	30	17	0.0000	0.0388	0.0000	0
37	8	30	0.0043	0.0504	0.5140	0
38	26	30	0.0080	0.0860	0.9080	0
39	17	31	0.0474	0.1563	0.0399	0
40	29	31	0.0108	0.0331	0.0083	0
41	23	32	0.0317	0.1153	0.1173	0
42	31	32	0.0298	0.0985	0.0251	0
43	27	32	0.0229	0.0755	0.0193	0
44	15	33	0.0380	0.1244	0.0319	0
45	19	34	0.0752	0.2470	0.0632	0
46	35	36	0.0022	0.0102	0.0027	0
47	35	37	0.0110	0.0497	0.0132	0
48	33	37	0.0415	0.1420	0.0366	0
49	34	36	0.0087	0.0268	0.0057	0
50	34	37	0.0026	0.0094	0.0098	0
51	38	37	0.0000	0.0375	0.0000	0
52	37	39	0.0321	0.1060	0.0270	0
53	37	40	0.0593	0.1680	0.0420	0
54	30	38	0.0046	0.0540	0.4220	0

Branch	From bus	To bus	$R$ (p.u.)	$X$ (p.u.)	$B_c$ (p.u.)	Line limit (MVA)
55	39	40	0.0184	0.0605	0.0155	0
56	40	41	0.0145	0.0487	0.0122	0
57	40	42	0.0555	0.1830	0.0466	0
58	41	42	0.0410	0.1350	0.0344	0
59	43	44	0.0608	0.2454	0.0607	0
60	34	43	0.0413	0.1681	0.0423	0
61	44	45	0.0224	0.0901	0.0224	0
62	45	46	0.0400	0.1356	0.0332	0
63	46	47	0.0380	0.1270	0.0316	0
64	46	48	0.0601	0.1890	0.0472	0
65	47	49	0.0191	0.0625	0.0160	0
66	42	49	0.0715	0.3230	0.0860	0
67	42	49	0.0715	0.3230	0.0860	0
68	45	49	0.0684	0.1860	0.0444	0
69	48	49	0.0179	0.0505	0.0126	0
70	49	50	0.0267	0.0752	0.0187	0
71	49	51	0.0486	0.1370	0.0342	0
72	51	52	0.0203	0.0588	0.0140	0
73	52	53	0.0405	0.1635	0.0406	0
74	53	54	0.0263	0.1220	0.0310	0
75	49	54	0.0730	0.2890	0.0738	0
76	49	54	0.0869	0.2910	0.0730	0
77	54	55	0.0169	0.0707	0.0202	0
78	54	56	0.0028	0.0096	0.0073	0
79	55	56	0.0049	0.0151	0.0037	0
80	56	57	0.0343	0.0966	0.0242	0
81	50	57	0.0474	0.1340	0.0332	0
82	56	58	0.0343	0.0966	0.0242	0



Branch	From bus	To bus	$R$ (p.u.)	$X$ (p.u.)	$B_c$ (p.u.)	Line limit (MVA)
83	51	58	0.0255	0.0719	0.0179	0
84	54	59	0.0503	0.2293	0.0598	0
85	56	59	0.0825	0.2510	0.0569	0
86	56	59	0.0803	0.2390	0.0536	0
87	55	59	0.0474	0.2158	0.0565	0
88	59	60	0.0317	0.1450	0.0376	0
89	59	61	0.0328	0.1500	0.0388	0
90	60	61	0.0026	0.0135	0.0146	0
91	60	62	0.0123	0.0561	0.0147	0
92	61	62	0.0082	0.0376	0.0098	0
93	63	59	0.0000	0.0386	0.0000	0
94	63	64	0.0017	0.0200	0.2160	0
95	64	61	0.0000	0.0268	0.0000	0
96	38	65	0.0090	0.0986	1.0460	0
97	64	65	0.0027	0.0302	0.3800	0
98	49	66	0.0180	0.0919	0.0248	0
99	49	66	0.0180	0.0919	0.0248	0
100	62	66	0.0482	0.2180	0.0578	0
101	62	67	0.0258	0.1170	0.0310	0
102	65	66	0.0000	0.0370	0.0000	0
103	66	67	0.0224	0.1015	0.0268	0
104	65	68	0.0014	0.0160	0.6380	0
105	47	69	0.0844	0.2778	0.0709	0
106	49	69	0.0985	0.3240	0.0828	0
107	68	69	0.0000	0.0370	0.0000	0
108	69	70	0.0300	0.1270	0.1220	0
109	24	70	0.0022	0.4115	0.1020	0
110	70	71	0.0088	0.0355	0.0088	0

Branch	From bus	To bus	$R$ (p.u.)	$X$ (p.u.)	$B_c$ (p.u.)	Line limit (MVA)
111	24	72	0.0488	0.1960	0.0488	0
112	71	72	0.0446	0.1800	0.0444	0
113	71	73	0.0087	0.0454	0.0118	0
114	70	74	0.0401	0.1323	0.0337	0
115	70	75	0.0428	0.1410	0.0360	0
116	69	75	0.0405	0.1220	0.1240	0
117	74	75	0.0123	0.0406	0.0103	0
118	76	77	0.0444	0.1480	0.0368	0
119	69	77	0.0309	0.1010	0.1038	0
120	75	77	0.0601	0.1999	0.0498	0
121	77	78	0.0038	0.0124	0.0126	0
122	78	79	0.0055	0.0244	0.0065	0
123	77	80	0.0170	0.0485	0.0472	0
124	77	80	0.0294	0.1050	0.0228	0
125	79	80	0.0156	0.0704	0.0187	0
126	68	81	0.0018	0.0202	0.8080	0
127	81	80	0.0000	0.0370	0.0000	0
128	77	82	0.0298	0.0853	0.0817	0
129	82	83	0.0112	0.0367	0.0380	0
130	83	84	0.0625	0.1320	0.0258	0
131	83	85	0.0430	0.1480	0.0348	0
132	84	85	0.0302	0.0641	0.0123	0
133	85	86	0.0350	0.1230	0.0276	0
134	86	87	0.0283	0.2074	0.0445	0
135	85	88	0.0200	0.1020	0.0276	0
136	85	89	0.0239	0.1730	0.0470	0
137	88	89	0.0139	0.0712	0.0193	0
138	89	90	0.0518	0.1880	0.0528	0

Branch	From bus	To bus	$R$ (p.u.)	$X$ (p.u.)	$B_c$ (p.u.)	Line limit (MVA)
139	89	90	0.0238	0.0997	0.1060	0
140	90	91	0.0254	0.0836	0.0214	0
141	89	92	0.0099	0.0505	0.0548	0
142	89	92	0.0393	0.1581	0.0414	0
143	91	92	0.0387	0.1272	0.0327	0
144	92	93	0.0258	0.0848	0.0218	0
145	92	94	0.0481	0.1580	0.0406	0
146	93	94	0.0223	0.0732	0.0188	0
147	94	95	0.0132	0.0434	0.0111	0
148	80	96	0.0356	0.1820	0.0494	0
149	82	96	0.0162	0.0530	0.0544	0
150	94	96	0.0269	0.0869	0.0230	0
151	80	97	0.0183	0.0934	0.0254	0
152	80	98	0.0238	0.1080	0.0286	0
153	80	99	0.0454	0.2060	0.0546	0
154	92	100	0.0648	0.2950	0.0472	0
155	94	100	0.0178	0.0580	0.0604	0
156	95	96	0.0171	0.0547	0.0147	0
157	96	97	0.0173	0.0885	0.0240	0
158	98	100	0.0397	0.1790	0.0476	0
159	99	100	0.0180	0.0813	0.0216	0
160	100	101	0.0277	0.1262	0.0328	0
161	92	102	0.0123	0.0559	0.0146	0
162	101	102	0.0246	0.1120	0.0294	0
163	100	103	0.0160	0.0525	0.0536	0
164	100	104	0.0451	0.2040	0.0541	0
165	103	104	0.0466	0.1584	0.0407	0
166	103	105	0.0535	0.1625	0.0408	0

Branch	From bus	To bus	$R$ (p.u.)	$X$ (p.u.)	$B_c$ (p.u.)	Line limit (MVA)
167	100	106	0.0605	0.2290	0.0620	0
168	104	105	0.0099	0.0378	0.0099	0
169	105	106	0.0140	0.0547	0.0143	0
170	105	107	0.0530	0.1830	0.0472	0
171	105	108	0.0261	0.0703	0.0184	0
172	106	107	0.0530	0.1830	0.0472	0
173	108	109	0.0105	0.0288	0.0076	0
174	103	110	0.0391	0.1813	0.0461	0
175	109	110	0.0278	0.0762	0.0202	0
176	110	111	0.0220	0.0755	0.0200	0
177	110	112	0.0247	0.0640	0.0620	0
178	17	113	0.0091	0.0301	0.0077	0
179	32	113	0.0615	0.2030	0.0518	0
180	32	114	0.0135	0.0612	0.0163	0
181	27	115	0.0164	0.0741	0.0197	0
182	114	115	0.0023	0.0104	0.0028	0
183	68	116	0.0003	0.0041	0.1640	0
184	12	117	0.0329	0.1400	0.0358	0
185	75	118	0.0145	0.0481	0.0120	0
186	76	118	0.0164	0.0544	0.0136	0

## B. Additional Results

### B.1 24-Bus Test System

The active and reactive power flow results and power loss of ACOPF with SOCP Relaxation on each branch are shown in Table B.1.

Table B.1 Branch data result in 24-bus test system

From Bus	To Bus	$P_{ij}$ (MW)	$Q_{ij}$ (MVAr)	$P_{ji}$ (MW)	$Q_{ji}$ (MVAr)	$P_{loss}$ (MW)	$Q_{loss}$ (MVAr)
1	2	28.78	-28.42	-28.75	-14.60	0.02	0.13
1	3	13.16	-6.36	-13.05	1.42	0.11	0.42
1	5	42.07	-29.39	-41.47	29.53	0.60	2.32
2	4	38.98	-2.50	-38.45	1.39	0.53	2.06
2	6	84.77	-52.90	-79.60	67.60	5.17	19.96
3	9	-10.34	-11.31	10.40	8.50	0.07	0.26
3	24	-156.62	-27.11	157.24	49.71	0.62	22.60
4	9	-35.55	-16.39	35.99	15.43	0.44	1.69
5	10	-29.53	-43.53	30.16	43.55	0.63	2.44
6	10	-56.40	-95.60	56.99	-165.46	0.59	2.57
7	8	156.15	31.44	-152.35	-18.46	3.80	14.68
8	9	-7.36	4.68	7.40	-8.88	0.04	0.17
8	10	-11.29	-21.22	11.51	17.48	0.21	0.82
9	11	-91.19	-29.80	91.41	37.77	0.22	7.98
9	12	-137.60	-21.26	138.06	38.07	0.46	16.81
10	11	-114.67	26.01	114.97	-15.04	0.30	10.97
10	12	-178.99	38.43	179.72	-11.85	0.73	26.58
11	13	-198.55	0.22	200.89	7.62	2.34	18.26
11	14	-7.82	-22.96	7.84	14.01	0.02	0.16
12	13	-179.56	-8.86	181.48	13.46	1.92	15.00
12	23	-138.22	-17.36	140.54	13.98	2.32	18.07
13	23	-56.38	-19.94	56.72	3.12	0.35	2.69
14	16	-201.84	-18.37	203.80	24.91	1.96	15.24
15	16	2.03	1.94	-2.03	-5.88	0.00	0.00
15	21	-131.52	-3.97	132.53	0.54	1.01	7.82
15	21	-131.52	-3.97	132.53	0.54	1.01	7.82

From Bus	To Bus	$P_{ij}$ (MW)	$Q_{ij}$ (MVar)	$P_{ji}$ (MW)	$Q_{ji}$ (MVar)	$P_{loss}$ (MW)	$Q_{loss}$ (MVar)
15	24	159.01	52.01	-157.24	-49.71	1.77	13.72
16	17	-159.11	-7.61	159.88	7.74	0.77	6.06
16	19	12.34	25.84	-12.31	-30.85	0.03	0.21
17	18	-122.44	1.67	122.69	-3.03	0.25	1.97
17	22	-37.44	-9.41	37.61	-13.56	0.17	1.35
18	21	-27.84	-3.39	27.87	-2.43	0.02	0.18
18	21	-27.84	-3.39	27.87	-2.43	0.02	0.18
19	20	-84.35	-3.07	84.69	-3.22	0.34	2.64
19	20	-84.35	-3.07	84.69	-3.22	0.34	2.64
20	23	-148.69	-9.78	149.26	9.29	0.58	4.45
20	23	-148.69	-9.78	149.26	9.29	0.58	4.45
21	22	-22.35	-4.82	22.39	-10.56	0.04	0.31

## B.2 33-Bus Test System

The branch results of ACOPF with SOCP relaxation are shown in Table B.2.

Table B.2 Branch data result in 33-bus test system

From Bus	To Bus	$P_{ij}$ (MW)	$Q_{ij}$ (MVar)	$P_{ji}$ (MW)	$Q_{ji}$ (MVar)	$P_{loss}$ (MW)	$Q_{loss}$ (MVar)
1	2	3.92	2.44	-3.91	-2.43	0.01	0.01
2	3	3.44	2.21	-3.39	-2.18	0.05	0.03
3	4	2.36	1.68	-2.34	-1.67	0.02	0.01
4	5	2.22	1.59	-2.20	-1.58	0.02	0.01
5	6	2.14	1.55	-2.11	-1.52	0.04	0.03
6	7	1.10	0.53	-1.09	-0.52	0.00	0.01
7	8	0.89	0.42	-0.89	-0.42	0.00	0.00
8	9	0.69	0.32	-0.68	-0.32	0.00	0.00
9	10	0.62	0.30	-0.62	-0.29	0.00	0.00

From Bus	To Bus	$P_{ij}$ (MW)	$Q_{ij}$ (MVar)	$P_{ji}$ (MW)	$Q_{ji}$ (MVar)	$P_{loss}$ (MW)	$Q_{loss}$ (MVar)
10	11	0.56	0.27	-0.56	-0.27	0.00	0.00
11	12	0.52	0.24	-0.51	-0.24	0.00	0.00
12	13	0.45	0.21	-0.45	-0.21	0.00	0.00
13	14	0.39	0.17	-0.39	-0.17	0.00	0.00
14	15	0.27	0.09	-0.27	-0.09	0.00	0.00
15	16	0.21	0.08	-0.21	-0.08	0.00	0.00
16	17	0.15	0.06	-0.15	-0.06	0.00	0.00
17	18	0.09	0.04	-0.09	-0.04	0.00	0.00
2	19	0.36	0.16	-0.36	-0.16	0.00	0.00
19	20	0.27	0.12	-0.27	-0.12	0.00	0.00
20	21	0.18	0.08	-0.18	-0.08	0.00	0.00
21	22	0.09	0.04	-0.09	-0.04	0.00	0.00
3	23	0.94	0.46	-0.94	-0.46	0.00	0.00
23	24	0.85	0.41	-0.84	-0.40	0.01	0.00
24	25	0.42	0.20	-0.42	-0.20	0.00	0.00
6	26	0.95	0.97	-0.95	-0.97	0.00	0.00
26	27	0.89	0.95	-0.88	-0.95	0.00	0.00
27	28	0.82	0.92	-0.81	-0.91	0.01	0.01
28	29	0.75	0.89	-0.75	-0.88	0.01	0.01
29	30	0.63	0.81	-0.62	-0.81	0.00	0.00
30	31	0.42	0.21	-0.42	-0.21	0.00	0.00
31	32	0.27	0.14	-0.27	-0.14	0.00	0.00
32	33	0.06	0.04	-0.06	-0.04	0.00	0.00

### B.3 118-Bus Test System

The bus data results of the conventional ACOPF and the proposed ACOPF are shown in Table B.3. The active and reactive power flow results on each branch of ACOPF with SOCP Relaxation are shown in Table B.4.

Table B.3 Comparison of bus data result in 118-bus test system

Bus	Conventional ACOPF			ACOPF with SOCP Relaxation		
	$V$ (p.u.)	$P_g$ (MW)	$Q_g$ (MVar)	$V$ (p.u.)	$P_g$ (MW)	$Q_g$ (MVar)
1	1.033	26.48	15.00	1.032	0.00	15.00
2	1.039	-	-	1.042	-	-
3	1.038	-	-	1.038	-	-
4	1.06	0.00	71.52	1.060	0.00	64.82
5	1.057	-	-	1.058	-	-
6	1.053	0.04	33.28	1.055	0.00	30.72
7	1.051	-	-	1.055	0.00	0.00
8	1.041	0.00	-78.64	1.047	0.00	-163.52
9	1.06	-	-	1.060	-	-
10	1.053	401.87	-99.68	1.044	349.20	-128.97
11	1.046	-	-	1.050	-	-
12	1.05	85.79	54.44	1.056	185.00	57.53
13	1.034	-	-	1.037	-	-
14	1.049	-	-	1.052	-	-
15	1.049	20.88	23.85	1.047	0.00	30.00
16	1.046	-	-	1.049	-	-
17	1.06	-	-	1.058	-	-
18	1.05	13.22	30.47	1.050	0.00	43.81
19	1.048	21.58	23.96	1.046	0.00	24.00
20	1.036	-	-	1.036	-	-
21	1.031	-	-	1.032	-	-
22	1.035	-	-	1.037	-	-
23	1.049	-	-	1.050	-	-
24	1.046	0.00	-7.30	1.046	0.00	-0.69
25	1.06	193.81	-470	1.060	200.22	99.61
26	1.027	279.76	-27.58	1.060	285.77	72.08
27	1.041	9.92	25.53	1.044	0.00	24.59



Bus	Conventional ACOPF			ACOPF with SOCP Relaxation		
	$V$ (p.u.)	$P_g$ (MW)	$Q_g$ (MVar)	$V$ (p.u.)	$P_g$ (MW)	$Q_g$ (MVar)
28	1.035	-	-	1.039	-	-
29	1.035	-	-	1.042	-	-
30	1.031	-	-	1.060	-	-
31	1.039	7.25	27.19	1.046	49.78	29.19
32	1.041	14.86	21.83	1.043	0.00	19.94
33	1.046	-	-	1.043	-	-
34	1.056	4.88	-7.93	1.053	0.00	24.00
35	1.054	-	-	1.050	-	-
36	1.054	10.66	19.77	1.051	0.00	24.00
37	1.06	-	-	1.056	-	-
38	1.015	-	-	1.060	-	-
39	1.042	-	-	1.036	-	-
40	1.042	49.32	28.75	1.036	0.00	41.55
41	1.035	-	-	1.030	-	-
42	1.041	40.99	22.10	1.037	0.00	32.08
43	1.04	-	-	1.035	-	-
44	1.031	-	-	1.025	-	-
45	1.025	-	-	1.028	-	-
46	1.038	19.04	-4.15	1.057	60.09	19.54
47	1.045	-	-	1.058	-	-
48	1.047	-	-	1.054	-	-
49	1.05	193.33	19.68	1.060	304.00	30.28
50	1.039	-	-	1.052	-	-
51	1.022	-	-	1.038	-	-
52	1.017	-	-	1.033	-	-
53	1.016	-	-	1.033	-	-
54	1.031	49.54	34.87	1.048	148.00	31.17
55	1.031	32.13	20.01	1.046	0.00	20.72

Bus	Conventional ACOPF			ACOPF with SOCP Relaxation		
	$V$ (p.u.)	$P_g$ (MW)	$Q_g$ (MVar)	$V$ (p.u.)	$P_g$ (MW)	$Q_g$ (MVar)
56	1.031	32.56	14.88	1.046	0.00	15.00
57	1.032	-	-	1.046	-	-
58	1.024	-	-	1.039	-	-
59	1.047	149.70	95.67	1.060	247.57	122.78
60	1.046	-	-	1.058	-	-
61	1.048	148.41	31.96	1.060	187.76	32.40
62	1.044	0.00	0.89	1.056	0.00	11.14
63	1.016	-	-	1.057	-	-
64	1.023	-	-	1.059	-	-
65	1.016	352.24	-66.99	1.060	276.42	40.48
66	1.06	348.86	-67.00	1.060	277.13	153.38
67	1.047	-	-	1.053	-	-
68	1.015	-	-	1.060	-	-
69	1.06	453.67	-111.09	1.060	425.45	76.47
70	1.039	0.00	28.87	1.039	0.00	32.00
71	1.039	-	-	1.040	-	-
72	1.04	0.00	-5.20	1.041	0.00	-4.49
73	1.038	0.00	-2.22	1.041	0.00	1.57
74	1.022	16.93	9	1.010	0.00	9.00
75	1.024	-	-	1.016	-	-
76	1.012	22.85	23	1.000	0.00	23.00
77	1.047	0.00	69.99	1.042	0.00	70.00
78	1.042	-	-	1.036	-	-
79	1.044	-	-	1.035	-	-
80	1.06	430.84	-9.42	1.060	447.85	125.73
81	1.011	-	-	1.059	-	-
82	1.038	-	-	1.025	-	-
83	1.04	-	-	1.027	-	-

Bus	Conventional ACOPF			ACOPF with SOCP Relaxation		
	$V$ (p.u.)	$P_g$ (MW)	$Q_g$ (MVar)	$V$ (p.u.)	$P_g$ (MW)	$Q_g$ (MVar)
84	1.043	-	-	1.034	-	-
85	1.051	0.00	23.00	1.044	0.00	23.00
86	1.044	-	-	1.041	-	-
87	1.057	3.63	3.54	1.056	11.92	3.80
88	1.048	-	-	1.046	-	-
89	1.06	501.84	-24.01	1.060	381.36	2.06
90	1.042	0.00	47.21	1.041	0.00	45.22
91	1.046	0.00	1.56	1.044	0.00	0.48
92	1.05	0.00	9.00	1.050	0.00	9.00
93	1.04	-	-	1.040	-	-
94	1.038	-	-	1.037	-	-
95	1.027	-	-	1.024	-	-
96	1.035	-	-	1.031	-	-
97	1.043	-	-	1.040	-	-
98	1.052	-	-	1.053	-	-
99	1.054	0.00	-3.17	1.055	0.00	-3.30
100	1.058	231.29	45.77	1.060	301.94	29.93
101	1.043	-	-	1.044	-	-
102	1.047	-	-	1.048	-	-
103	1.051	38.25	11.72	1.059	95.99	20.12
104	1.043	0	22.87	1.042	0.00	23.00
105	1.04	5.16	9.31	1.038	0.00	23.00
106	1.034	-	-	1.032	-	-
107	1.034	29.03	3.26	1.029	0.00	16.10
108	1.039	-	-	1.039	-	-
109	1.039	-	-	1.039	-	-
110	1.041	7.03	19.67	1.043	0.00	23.00
111	1.049	35.24	-0.25	1.060	79.07	1.31

Bus	Conventional ACOPF			ACOPF with SOCP Relaxation		
	$V$ (p.u.)	$P_g$ (MW)	$Q_g$ (MVar)	$V$ (p.u.)	$P_g$ (MW)	$Q_g$ (MVar)
112	1.034	36.48	10.28	1.030	0.00	16.58
113	1.055	0.00	-10.23	1.057	0.00	2.85
114	1.037	-	-	1.039	-	-
115	1.036	-	-	1.038	-	-
116	1.015	0.00	6.41	1.059	0.00	-7.97
117	1.035	-	-	1.041	-	-
118	1.012	-	-	1.002	-	-

Table B.4 Branch data result in 118-bus test system

From Bus	To Bus	$P_{ij}$ (MW)	$Q_{ij}$ (MVar)	$P_{ji}$ (MW)	$Q_{ji}$ (MVar)	$P_{loss}$ (MW)	$Q_{loss}$ (MVar)
1	2	-16.47	-6.58	16.56	4.14	0.09	0.28
1	3	-34.53	-5.42	34.67	4.74	0.15	0.48
4	5	-74.87	48.20	74.99	-47.87	0.12	0.56
3	5	-58.56	-5.83	59.33	6.17	0.77	3.46
5	6	63.36	-8.51	-62.93	8.89	0.43	1.97
6	7	10.93	-0.17	-10.92	-0.42	0.00	0.02
8	9	-343.59	-66.02	346.22	-30.02	2.63	32.88
8	5	240.46	-36.39	-240.46	50.81	0.00	14.42
9	10	-346.22	30.02	349.20	-128.97	2.98	37.17
4	11	35.87	4.61	-35.62	-5.75	0.25	0.81
5	11	42.78	-0.59	-42.45	-0.22	0.33	1.12
11	12	-25.57	-24.31	25.63	23.97	0.07	0.22
2	12	-36.56	-13.14	36.81	12.25	0.26	0.84
3	12	-15.12	-8.92	15.24	4.87	0.12	0.41
7	12	-8.08	-1.58	8.09	0.63	0.01	0.02
11	13	33.64	7.28	-33.40	-8.53	0.24	0.80
12	14	21.18	-2.69	-21.09	0.96	0.09	0.29

From Bus	To Bus	$P_{ij}$ (MW)	$Q_{ij}$ (MVar)	$P_{ji}$ (MW)	$Q_{ji}$ (MVar)	$P_{loss}$ (MW)	$Q_{loss}$ (MVar)
13	15	-0.60	-7.47	0.62	0.71	0.01	0.04
14	15	7.09	-1.96	-7.06	-3.48	0.03	0.09
12	16	10.92	3.86	-10.89	-6.12	0.03	0.11
15	17	-96.62	2.30	97.75	-3.49	1.13	3.73
16	17	-14.11	-3.88	14.19	-0.97	0.08	0.33
17	18	91.50	-4.97	-90.57	7.32	0.92	3.79
18	19	30.57	2.49	-30.48	-3.32	0.10	0.42
19	20	12.19	4.44	-12.15	-7.47	0.04	0.20
15	19	14.23	-1.36	-14.21	0.33	0.02	0.07
20	21	-5.85	4.47	5.86	-6.72	0.01	0.05
21	22	-19.86	-1.28	19.94	-1.00	0.08	0.36
22	23	-29.94	-4.00	30.23	0.94	0.29	1.33
23	24	50.35	-7.54	-50.04	3.21	0.31	1.14
23	25	-130.33	14.30	132.78	-11.33	2.45	12.58
26	25	38.85	122.50	-38.85	122.50	0.00	245.00
25	27	106.30	-11.56	-103.10	8.44	3.20	16.39
27	28	13.13	1.63	-13.10	-3.83	0.03	0.14
28	29	-3.90	-3.17	3.90	0.61	0.00	0.02
30	17	270.19	24.99	-270.19	13.71	0.00	38.70
8	30	75.13	-61.10	-74.87	7.17	0.26	3.10
26	30	246.92	-50.42	-242.58	-4.94	4.34	46.67
17	31	28.44	-2.08	-28.10	-1.21	0.34	1.13
29	31	-27.90	-4.61	27.98	3.95	0.08	0.24
23	32	42.75	-10.70	-42.22	-0.23	0.53	1.93
31	32	6.90	-0.55	-6.89	-2.14	0.01	0.04
27	32	2.79	-1.17	-2.79	-0.92	0.00	0.01
15	33	-1.17	1.84	1.17	-5.31	0.00	0.02
19	34	-12.50	-2.44	12.61	-4.16	0.11	0.36

From Bus	To Bus	$P_{ij}$ (MW)	$Q_{ij}$ (MVar)	$P_{ji}$ (MW)	$Q_{ji}$ (MVar)	$P_{loss}$ (MW)	$Q_{loss}$ (MVar)
35	36	8.74	-7.15	-8.74	6.86	0.00	0.01
35	37	-41.74	-1.85	41.92	1.18	0.17	0.79
33	37	-24.17	-3.69	24.40	0.42	0.22	0.77
34	36	22.30	-0.65	-22.26	0.14	0.04	0.12
34	37	-112.11	-1.39	112.40	1.36	0.29	1.07
38	37	294.07	27.21	-294.07	1.90	0.00	29.11
37	39	66.81	0.22	-65.52	1.08	1.29	4.25
37	40	48.55	-5.09	-47.29	4.06	1.26	3.57
30	38	47.27	-27.23	-47.17	-19.11	0.09	1.08
39	40	38.52	-12.08	-38.25	11.32	0.28	0.91
40	41	23.49	5.42	-23.41	-6.45	0.08	0.27
40	42	-3.95	-2.26	3.96	-2.72	0.01	0.03
41	42	-13.59	-3.55	13.66	0.11	0.07	0.24
43	44	0.05	1.23	-0.04	-7.63	0.01	0.05
34	43	18.19	4.19	-18.05	-8.23	0.14	0.57
44	45	-15.96	-0.37	16.01	-1.77	0.05	0.22
45	46	-38.05	-12.11	38.64	10.50	0.59	2.00
46	47	-3.46	-1.23	3.46	-2.29	0.00	0.01
46	48	-3.09	0.27	3.10	-5.49	0.01	0.03
47	49	-24.81	3.05	24.92	-4.49	0.11	0.35
42	49	-56.81	5.84	59.03	-5.29	2.22	10.02
42	49	-56.81	5.84	59.03	-5.29	2.22	10.02
45	49	-30.96	-8.12	31.61	5.03	0.64	1.75
48	49	-23.10	-5.51	23.19	4.35	0.09	0.25
49	50	30.90	0.16	-30.68	-1.61	0.23	0.64
49	51	36.52	3.23	-35.93	-5.34	0.59	1.66
51	52	16.30	1.75	-16.25	-3.09	0.05	0.15
52	53	-1.75	-1.91	1.75	-2.42	0.00	0.00

From Bus	To Bus	$P_{ij}$ (MW)	$Q_{ij}$ (MVar)	$P_{ji}$ (MW)	$Q_{ji}$ (MVar)	$P_{loss}$ (MW)	$Q_{loss}$ (MVar)
53	54	-24.75	-8.58	24.91	5.98	0.16	0.75
49	54	18.77	-4.07	-18.54	-3.23	0.23	0.91
49	54	15.74	-4.15	-15.55	-3.32	0.19	0.64
54	55	13.48	-0.89	-13.46	-1.20	0.03	0.12
54	56	61.75	1.51	-61.65	-1.99	0.10	0.33
55	56	-11.91	0.19	11.91	-0.58	0.01	0.02
56	57	-1.59	-0.68	1.60	-1.96	0.00	0.00
50	57	13.68	-2.39	-13.60	-1.04	0.08	0.23
56	58	9.41	2.96	-9.38	-5.50	0.03	0.09
51	58	2.62	-4.41	-2.62	2.50	0.00	0.01
54	59	-31.06	-0.88	31.50	-3.74	0.44	2.03
56	59	-20.76	-1.47	21.09	-3.84	0.33	0.99
56	59	-21.32	-1.24	21.65	-3.71	0.34	1.00
55	59	-37.64	-0.26	38.26	-3.19	0.62	2.81
59	60	0.54	-0.66	-0.54	-3.55	0.00	0.00
59	61	-6.82	-0.65	6.84	-3.64	0.01	0.07
60	61	-91.09	0.71	91.28	-1.34	0.20	1.00
60	62	13.62	-0.16	-13.60	-1.39	0.02	0.09
61	62	49.59	0.42	-49.41	-0.69	0.18	0.82
63	59	135.64	8.77	-135.64	25.58	0.00	34.35
63	64	-135.64	-8.77	135.92	-12.11	0.28	3.30
64	61	-40.05	27.72	40.05	36.96	0.00	64.68
38	65	-246.90	-8.10	251.99	-53.69	5.09	55.75
64	65	-95.88	-15.61	96.10	-24.55	0.22	2.49
49	66	-38.32	6.76	38.57	-8.30	0.25	1.26
49	66	-38.32	6.76	38.57	-8.30	0.25	1.26
62	66	-13.54	-2.01	13.62	-4.10	0.08	0.36
62	67	-0.45	1.23	0.45	-4.67	0.00	0.01

From Bus	To Bus	$P_{ij}$ (MW)	$Q_{ij}$ (MVar)	$P_{ji}$ (MW)	$Q_{ji}$ (MVar)	$P_{loss}$ (MW)	$Q_{loss}$ (MVar)
65	66	-118.77	155.99	118.77	155.99	0.00	311.99
66	67	28.62	0.08	-28.45	-2.33	0.16	0.74
65	68	47.10	-37.28	-47.07	-34.07	0.03	0.32
47	69	-12.65	-0.76	12.78	-6.77	0.13	0.42
49	69	-6.06	-2.75	6.09	-6.44	0.04	0.12
68	69	-173.59	88.64	173.59	90.77	0.00	179.41
69	70	95.36	-6.39	-92.94	3.23	2.43	10.28
24	70	29.24	-2.20	-29.23	-5.63	0.02	3.26
70	71	10.26	-7.53	-10.24	6.63	0.01	0.05
24	72	7.80	-1.70	-7.77	-3.51	0.03	0.11
71	72	4.24	-3.80	-4.23	-0.98	0.01	0.03
71	73	6.00	-2.83	-6.00	1.57	0.00	0.02
70	74	29.66	12.09	-29.26	-14.31	0.40	1.32
70	75	16.24	9.84	-16.08	-13.11	0.16	0.53
69	75	85.66	6.40	-82.95	-11.60	2.71	8.16
74	75	-38.74	-3.69	38.92	3.23	0.18	0.60
76	77	-57.94	-10.50	59.46	11.75	1.52	5.08
69	77	51.97	-1.10	-51.22	-7.91	0.75	2.45
75	77	-30.27	-5.49	30.80	2.01	0.54	1.79
77	78	25.14	39.54	-25.06	-40.65	0.08	0.26
78	79	-45.94	14.65	46.06	-14.81	0.12	0.53
77	80	-90.03	-9.13	91.31	7.57	1.28	3.64
77	80	-51.86	-3.87	52.59	3.96	0.73	2.61
79	80	-85.06	-17.19	86.15	20.07	1.09	4.93
68	81	36.55	-45.36	-36.53	-45.07	0.02	0.24
81	80	36.53	45.07	-36.53	50.53	0.00	95.60
77	82	16.71	9.60	-16.58	-17.96	0.13	0.37
82	83	-5.12	-5.96	5.12	1.98	0.00	0.01



From Bus	To Bus	$P_{ij}$ (MW)	$Q_{ij}$ (MVAr)	$P_{ji}$ (MW)	$Q_{ji}$ (MVAr)	$P_{loss}$ (MW)	$Q_{loss}$ (MVAr)
83	84	-5.94	-4.13	5.97	1.44	0.03	0.05
83	85	-19.18	-7.85	19.35	4.69	0.16	0.57
84	85	-16.97	-8.44	17.07	7.32	0.10	0.21
85	86	9.16	-1.26	-9.13	-1.65	0.03	0.09
86	87	-11.87	-8.35	11.92	3.80	0.05	0.34
85	88	-17.27	-0.01	17.32	-2.72	0.06	0.28
85	89	-52.30	-2.73	52.90	1.87	0.60	4.34
88	89	-65.32	-7.28	65.87	7.93	0.55	2.80
89	90	46.86	-3.11	-45.85	0.95	1.01	3.67
89	90	102.17	-5.09	-99.96	2.66	2.21	9.26
90	91	-17.20	-0.39	17.27	-1.70	0.07	0.23
89	92	90.73	1.53	-90.00	-3.92	0.73	3.71
89	92	22.84	-1.07	-22.66	-2.80	0.18	0.74
91	92	-27.27	2.18	27.54	-4.88	0.27	0.89
92	93	15.25	7.30	-15.18	-9.45	0.07	0.23
92	94	9.64	3.96	-9.59	-8.20	0.06	0.19
93	94	3.18	2.45	-3.18	-4.46	0.00	0.02
94	95	32.37	20.06	-32.19	-20.64	0.18	0.60
80	96	39.70	7.78	-39.16	-10.44	0.53	2.73
82	96	-32.30	-3.08	32.46	-2.14	0.16	0.53
94	96	9.74	2.87	-9.72	-5.23	0.03	0.09
80	97	46.98	12.55	-46.59	-13.35	0.39	2.00
80	98	23.51	0.77	-23.39	-3.43	0.12	0.54
80	99	14.15	-3.49	-14.07	-2.25	0.08	0.37
92	100	-9.17	-3.97	9.22	-1.05	0.05	0.23
94	100	-59.35	-26.27	60.02	21.82	0.67	2.19
95	96	-9.81	-10.36	9.84	8.90	0.03	0.10
96	97	-31.43	-6.08	31.59	4.35	0.16	0.84

From Bus	To Bus	$P_{ij}$ (MW)	$Q_{ij}$ (MVar)	$P_{ji}$ (MW)	$Q_{ji}$ (MVar)	$P_{loss}$ (MW)	$Q_{loss}$ (MVar)
98	100	-10.61	-4.57	10.65	-0.55	0.04	0.19
99	100	-27.93	-1.06	28.06	-0.79	0.13	0.57
100	101	22.75	6.94	-22.60	-9.90	0.15	0.67
92	102	4.40	3.30	-4.40	-4.90	0.00	0.02
101	102	0.60	-5.10	-0.60	1.90	0.00	0.01
100	103	38.83	-11.38	-38.60	6.10	0.22	0.74
100	104	48.26	-2.35	-47.33	0.61	0.94	4.23
103	104	33.14	-0.43	-32.69	-2.50	0.46	1.56
103	105	36.78	-0.23	-36.13	-2.29	0.65	1.97
100	106	47.14	-0.70	-45.94	-1.54	1.20	4.54
104	105	42.01	-0.11	-41.85	-0.35	0.16	0.61
105	106	19.67	6.13	-19.62	-7.45	0.06	0.22
105	107	28.10	-4.88	-27.71	1.19	0.39	1.35
105	108	-0.79	-1.61	0.79	-0.37	0.00	0.00
106	107	22.56	-7.02	-22.29	2.91	0.26	0.91
108	109	-2.79	-0.63	2.79	-0.19	0.00	0.00
103	110	41.67	-1.32	-41.07	-0.96	0.61	2.81
109	110	-10.79	-2.81	10.82	0.70	0.03	0.08
110	111	-77.85	0.69	79.07	1.31	1.23	4.21
110	112	69.09	-7.43	-68.00	3.58	1.09	2.82
17	113	27.31	-5.20	-27.25	4.55	0.06	0.21
32	113	-21.00	-3.19	21.25	-1.70	0.25	0.82
32	114	13.90	3.41	-13.87	-5.06	0.03	0.12
27	115	16.17	2.70	-16.13	-4.65	0.04	0.19
114	115	5.87	2.06	-5.87	-2.35	0.00	0.00
68	116	184.10	-9.21	-184.00	-7.97	0.10	1.22
12	117	20.13	4.63	-20.00	-8.00	0.13	0.56
75	118	43.38	15.98	-43.08	-16.19	0.30	1.00
76	118	-10.06	-2.50	10.08	1.19	0.02	0.06

## VITA

**NAME** Akira Chuppawa

**DATE OF BIRTH** 23 January 1997

**PLACE OF BIRTH** Bangkok, Thailand

**INSTITUTIONS ATTENDED** B. Eng. (Electrical Eng.) at Chulalongkorn University  
M. Eng. (Electrical Eng.) at Chulalongkorn University

**HOME ADDRESS** Power System Research Lab (PSRL) 12th floor, Building 4,  
Department of Electrical Engineering, Faculty of  
Engineering, Chulalongkorn University

